



FUZZY LOGIC BASED EXACT SENSORLESS
SPEED CONTROL OF INDUCTION MOTOR
AT LOW RANGE OF OPERATIONS

BY

Abdul-Fattah Al-Batran

Supervisor

Dr. Haithem Abu-Rub

This thesis was submitted in partial fulfillment of the requirements for the
Master Degree in Scientific Computing from the faculty of graduate
studies at Birzeit University – Palestine.

December, 2004

TO MY FAMILY

بِسْمِ اللّٰهِ الرَّحْمٰنِ الرَّحِیْمِ

مَنْ جَاءَ بِالْحَسَنَةِ فَلَهُ عَشْرُ أَمْثَالِهَا وَمَنْ جَاءَ بِالسَّيِّئَةِ فَلَا يُجْزَى إِلَّا مِثْلَهَا وَهُمْ لَا يُظْلَمُونَ
160 قُلْ إِنِّي هَدَانِي رَبِّي إِلَى صِرَاطٍ مُسْتَقِيمٍ دِينًا قَدِيمًا مِّلَّةَ إِبْرَاهِيمَ حَنِيفًا وَمَا
كَانَ مِنَ الْمُشْرِكِينَ 161 قُلْ إِنْ صَلَاتِي وَنُسُكِي وَمَحْيَايَ وَمَمَاتِي لِلَّهِ رَبِّ
العَالَمِينَ 162 لَا شَرِيكَ لَهُ وَبِذَلِكَ أُمِرْتُ وَأَنَا أَوَّلُ الْمُسْلِمِينَ 163 قُلْ أَحْسِرَ اللَّهُ
أُبْغِي رِبًّا وَهُوَ رَبُّ كُلِّ شَيْءٍ وَلَا تَكْسِبُ كُلُّ نَفْسٍ إِلَّا عَلَيْهَا وَلَا تَزِرُ وَازِرَةٌ وِزْرَ
أُخْرَى ثُمَّ إِلَىٰ رَبِّكُمْ مَرْجِعُكُمْ فَيُنَبِّئُكُمْ بِمَا كُنْتُمْ فِيهِ تَخْتَلِفُونَ 164 وَهُوَ الَّذِي
جَعَلَكُمْ خَلَائِفَتهَ الْأَرْضِ وَرَفَعَ بَعْضَكُمْ فَوْقَ بَعْضٍ دَرَجَاتٍ لِّيُبْلُوَكُمْ فِي مَا آتَاكُمْ إِنَّ
رَبَّكَ سَرِيعُ الْعِقَابِ وَإِنَّهُ لَغَفُورٌ رَّحِيمٌ 165

صدق الله العظيم

ABSTRACT

In this thesis, the field orientation control, which is the most popular control algorithm of induction motor, beside the fuzzy logic controller to compensate the speed is used.

One of the most important reasons of spreading the use of the fuzzy logic is that the structure of the fuzzy logic is very similar to the human way of thinking. Accordingly, some of the technological problems can be solved easier. Therefore, this method is used in the proposed control algorithm.

Controlled induction motor drives without mechanical speed sensors at the motor shaft have the attractions of low cost and high reliability. To replace the sensor the information on the rotor speed is extracted from measured stator voltages and currents at the motor terminals. Vector-controlled drives require estimating the magnitude and spatial orientation of the fundamental magnetic flux waves in the stator or in the rotor. Luenberger state observer is used for this purpose. Very low errors between the estimated and real rotor angular velocity in steady states and transients have been observed for values very close or equal to zero. The used motor is fed by voltage source inverter with hysteresis current controllers. Properties of the control system with the speed observer have been investigated and results of simulations are presented, for extremely low speeds operation under different load conditions.

المستخلص

إن المحرك الحثي يمتاز بكثير من الميزات من أهمها الصلابة وقوة التحمل وانخفاض السعر وقلة الحاجة إلى الصيانة مما تجعله من أهم المحركات المستخدمة في الحياة العملية، إلا أن الطرق التقليدية المستخدمة في التحكم بسرعة هذا النوع من المحركات باتت لا تفي بالغرض. في هذا العمل، استخدمت أهم طرق التحكم الحديثة وهي طريقة الحقل الموجه إلى جانب استخدام تقنية من تقنيات الذكاء الصناعي وهي المنطق الضبابي.

والمنطق الضبابي انتشر انتشاراً كبيراً بسبب سهولته ومحاكاته لطريقة التفكير عند البشر، ومن خلالها يمكن حل المشاكل المعقدة التي يتطلب حلها بالطرق التقليدية كثير من الوقت والجهد بشكل بسيط وبتكاليف أقل.

إن التحكم بالمحرك الحثي بدون استخدام مجسات لقياس السرعة والتدفق المغناطيسي للعضو المتحرك للمحرك حاز على اهتمام كبير بسبب فعاليته وتقليل سعر التكلفة بشكل كبير، حيث أنه من خلال قياس متجهات التيار والفولتية الخاصة بالعضو الثابت –وهي سهولة القياس- يمكن حساب المتغيرات الخاصة بالعضو المتحرك من خلال مراقب فعال يمكنه إعطاء حسابات دقيقة جداً خصوصاً على سرعات منخفضة، حيث أن هذه المتغيرات المحسوبة تشكل المعطيات الأساسية لخوارزمية الحقل الموجه للحصول على نموذج تحكم فعال على سرعات متدنية.

في هذا التقرير تُرى نتائج البحث أن هذه الطريقة في التحكم وباستخدام المنطق الضبابي تعطي نتائج جيدة جداً ونسبة الخطأ فيها صغيرة جداً.

ACKNOWLEDGMENTS

I would like to express my sincere gratitude and deep appreciation to my supervisor Dr. Haithem Abu-Rub for his encouragement and guidance throughout the study.

Special thanks go to Dr. Wael Hashlamoun and Mohammad Karaen from the office of the dean in the faculty of engineering.

Finally and most of all, I would like to thank my family for their support, encouragement and patience during all years of my study.

TABLE OF CONTENTS

Abstract.....	I
المستخلص.....	II
Acknowledgments.....	III
Table of Contents.....	IV
List of Tables.....	VI
List of Figures.....	VII
Nomenclature.....	X
Abbreviations	X
Symbols.....	XI
Superscripts.....	XIII
Subscripts.....	XIII
Introduction.....	1
Overview of the chapters.....	5
Chapter 1 Fuzzy Logic.....	8
Introduction.....	8
Fuzzy logic, Definition.....	11
Fuzzy Sets versus Crisp Sets.....	13
Membership Functions.....	17
Operations on Fuzzy Sets.....	19
If-Then Rules.....	20
Fuzzy Inference System (Mamdani models).....	21
Basic Idea.....	21
Fuzzification.....	23
Fuzzy Inference (Rule Evaluation).....	23
Defuzzification.....	25
Induction Motors.....	28
Induction Motor Construction and Operation.....	28
Induction machine control.....	30
Decoupling idea using separately excited DC Motors.....	31
Induction Motor Equivalent Circuit.....	33
Field Orientation Control.....	37
What is Field Orientation Control (FOC).....	37
Space Vector Definition and Projection.....	38
Application of FOC on Induction motor.....	42
Main principle: Decoupling	42
Mathematical model of Induction motor.....	46

The basic scheme for the FOC.....	47
Direct and Indirect Field Orientation Control	49
Inverters and PWM.....	52
Inverters.....	52
Types of Switching Devices used in Inverters.....	54
Quick comparison between VSI and CSI.....	56
Voltage Source Inverter.....	57
Current Control of VSI Pulse Width Modulator	58
Introduction.....	58
General properties.....	59
Switching states.....	60
Switching frequency.....	61
Hysteresis Controller: Three Independent Controllers.....	62
Sensorless Control of IM.....	65
Introduction.....	65
Observers of an IM.....	66
Luenberger Observer.....	67
Flux Observer	68
Speed Observer	70
Simulations and Results.....	75
Working with Simulink.....	75
Fuzzy Logic Controller.....	76
Induction Motor Model Implementation.....	80
Implementing FOC with speed and flux measurements	83
Implementing FOC with Luenberger Observer.....	89
Chapter 7 Conclusion and Future Works.....	97
Conclusion.....	97
Future Works.....	98
Appendices.....	100
Per Unit notation (p.u.).....	100
Per Unit System.....	100
Per unit in Three phase.....	101
Torque Constant.....	102
Published Works.....	103
Simulink Models and Parameters.....	108
Induction Motor Parameters.....	108
PWM & Inverter Simulink model.....	109
Simulink model of the control system with speed and flux measurements	111
Simulink model for the sensorless control system	113
References.....	115

LIST OF TABLES

Table 4.1: Switches Comparisons.....	56
Table 6.2: Conclusion Rules.....	78
Table A.3: Torque constant values.....	102

LIST OF FIGURES

Figure 1.1: Precision and Significance in the Real World.....	12
Figure 1.2: Classical set –days of the week.....	14
Figure 1.3: Fuzzy set – days of weekend.....	15
Figure 1.4: Plotting the truth values in both two-valued and multi-valued membership.....	16
Figure 1.5: Plotting the truth values in both two-valued and multi-valued membership (continuous time scale).....	16
Figure 1.6: S, Π and Triangular- Membership functions.....	19
Figure 1.7: Truth table of fuzzy logic operation.....	19
Figure 1.8: Fuzzy logic operation for tow and multi-valued logic.....	20
Figure 1.9: Fuzzy Inference system.....	22
Figure 1.10: suggested membership functions for tallness.....	23
Figure 1.11: Fuzzify input, apply operator and apply implication operator..	24
Figure 1.12 Result of aggregation.....	25
Figure 1.13: The Defuzzification process.....	26
Figure 2.14: (a) A typical structure of stator core and (b) the rotor in squirrel-cage induction motor.....	29
Figure 2.15: A squirrel cage induction motor.	29
Figure 2.16: V/f open loop (scalar) control.....	31
Figure 2.17: (a) Equivalent circuit of separately excited DC motor, (b) layout of two-winding model and (c) vector diagram.....	32
Figure 2.18: The equivalent circuit of induction motor.....	34
Figure 3.19: The schematic of rotating magnetic fields with rotor speed.....	39
Figure 3.20: Stator current space vector and its components in (a,b,c).....	40
Figure 3.21: (a) Stator current space vector and its components in (α , β) and (b) Transformation from (α , β) to (d, q).....	41
Figure 3.22: Angular relations of current vectors.....	46
Figure 3.23: Basic scheme of FOC for AC-motor.....	49

Figure 3.24: Calculation of rotor flux and rotor flux angle in Direct field Orientation.....	50
Figure 4.25: (a) CSI, (b) VSI, (c) waveform of current and voltage of CSI and (d) waveform of current and voltage of VSI.....	53
Figure 4.26: Symbols of different types of switches used in inverters, (a) BJT, (b) MOSFET (c) IGBT and (d) GTO.....	55
Figure 4.27: Circuit diagram of three phase VSI.....	58
Figure 4.28: Basic diagram of PWM current controller.....	59
Figure 4.29: Eight switching state topology (a) The six nonzero voltage vectors, (b) the two zero voltage vectors and (c) nonzero voltages vectors associated with VSI inverter.....	60
Figure 4.30: Hysteresis Controller for one phase.....	62
Figure 4.31: Hysteresis bands (HB) around the reference currents i_a; i_b; i_c.63	
Figure 5.32: Structure of the conventional rotor flux observer.....	70
Figure 5.33: Structure of the proposed rotor flux and rotor speed observer.73	
Figure 6.34: Fuzzy logic controller.....	77
Figure 6.35: Membership functions plots for A) e, B) Δe and C) Δu.....	79
Figure 6.36: Control surface.....	79
Figure 6.37: Squirrel Cage Induction Motor Model.....	80
Figure 6.38: Simulation result in p.u. for IM model (a) No load and (b) Full load.....	82
Figure 6.39: Simulink FOC model of induction motor.....	84
Figure 6.40: Pulse Generator using three independent hysteresis current controllers.....	85
Figure 6.41: Simulink Fuzzy logic controller.....	86
Figure 6.42: Simulation results for the control system (a) PI controller (b) FLC for speed=1p.u.....	86
Figure 6.43: The measured i_{abc} in transient, steady state and applying disturbance (changing torque).....	86
Figure 6.44: Command i_{abc}, very small change during changing the torque.	87

Figure 6.45: Speed response for FLC and PI controller.....	87
Figure 6.46: Simulation results for the FOC system (a) PI controller (b) FLC for variable speed.....	88
Figure 6.47: Speed response for FLC and PI controller for variable speed...	88
Figure 6.48: The control model with the observer system.....	89
Figure 6.49: Luenberger speed observer.....	90
Figure 6.50: Simulation results for the sensorless control system (a) PI controller (b) FLC for constant speed and step change of load torque.....	91
Figure 6.51: The plot of the rotor speed, and the Error plot at 0.3 p.u. command speed.....	91
Figure 6.52: The plot of the rotor speed, and the absolute error plot at 0.5 p.u. command speed.....	92
Figure 6.53: The plot of the rotor speed, and the absolute error plot at 0.1 p.u. command speed.....	93
Figure 6.54: Speed response at zero speed with a step change of torque.....	93
Figure 6.55: The iabc command and actual for the sensorless model.....	94
Figure 6.56: Result of control system after ramp speed change and the absolute error.....	94
Figure 6.57: Result of control system after negative ramp speed change and the absolute error.....	94
Figure 6.58: Results of control system after speed changes and step load changes. $i_{s\alpha}$, $i_{s\beta}$, $\psi_{r\alpha}$, and $\psi_{r\beta}$ are also shown.....	95

NOMENCLATURE

Abbreviations

AC	Alternating Current
DC	Direct Current
IM	Induction motor
FOC	Field Orientation Control
DFOC	Direct Field Oriented Control
ILOC	Indirect Field Oriented Control
AI	Artificial Intelligence
ANN	Artificial Neural Networks
GA	Genetic Algorithm
FL	Fuzzy Logic
FLC	Fuzzy Logic Controller
PI	Proportion Integral controller
SOM	Smallest of maximum
MOM	Mean of maximum
LOM	Large of maximum
BOA	Bisector of area
COA	Centroid of area
MMF	Magneto-motive force
abc	A, B, C Frame

$\alpha\beta$	Stationary frame
dq	Rotating frame
p.u.	Per Unit value
VSI	Voltage Source Inverter
CSI	Current Source Inverter
PWM	Pulse-Width Modulation
HB	Hysteresis Band
BJT	Bipolar Junction Transistor
GTO	Gate Turn-Off Thyristor
IGBT	Insulated Gate Bipolar Transistor
MOSFET	Meta Oxide Semiconductor Field Effect Transistor

Symbols

μ	Membership Function
n_{sync}	Synchronous speed
n_m	Mechanical speed
n_{slip}	Slip speed
s	Slip
ω_{sync}	Synchronous speed (rotational)
ω_m	Mechanical speed (rotational)
T_a	Electromagnetic time constant of the armature current
T_{fn}	Rated electromagnetic time constant of the excitation circuit
T_M	Mechanical constant

i	Current
u	Voltage
\underline{v}	Voltage vector
e	Counter EMF induced in the rotor
ψ	Flux
M	Mechanical load Torque
M	Mutual Inductance
R	Resistance
L	Inductance
C	Capacitance
t	Time
ε	Rotor angle
θ	Rotor angle
J	Moment of inertia
C	Constant
K	Space vector
m	Mechanical torque (p. u.)
X	Relactance
T_o	Load torque
x, u, y, z	Vectors of state, control, output and disturbance variable
A, B, C	Matrices of coefficients
K_x, K_z	Matrices of gain coefficients
k_i, k_{j1}, k_{j2}	Gain coefficients of observer

Superscripts

$\hat{}$ Estimated value

Subscripts

a	Armature
a	Phase A
a	Constant
b	Phase B
c	Phase C
f	Field
r	Rotor
s	Stator
L	Load
M	Mutual
α	α component in $\alpha\beta$ frame
β	β component in $\alpha\beta$ frame
d	d component in dq frame
q	q component in dq frame
ref	reference or command value

INTRODUCTION

Electric motors use 60% of the electrical energy generated in the industrial countries. About 8% of this energy is taken up by dc motors, thus most of the energy is used by ac motors. An improvement of 1% in all electric motors operating efficiency could result in reduced coal combustion of 6.5 to 10 million tons per year [27]. The most important challenge to reducing motor power consumption is to properly vary the shaft speed of motors that are designed as constant-speed machines.

Induction motors are relatively rugged and inexpensive machines. Therefore much attention is given to their control for various applications with different control requirements. An induction machine, especially squirrel cage induction machine, has many advantages when compared with DC machine. First of all, it is very cheap. Next, it has very compact structure and insensitive to environment. Furthermore, it does not require periodic maintenance like DC motors. However, because of its highly non-linear and coupled dynamic structure, an induction machine requires more complex control schemes than DC motors. Traditional open-loop control of the induction machine with variable frequency may provide a satisfactory solution under limited conditions. However, when high performance dynamic operation is required, these methods are unsatisfactory. Therefore, more sophisticated control methods are needed to make the performance of the induction motor comparable with DC motors. Recent

developments in the area of drive control techniques, fast semiconductor power switches, powerful and cheap microcontrollers made induction motors alternatives of DC motors in industry [7].

The most popular induction motor drive control method has been the field oriented control (FOC) in the past two decades. Furthermore, the recent trend in FOC is towards the use of sensorless techniques that avoid the use of speed sensor and flux sensor. The sensors in the hardware of the drive are replaced with state observers to minimize the cost and increase the reliability [12]. One of the most important states observers to estimate the states that are used in the FOC algorithm to estimate the rotor speed and rotor flux is Luenberger Observer, which gives acceptable results especially at low ranges of operations, even at zero speed. FOC needs a huge amount of computations, and in the case of using Luenberger observer the computation amount is extremely increased. The induction motor is fed by the voltage source inverter with hysteresis current controllers.

A speed sensor is inconvenient and has many defects [36] – [47]. Among the problems it presents are the spoiling of the ruggedness and the simplicity of AC motors. The encoder is a cost factor, since the provision of special motor-shaft extension encoder mounting surfaces leads to more expensive machines. The use of the delicate optical encoders lowers system reliability, especially in hostile environments. Because of these problems, it is important to eliminate the speed

sensor from control systems. Thus, for two decades there have been serious trends throughout the world to use sensorless control of electrical machines.

In high performance motor control systems current controller is the most often used one. In the literature different current controllers are used.

The performance of sensorless controlled induction motors is poor at very low speed and zero stator frequency. There are limits of stable operation at very low speed that should be solved.

When the field oriented control system is used for sensorless drive system, the field angle, and also the mechanical speed, are estimated using the stator current vector and the stator voltage vector as input variables. Their accurate acquisition is a major concern for stable operation at very low speed. The reason is the limited accuracy of stator voltage acquisition and the presence of offset and drift components in the acquired signals [48].

The direct measurement of the stator voltages at the machine terminals is most accurate, but hardware requirements are quite substantial. The switched stator voltage waveforms require a large signal acquisition bandwidth, and the electric isolation must be maintained between the power circuit and the electronic control system. However, the processing of the analog signals introduces errors and offset. Using the reference voltage of the PWM modulator avoids all these problems. This signal is readily available in the control unit, and it is free from harmonic components. It does not exactly represent the stator voltages, though, as

distortions are introduced by the dead time effect which cannot be completely eliminated even by the most sophisticated compensation strategies [48].

The use of speed observer system eliminates these problems for low speed ranges and gives it possible to present extremely low speed control.

Artificial Intelligence (AI), such Artificial Neural Networks (ANN), Genetic Algorithm (GA) and Fuzzy Logic Control (FLC) or a combinations among them are become an important techniques to extract the ultimate performance from modern motors. Fuzzy logic control is used and implemented in this thesis, because of its simple structure and good results in the area of control.

Fuzzy logic control is the process of employing fuzzy logic concept in system control applications. Fuzzy logic is a kind of logic that deals with the concept of partial truthness, so it can be thought of as the super-set of the conventional, true or false, Boolean logic. The fuzzy logic approach allows the designer to handle efficiently very complex closed-loop control problems, reducing in many cases, engineering time and cost. Also it supports nonlinear design techniques that are now being used in motor control application. Moreover, FLC relatively needs less computation than ANN and GA.

The induction motor used is fed by a voltage source inverter with hysteresis current controllers; this controller is widely used because of its simplicity.

Overview of the chapters

The first five chapters are discussing a brief backgrounds and mathematical models of the main elements in the different system models.

Chapter one presents the basic idea of fuzzy logic and compared it with the Boolean logic, also it presents the membership functions, the operations on fuzzy logic, and the inference system.

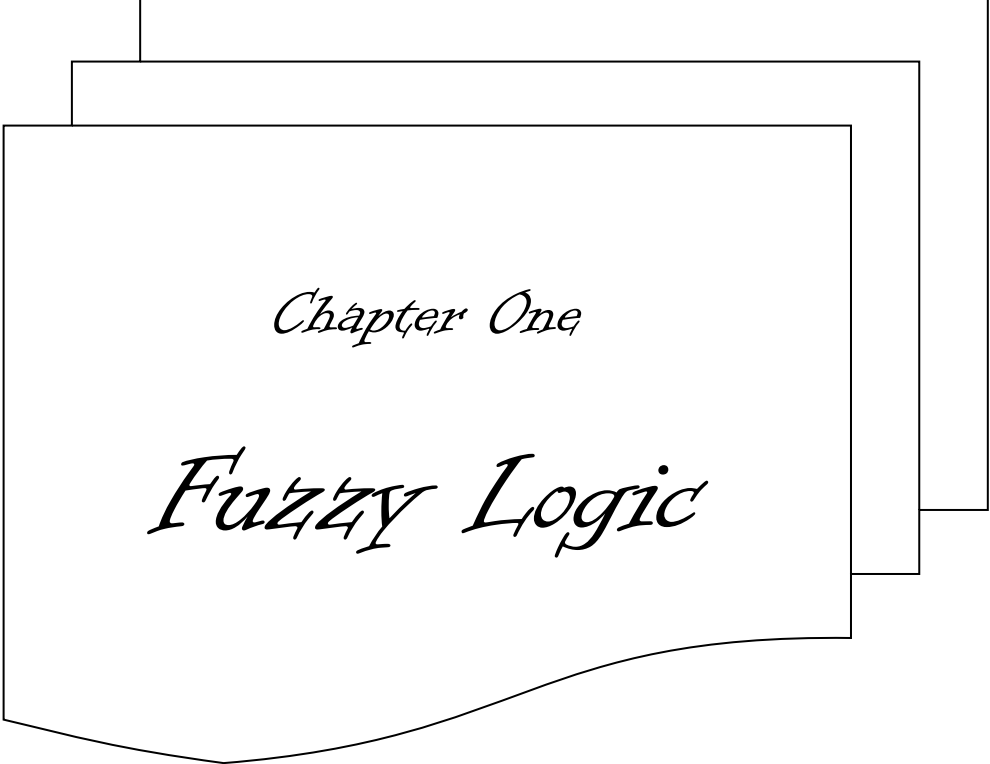
Chapter two presents a brief description of induction motor, the construction of the IM, the induction machine control and comparison with DC motor control, and the mathematical model of the induction motor based on the equivalent circuit.

Chapter three and chapter five show a detailed description of the field orientation control, the derivation of the main equations and the implementation of the FOC on the induction motor and introducing the mathematical model of the induction motor is the rotating frame. Then, describing the sensorless control of IM with the use of Luenberger observer, and showing the benefits of sensorless control over the traditional FOC.

Chapter four demonstrates the voltage source inverter and current source inverter, and focuses mainly on the current-controlled voltage source inverter pulse width modulation and the use of hysteresis current controllers. And it

introduces a brief comparison between the main types of switching devices used in inverters.

And at last, in chapter six, design of the Fuzzy Logic Controller and the implementation of induction motor are introduced firstly and then discussion of simulation results at low speeds: Firstly, for the FOC system with speed and flux measurement with the use of traditional PI controller and the FLC, secondly, for the sensorless control model with Luenberger observer with FLC and PI controllers. The complete Simulink models were introduced in Appendix A.4.



Chapter One

Fuzzy Logic

CHAPTER 1 FUZZY LOGIC

Introduction

Consider the following paradox statements and questions: When the first plank was replaced in the ship, everyone agreed it was still the same ship. Replacing a second plank made no difference either. At some point, all planks may have replaced. Was it a different ship? At what point did it become new one?. Or consider a heap of sand. Is it still a heap if we remove one grain of sand? How about two grains? Three?! If we continue in this way, we eventually remove all grains and still conclude that a heap remains, or that it has suddenly vanished. No single grain takes us from heap to nonheap.

If a barber says: “I shave all, and only, those men who don’t shave themselves!! “...Who shaves the barber?! If he shaves him self, then according to what he said he does not. If he doesn’t, then again, according to his saying, He does. Consider the card that says on one side “the sentence on the other side is TRUE”, and the other side says: “the sentence on the other side is FALSE” [1]. Or consider a one who said to you: “don’t trust me”. Should you trust him?

Questions of the above nature, bothered people acquainted with a classical logic for ages. The classical logic concept of the excluded middle, where every logical proposition has to either be completely true or false, does not seem to fulfill expectations of nowadays very technical and logic dependent world.

Nevertheless, most computer, control system engineers and many other people involved in modeling and programming behavior still rely on the True/False conditions and differential equations. There were several people who tried to adjust classical logic to accept a broader concept of something being true or false. In the early 1900's, Lukasiewicz presented his three-valued logic, where the third value proposed could be described as "possible", and had a numeric value between True and False [1] [2].

When Lotfi Zadeh¹ published his works on fuzzy sets and math accompanying them in 1965 the theory quickly was branded fuzzy logic. It created a lot of new possibilities along with controversy and misunderstandings. Here some of the reactions on the Zadeh's works:

***Rudolph E. Kalman said in 1972:** "I would like to comment briefly on Prof. Zadeh's presentation. His proposals could be severely, ferociously, even brutally criticized from a technical point of view. This would be out of place here. But a blunt question remains: Is Prof. Zadeh presenting important ideas or is he indulging in wishful thinking? No doubt Prof. Zadeh's enthusiasm for fuzziness has been reinforced by the prevailing climate in the US --- one of unprecedented permissiveness. 'Fuzzification' is a kind of scientific permissiveness; it tends to result in socially appealing slogans unaccompanied by the discipline of hard scientific work and patient observation."*[3].

¹ The creator of Fuzzy logic.

Prof. William Kahan said in 1975²: "Fuzzy theory is wrong, wrong, and pernicious. I cannot think of any problem that could not be solved better by ordinary logic. What Zadeh is saying is the same sort of things: Technology got us into this mess and now it can't get us out. Well, technology did not get us into this mess. Greed and weakness and ambivalence got us into this mess. What we need is more logical thinking, not less. The danger of fuzzy theory is that it will encourage the sort of imprecise thinking that has brought us so much trouble." [3].

Even in the 1990s when there have been hundreds of successful applications of fuzzy logic, some scientists still condemn the concept, like what **Jon Konieki** stated in AI Expert in 1991: *"Fuzzy logic is based on fuzzy thinking. It fails to distinguish between the issues specifically addressed by the traditional methods of logic, definition, and statistical decision-making."* [3]

Despite of the above opinions fuzzy theory especially in control fields has been and continues to be very active and fruitful research field and has rapidly become one of the most successful of today's technologies for developing sophisticated control systems. It fills an important gap in engineering design methods left vacant by purely mathematical approaches (e.g. linear control design), and purely logic-based approaches (e.g. expert systems) in system design. The impetus behind this lies largely on the fact that numerous applications of fuzzy control emerged covering a wide range of practice arias, beside it deals with

² Prof. William Kahan: An esteemed and brilliant colleague whose Evans Hall office is a few doors from Zadeh's.

such applications perfectly as it resembles human decision making with an ability to generate precise solutions from certain or approximate information, also the simplicity of understanding and dealing with this theory.

Fuzzy logic, Definition

Most of references on fuzzy logic begin with a few quotes, here some of them: “Precision is not truth” –Henri Matisse, “Sometimes the more measurable drives out the most important.” – René Dubos, “As complexity rises, precise statements lose meaning and meaningful statements lose precision. “ - Lotfi Zadeh and “Don't lose sight of the forest for the trees. “ and “Don't be penny wise and pound foolish.” - Some folk saying.

Fuzzy logic is all about relative importance of precision: how important is it to be exactly right when a violent answer will do? –See Figure 1.1- Or it is a superset of conventional(Boolean) logic that has been extended to handle the concept of partial truth- truth values between "completely true" and "completely false" [4]. As its name suggests, it is the logic underlying modes of reasoning which are approximate rather than exact. Another definition by Lotfi Zadeh: Fuzzy logic has two different meanings. *In a narrow sense*, fuzzy logic is a logical system, which is an extension of multivalued logic. *But in a wider sense*, which is in predominant use today, fuzzy logic (FL) is almost synonymous with the theory of fuzzy sets, a theory which relates to classes of objects with unsharp boundaries in which membership is a matter of degree. In this perspective, fuzzy logic in its narrow sense is a branch of FL. What is important to recognize is that, even in its

narrow sense, the agenda of fuzzy logic is very different both in spirit and substance from the agendas of traditional multivalued logical systems. [5]

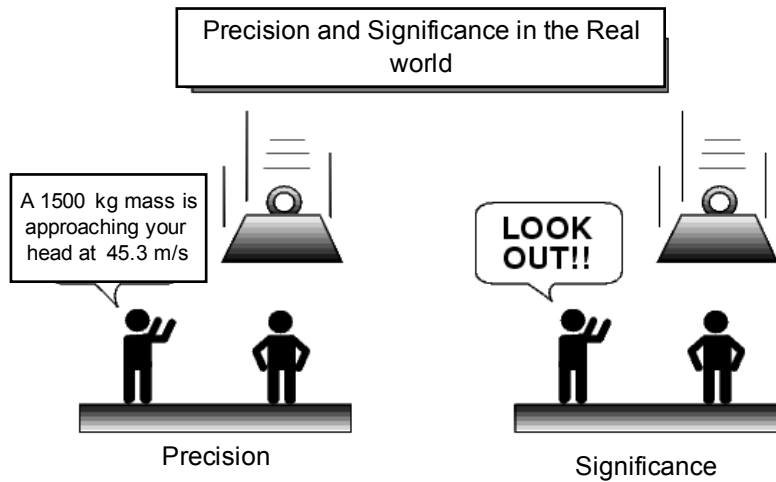


Figure 1.1: Precision and Significance in the Real World.

The essential characteristics of fuzzy logic as founded by Zadeh Lotfi are as follows [4]:

- In fuzzy logic, exact reasoning is viewed as a limiting case of approximate reasoning.
- In fuzzy logic everything is a matter of degree.
- Any logical system can be fuzzified³.
- In fuzzy logic, knowledge is interpreted as a collection of elastic or, equivalently, fuzzy constraint on a collection of variables

³ Defining Boolean logic as a subset of Fuzzy logic.

- Inference is viewed as a process of propagation of elastic constraints.

Fuzzy Sets versus Crisp Sets

An ordinary set is simply a collection of things; the things themselves could be almost anything, such as numbers, cars, specific countries, specific ideas, and so on. If we have a particular set, say cars, any object that you can think of either belongs or doesn't belong to the set; there is nothing in between belonging and not belonging. Such sets are called *crisp*; there are no gradations of membership. If we imagine a set of true statements, then a statement is either true or false, with no gradations of truth. Like saying: you are at home or not, you have car or not, or defining the set of real numbers.

Any statement can be fuzzy. The tool that fuzzy reasoning gives the ability to reply to a yes-no question with a not-quite-yes-or-no answer. This is the kind of thing that humans do all the time (think how rarely you get a straight answer to a seemingly simple question) but it's a rather new trick for computers [5].

Fuzzy mathematics defines a different kind of set, and a different measure of truth, which are sets that have *gradation* of belonging. The real world is not all True and False, i.e. using linguistic terms like: “tall”, “fast”, “big”, “near”, “Green” are matter of degree, in fact, to deal with such terms mostly one may use some fuzzy qualifiers like: “very”, “more”, “less”, “slightly”, “some” ...etc. If one defines a fuzzy set of true statements, a real statement will belong to the set

more or less depending on how true the statement is. If one defines a set (for example, tall people) a real person will belong to the set to some degree, depending on how tall he/she is. Here, a member of a fuzzy set has a grade (*confidence*) of *membership* indicating how sure we are that the member belongs to the fuzzy set.

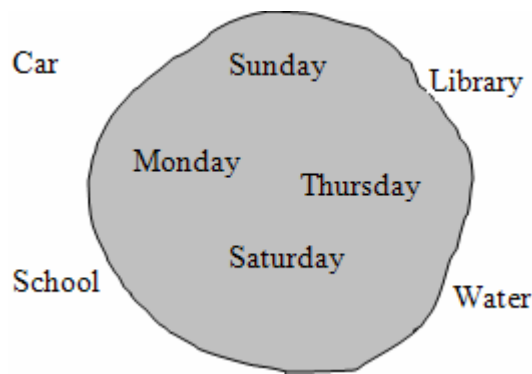


Figure 1.2: Classical set –days of the week.

Here a good clarification of the idea of fuzzy and crisp sets. Consider this example⁴, the set of days of the week indubitably includes Sunday, Monday, and Saturday. It just as indubitably excludes car, liberty, and school, and so on, as in Figure 1.2. But a set of days of weekend may be represented graphically as in Figure 1.3.

⁴ This example is largely based on a similar example from Mathworks site (fuzzy tutorial section)

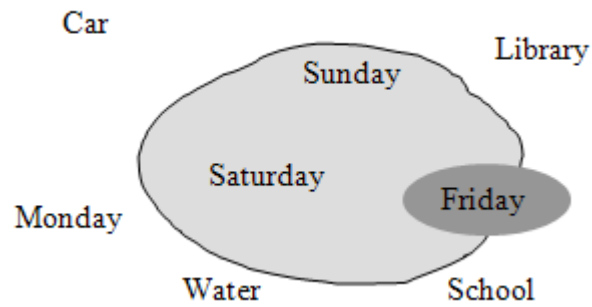


Figure 1.3: Fuzzy set – days of weekend

Most would agree that Saturday and Sunday belong to the set of days of weekend, but what about Friday? It "feels" like a part of the weekend, but somehow it seems like it should be technically excluded. So in Figure 1.3 Friday locates on the fence. Classical or "crisp" sets wouldn't tolerate this kind of thing.

Reasoning in fuzzy logic is –as clarified above- just a matter of generalizing the familiar yes-no (Boolean) logic. If we give "true" the numerical value of 1 and "false" the numerical value of 0, we're saying that fuzzy logic also permits in-between values like 0.2 and 0.7453. For instance, consider the following list of questions and answers:

Q: Is Saturday a weekend day? **A:** 1 (yes, or true).

Q: Is Tuesday a weekend day? **A:** 0 (no, or false)

Q: Is Friday a weekend day? **A:** 0.8 (for the most part yes, but not completely)

Q: Is Sunday a weekend day? **A:** 0.95 (yes, but not quite as much as Saturday).

In Figure 1.4 on the left is a plot that shows the truth values for "weekendness" if the response is absolute yes or no. where the right plot shows the truth

value for “weekend-ness” if it allowed responding with fuzzy in-between values.

And Figure 1.5 is the same plots but in continuous scale time.

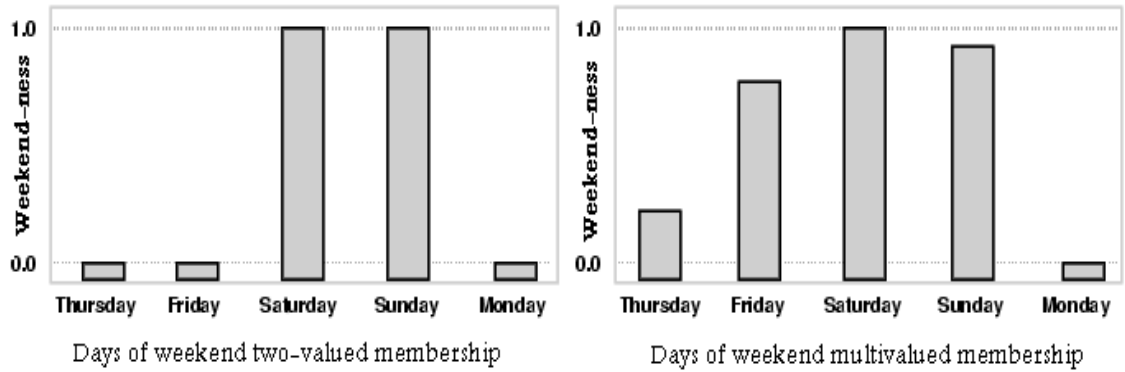


Figure 1.4: Plotting the truth values in both two-valued and multi-valued membership.

By making the plot continuous, we're defining the degree to which any given instant belongs in the weekend rather than an entire day. In the plot on the left, notice that at midnight on Friday, just as the second hand sweeps past 12, the weekend-ness truth value jumps discontinuously from 0 to 1. This is one way to define the weekend, and while it may be useful to an accountant, it doesn't really connect with our real-world experience of weekend-ness.

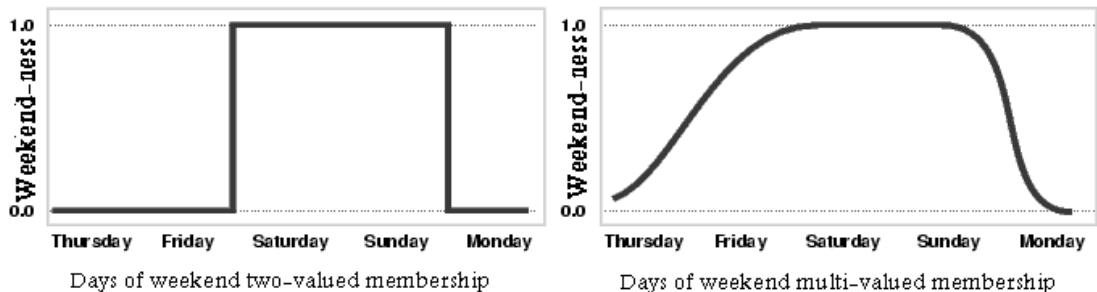


Figure 1.5: Plotting the truth values in both two-valued and multi-valued membership (continuous time scale)

The plot on the right shows a smoothly varying curve that accounts for the fact that all of Friday, and, to a small degree, parts of Thursday, partake of the quality of weekend-ness and thus deserve partial membership in the fuzzy set of weekend moments. The curve that defines the weekend-ness of any instant in time is a function that maps the input space (time of the week) to the output space (weekend-ness). Specifically it is known as a *membership function*. More detail is in the next section.

Membership Functions

A membership function is a curve that defines how each point in the input space is mapped to a membership value (or degree of membership). In classical sets membership function (μ) is defined as in equation 1.1, where an element x belongs to the set A or not. On the other hand, membership functions of fuzzy sets can be an arbitrary curve whose shape differ from one application to another according to the application it self or the simplicity, speed efficiency of computation or implementations but its value is banded between 0 and 1, i.e. $0 \leq \mu_A(x) \leq 1$.

$$\mu_{Crisp}(x) = \begin{cases} 1 & \text{if } x \in A \\ 0 & \text{if } x \notin A \end{cases} \quad (1.1)$$

Since the membership function is a curve which is mapped input space to a membership value, there are many membership functions could be defined, but as an example of well-known membership function is the *S-function* and *Π -function* which defined in equation 1.2 and 1.3 respectively. Another function

which is easier to represent and save computation is the *Triangular function*, which defined in equation 1.4. These functions are plotted in Figure 1.6.

$$S(x, a, b, c) = \begin{cases} 0 & x \leq a \\ 2\left(\frac{x-a}{c-a}\right)^2 & a \leq x \leq b \\ 1-2\left(\frac{x-a}{c-a}\right)^2 & b \leq x \leq c \\ 1 & x \geq c \end{cases} \quad (1.2)$$

$$\pi(x, a, b) = \begin{cases} s(x, b-a, b-a/2, b) & x \leq b \\ 1-s(x, b, b+a/2, a+b) & x \geq b \end{cases} \quad (1.3)$$

$$T(x, a, b, c) = \begin{cases} 0 & x \leq a \text{ or } x \geq c \\ \frac{x-a}{b-a} & a \leq x \leq b \\ -\frac{x-c}{c-b} & b \leq x \leq c \end{cases} \quad (1.4)$$

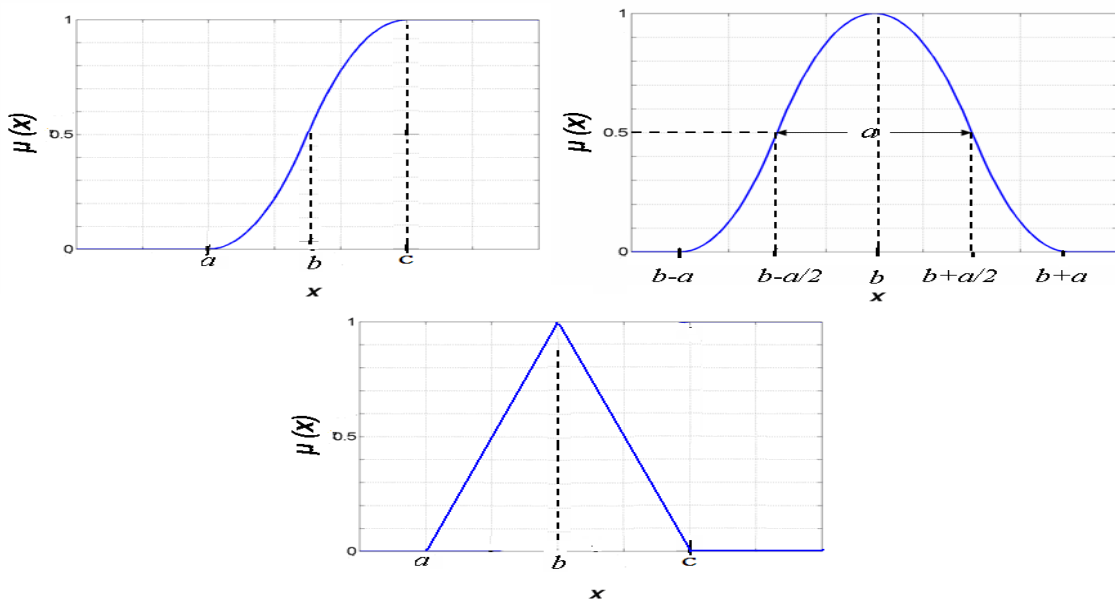


Figure 1.6: S, Π and Triangular- Membership functions

Operations on Fuzzy Sets

Firstly, to prove that fuzzy logic is a superset of standard Boolean logic, $\min(A,B)$, $\max(A,B)$ and $(1- A)$ operations are used to resolve **AND**, **OR** and **NOT** operations respectively of Boolean logic, where A and B are limited to the range $(0,1)$. Moreover, since there is a function behind the truth table rather than just the truth table itself, we can now consider values other than 1 and 0. Figure 1.7 and Figure 1.8 summarize this point.

A	B	$\min(A,B)$
0	0	0
0	1	0
1	0	0
1	1	1

AND

A	B	$\max(A,B)$
0	0	0
0	1	1
1	0	1
1	1	1

OR

A	$1-A$
0	1
1	0

NOT

Figure 1.7: Truth table of fuzzy logic operation.

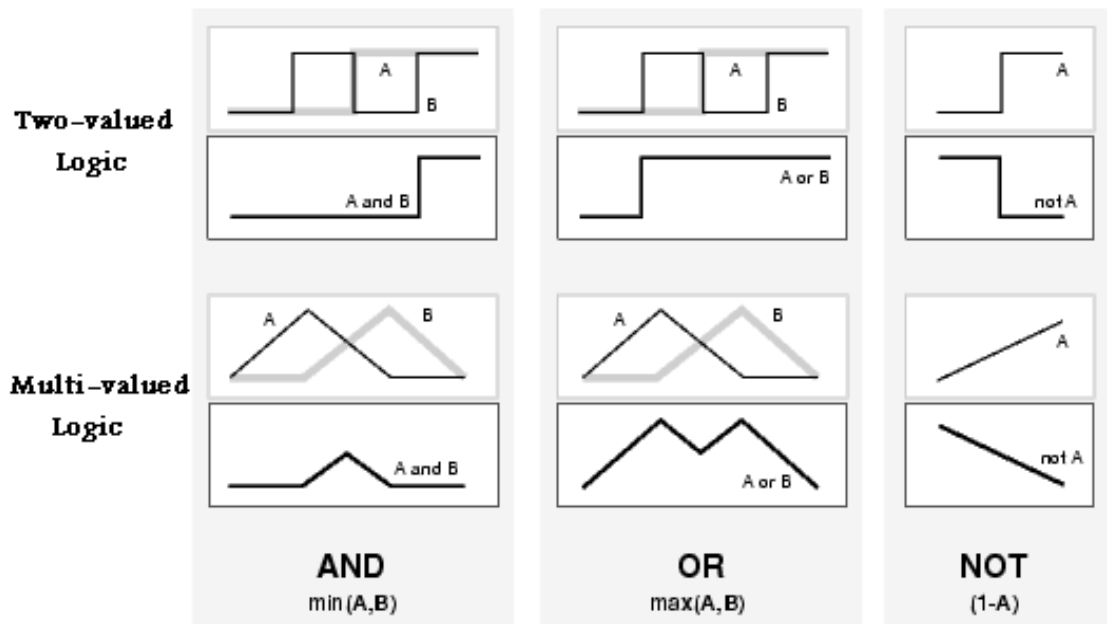


Figure 1.8: Fuzzy logic operation for tow and multi-valued logic.

$Min(A,B)$, $max(A,B)$ and $(1- A)$ operations represent the intersection, union and complement respectively. Moreover, De Morgans law, Associativity, Commutativity and Distributivity are common in classical set theory also apply to Fuzzy set theory.

If-Then Rules

Fuzzy sets and fuzzy operators are the subjects and verbs of fuzzy logic. These if-then rule statements are used to formulate the conditional statements that comprise fuzzy logic. A single fuzzy if-then rule assumes the form

$$if\ x\ is\ A\ then\ y\ is\ B$$

where A and B are linguistic values defined by fuzzy sets on the ranges (universes of discourse) X and Y, respectively [5]. The if-part of the rule "x is A" is called

the *antecedent* or *premise*, while the then-part of the rule "y is B" is called the *consequent* or *conclusion*. An example of such a rule might be

If service is good then tip is average

Interpreting if-then rules is a three-part process [5]. This process is explained in detail in the next section:

1. ***Fuzzify inputs:*** Resolve all fuzzy statements in the antecedent to a degree of membership between 0 and 1. If there is only one part to the antecedent, this is the degree of support for the rule.
2. ***Apply fuzzy operator to multiple part antecedents:*** If there are multiple parts to the antecedent, apply fuzzy logic operators and resolve the antecedent to a single number between 0 and 1. This is the degree of support for the rule.
3. ***Apply/implication method:*** Use the degree of support for the entire rule to shape the output fuzzy set. The consequent of a fuzzy rule assigns an entire fuzzy set to the output. This fuzzy set is represented by a membership function that is chosen to indicate the qualities of the consequent. If the antecedent is only partially true, (i.e., is assigned a value less than 1), then the output fuzzy set is truncated according to the implication method.

Fuzzy Inference System (Mamdani models)

Basic Idea

Assume that -for a specific system- a set of inputs X and outputs Y , a rule-base R . with the aid of fuzzy set and fuzzy logic theory, a fuzzy system at linguistic level can be established as shown in Figure 1.9.

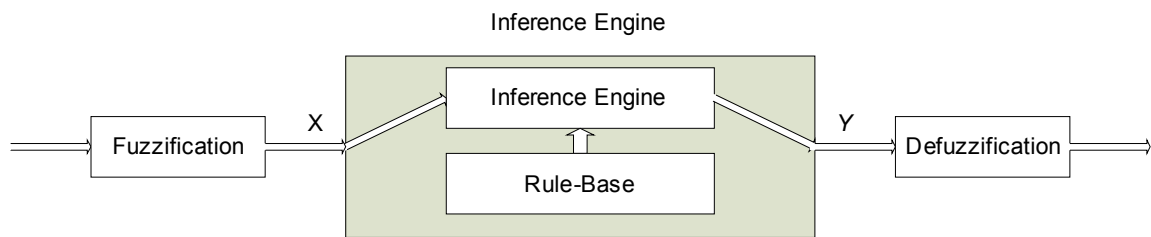


Figure 1.9: Fuzzy Inference system

The mechanism of deriving a reasonable *action* (conclusion) Y_o with respect to X_o can be interpreted as performing a two-stage reasoning process. Viewing the rule-base B as a prototype, the inference engine E first checks the IF-part of the rules. And to deduce the action the inference engine checks the THEN-part of the rules.

To implement a fuzzy system in a computational form, one of the methods used widely in the fuzzy community is to construct a relation matrix R from the available rule-base and then the current output Y is calculated by a relation equation $Y=XOR$, where O denotes a logical operator performing composition of inference [2]. From a system's viewpoint, the relation equation provides a compact formulation, analogous, for example, to the convolution equation in linear systems theory, with the relation matrix as the equivalent of the impulse response function and the composition operator corresponding to the convolution operator [2].

As Figure 1.9 shows, the inference procedure will pass through the three stages, Fuzzification, Inference (rule evaluation) and Defuzzification process.

Fuzzification

Fuzzification is the first step in the inference process in fuzzy logic, which is to take the inputs and determine the degree to which they belong to each of the appropriate fuzzy sets via membership functions. As an example shown in Figure 1.10, for the numerical variable *height* which has a given value of 160 cm is fuzzified using the shown membership functions as: linguistic variable *height* has linguistic values of "*short*" with a degree of membership of 0.5, "*medium*" with a degree of 0.5, and for the remaining linguistic value "*tall*" with a degree of 0.0.

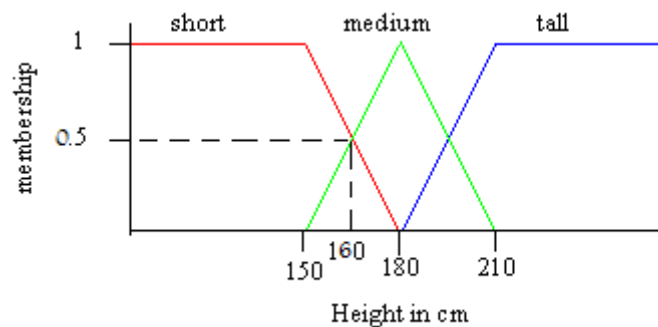


Figure 1.10: suggested membership functions for tallness.

Fuzzy Inference (Rule Evaluation)

Once the inputs have been fuzzified, we know the degree to which each part of the antecedent has been satisfied for each rule. If the antecedent of a given rule has more than one part, the fuzzy operator is applied to obtain one number that represents the result of the antecedent for that rule. This number will then be

applied to the output function. The input to the fuzzy operator is two or more membership values from fuzzified input variables. The output is a single truth value.

Consider the following rule as an example:

“IF (Temperature is warm OR Pressure is increasing) THEN Sky is grey”

And assuming that the given numeric values for *Temperature* and *Pressure* are T_o and P_o respectively, and according to the membership functions defined in Figure 1.11 applying **OR** or *max* operator in the IF-part of the rule giving a scalar number which is 0.75. And then, applying this result to the consequent function -THEN-part of the rule-. When antecedent is a fuzzy statement so that is true to some degree of membership, then the consequent is also true to that same degree.

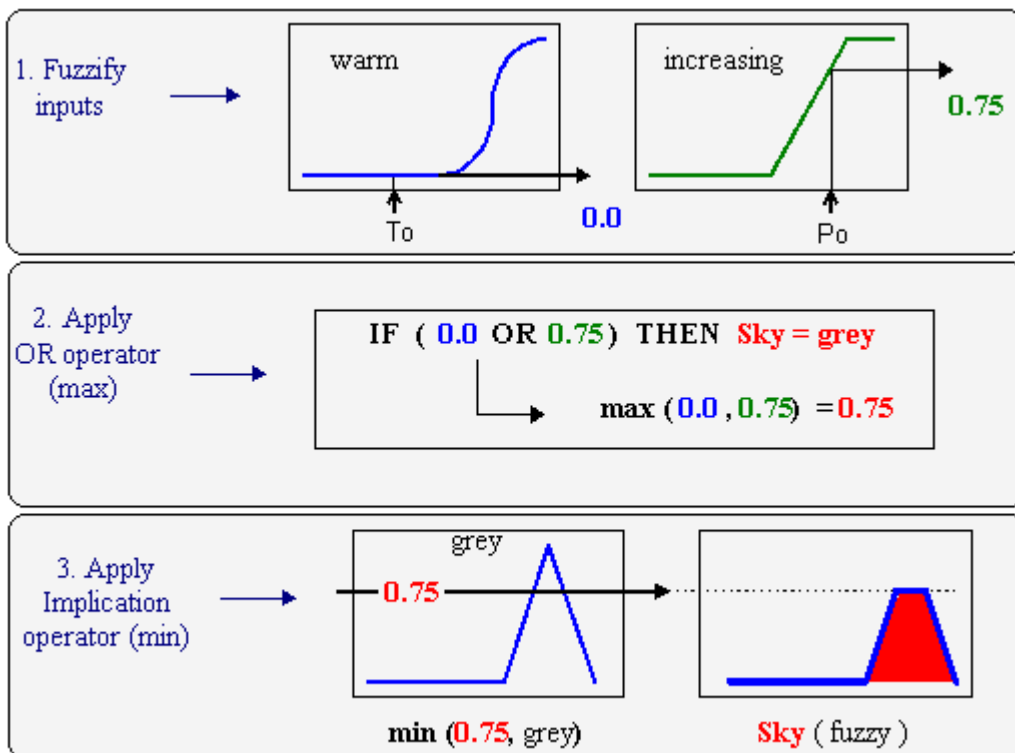


Figure 1.11: Fuzzify input, apply operator and apply implication operator

Then the rules must be combined in some manner in order to make a decision. **Aggregation** is the process by which the fuzzy sets that represent the outputs of each rule are combined into a single fuzzy set. Aggregation only occurs once for each output variable, just prior to the fifth and final step, **defuzzification**. The input of the aggregation process is the list of truncated output functions returned by the implication process for each rule. The output of the aggregation process is one fuzzy set for each output variable [5].

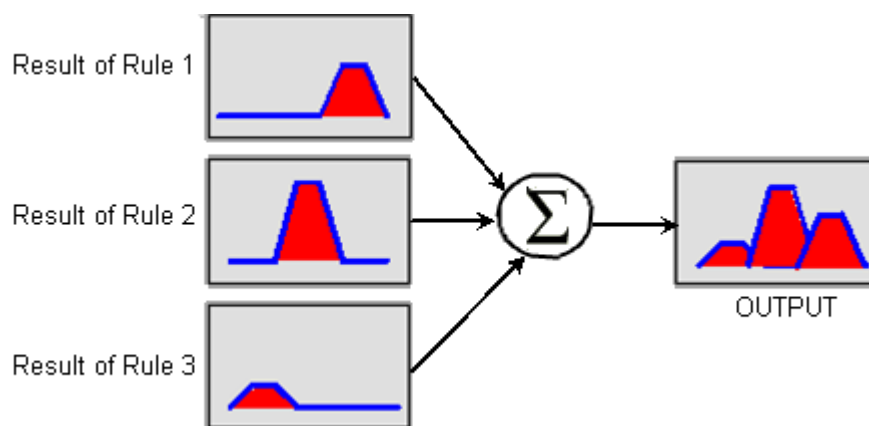


Figure 1.12 Result of aggregation

Defuzzification

Defuzzification is the process of transforming a fuzzy output of a fuzzy inference system into a crisp output. The input for the defuzzification process is a fuzzy set (the aggregate output fuzzy set) and the output is a single crisp number. As much as fuzziness helps the rule evaluation during the intermediate steps, the final desired output for each variable is generally a single number [5].

There are different methods in order to obtain a single number as output result. Since there is not any procedural method to chose which method is more suitable, most common used are: *Smallest of maximum (SOM)*, *mean of maximum (MOM)*, *largest of maximum (LOM)*, *Bisecter of area (BOA)* and *centroid of area (COA)*. Figure 1.13 is an example of the defuzzification process.

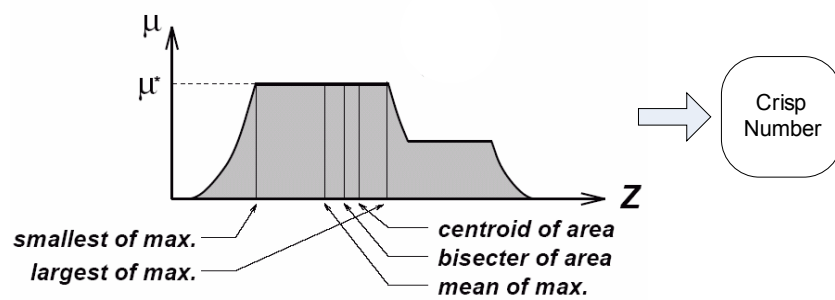
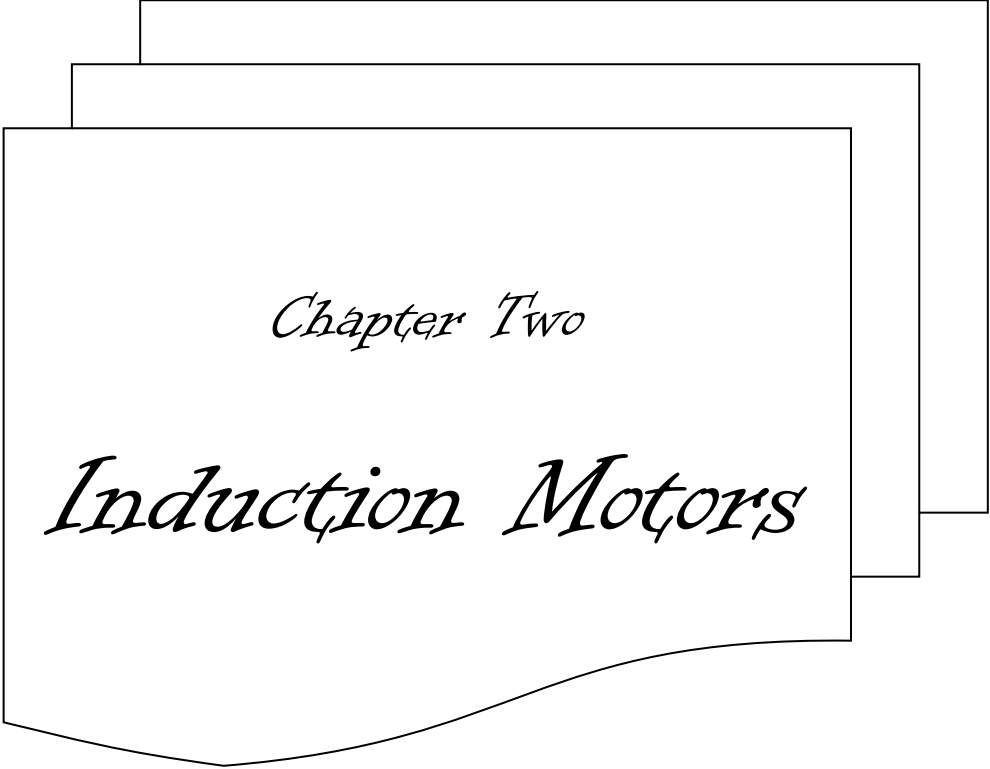


Figure 1.13: The Defuzzification process.



Chapter Two

Induction Motors

INDUCTION MOTORS

Induction Motor Construction and Operation

What makes the induction motors are the most important electrical motors are lot of advantages such as: its simple design, reliable operation, the simplicity of speed control and the high efficiency. Induction motor main components are the *stator* and the *rotor*. The rotor is constructed of a number of conducting bars running parallel to the axis of the motor and two conducting rings on the ends. The assembly –Figure 2.1-b - resembles a squirrel cage, thus this type of motor is often called a *squirrel-cage* motor. The stator –which is the outer body of the motor -contains a pattern of copper or aluminum coils arranged in windings – Figure 2.1-a -. As alternating current (AC) is passed through the stator windings, a rotating magnetic field is formed near the stator; the speed of rotation is called *synchronous speed*⁵ (n_{sync}). This induces a current in the rotor, creating its own magnetic field. The interaction of these fields produces a torque on the rotor. The speed of the rotor which is called *mechanical speed* (n_m) will be slightly less than the synchronous speed; the difference is called the *slip speed* (n_{slip}). Also *slip* is defined as equation 2.1.

⁵ Synchronous speed of three phase induction motor is determined by two factors: number of poles and the AC supply frequency.

$$s = \frac{\omega_{sync} - \omega_m}{\omega_{sync}} (\times 100\%) \quad (2.1)$$

Note that there is no direct electrical connection between the stator and the rotor. Figure 2.2 shows a typical induction motor. For that reason, the induction machine is called *rotating transformer*, like transformer the primary (stator) induce a voltage in the secondary (rotor), but unlike the transformer, the secondary frequency is not necessary the same as the primary frequency [6].

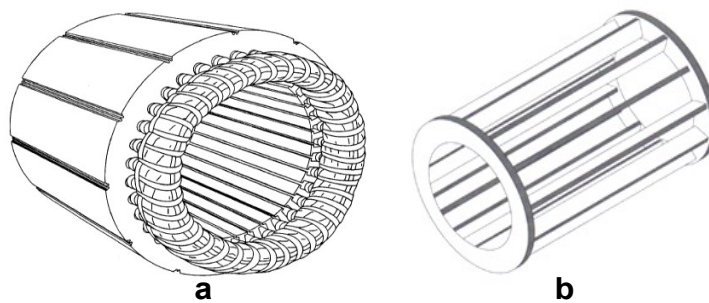


Figure 2.14: (a) A typical structure of stator core and (b) the rotor in squirrel-cage induction motor.



Figure 2.15: A squirrel cage induction motor.

One of the main characteristics of induction motor is the efficiency of an induction motor is inversely proportional to slip. A motor with a lower value of

slip will be more efficient than a motor with a higher slip because of the increased losses in the rotor of the latter. The efficiency of three phase induction motors varies with type, size and load. It ranges from 85% to 99%.

Induction machine control

The controllers required for induction motor drives can be divided into two major types: a conventional low cost volts per hertz v/f controller and torque controller [13]-[15]. In v/f control, the magnitudes of the voltage and frequency are kept in proportion. The performance of the v/f control is not satisfactory, because the rate of change of voltage and frequency has to be low. A sudden acceleration or deceleration of the voltage and frequency can cause a transient change in the current, which can result in drastic problems. Figure 2.3 shows a schematic of a scalar control method.

Some efforts were made to improve v/f control performance, but none of these improvements could yield a v/f torque controlled drive systems and this made DC motors a prominent choice for variable speed applications. This began to change when the theory of field orientation was introduced by Hasse and Blaschke. Field orientation control is considerably more complicated than DC motor control. The most popular class of the successful controllers uses the vector control technique because it controls both the amplitude and phase of AC

excitation. This technique results in an orthogonal spatial orientation of the electromagnetic field and torque, commonly known as Field Oriented Control.

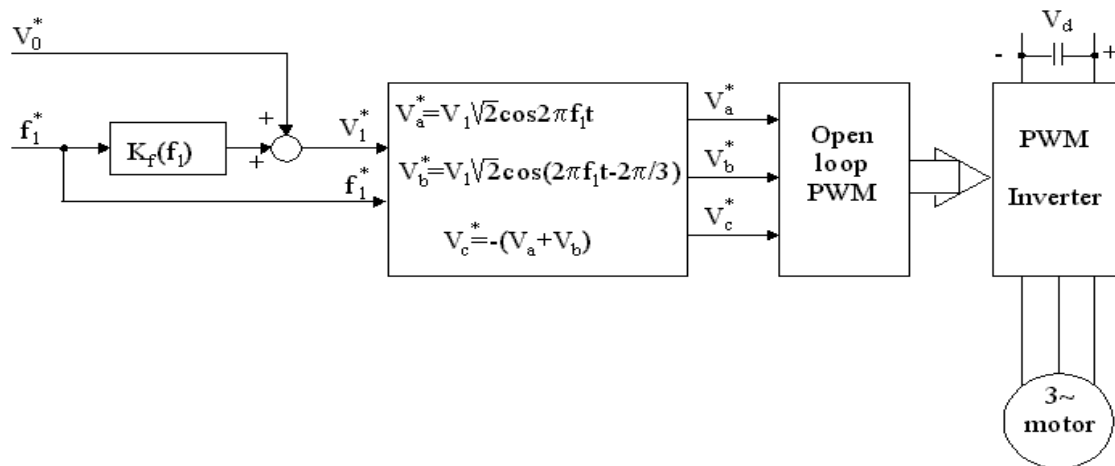


Figure 2.16: V/f open loop (scalar) control

Decoupling idea using separately excited DC Motors

The separately excited DC motor is a motor whose field circuit is supplied from a separate constant voltage power supply [6]. Its equivalent circuit is shown in Figure 2.4-a. An ideal model of a separately excited motor is shown in Figures 2.4-b and 2.4-c where there are two electrically separated and magnetically decoupled windings in the stator and rotor [7]. This means that the magnetomotive forces established by the currents in these windings are also orthogonal. Equations 2.2-4 describe the mathematical model of this system. And Equation 2.5 represents the torque equation. This means that the flux is dependent on the

field winding current. If the flux is fixed then the torque is varied directly by the armature current. It is for this reason that DC machines are said to have decoupled or independent control over torque and flux.

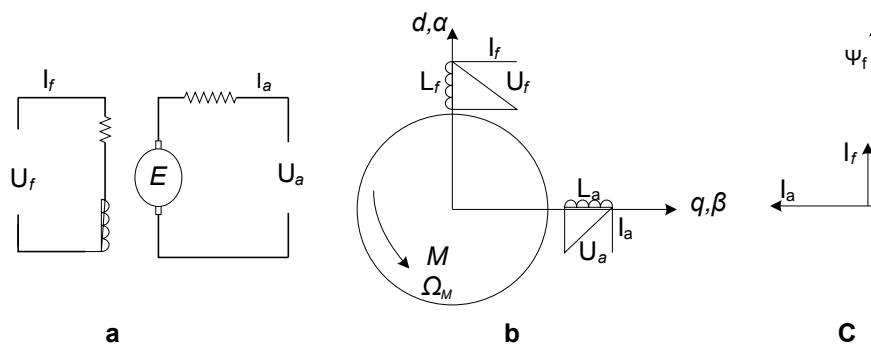


Figure 2.17: (a) Equivalent circuit of separately excited DC motor, (b) layout of two-winding model and (c) vector diagram.

$$T_a \frac{di_a}{dt} = -i_a + K_a (u_a - \psi_f \omega_m) \quad (2.2)$$

$$T_{fN} \frac{d\psi_f}{dt} = -F(\psi_f) + u_f \quad (2.3)$$

$$T_M \frac{d\omega_m}{dt} = \psi_f i_a - m_L \quad (2.4)$$

$$T_{em} = k \psi_f i_a \quad (2.5)$$

Where:

T_a : The electromagnetic time constant of the armature circuit,

T_{IN} : The rated electromagnetic time constant of the excitation circuit,

T_M : The mechanical constant,

i_a : The armature current and

ψ_f : The flux induced by I_f .

Induction Motor Equivalent Circuit

The steady state behavior of an induction motor can be predicted with good accuracy by the use of the equivalent circuit of figure 2.5 in which R_s is the resistance of the stator phase winding, L_o is the magnetizing inductance carrying the magnetizing component I_m of the stator phase current I_s , L_{ls} and L_{lr} are stator and rotor leakage inductance respectively, R_R is the rotor winding resistance, and the rotor resistance and load is represented by R_R/S , where S is the slip. The complete mathematical model of the induction motor is expressed by equations 2.6-2.9.

The equivalent circuit allows calculation of the basic quantities of a given motor. Such as stator current, power factor and developed torque. When the motor operates in steady state, constant speed and fixed balanced sinusoidal supply voltage, the electrical quantities are represented as phasors and the developed

torque is calculated as the output power divided by the angular velocity of the rotor.

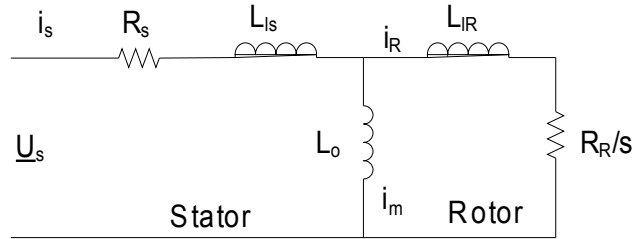


Figure 2.18: The equivalent circuit of induction motor.

The equivalent circuit is therefore insufficient for analysis of transient conditions. The dynamic model is based on the concept of vector quantities of AC machine. The motor can be represented either of the form of an equivalent circuit or a set of equations, this procedure allows analysis of the dynamics of the motor which can then be supplied with any kind of voltage, not necessarily a sinusoidal one.

$$R_S \underline{i}_s + L_S \frac{d \underline{i}_s}{dt} + L_o \frac{d}{dt} (\underline{i}_R e^{j\varepsilon}) = \underline{u}_s \quad (2.6)$$

$$R_R \underline{i}_R + L_R \frac{d \underline{i}_R}{dt} + L_o \frac{d}{dt} (\underline{i}_R e^{-j\varepsilon}) = 0 \quad (2.7)$$

$$J \frac{d \omega}{dt} = \frac{2}{3} \frac{|\psi_R|}{R_R} \omega_{sl} - m_L \quad (2.8)$$

$$\frac{d \varepsilon}{dt} = \omega \quad (2.9)$$

Where:

ϵ is the rotor angle, J is the inertia and m_L is the mechanical load.

Chapter Three

*Field Orientation
Control*

FIELD ORIENTATION CONTROL

What is Field Orientation Control (FOC)

Field orientation is a method of control using moving coordinates (Frames of reference determined by the angular position of flux waves), this application requires extensive on line processing that can only be achieved economically by using microprocessors or special digital hardware.

AC machines can not be controlled in a simple manner as the separately excited DC machine; in which, the magnetic flux and torque are decoupled. So, it is easy to design control drives with high dynamic performance, field weakening and torque limit as described in section 2.3. In the AC machines, the problem is in the dynamic interactions that are more complex than those in the DC machine are. The flux and Magneto-motive force (MMF) distribution are no longer stationary but moving with different velocities, forming varying angles, which depend on the dynamic state of the machine.

Using space vector for modeling AC machines led to control schemes functioning in moving coordinates, defined by the flux waves or rotor position. The subsequent development of field or rotor oriented control methods made it

possible to transform the complex structure of an AC machine into that of an equivalent DC machines so that the design of high performance AC drives became a forward task.

In general, an electrical motor can be thought of as a controlled source of torque. Accurate control of instantaneous torque produced by a motor is required in high performance control system, e.g., those used for position control. The torque developed in the motor is a result of the interaction between current in the armature winding and the magnetic field produced in the field system of the motor. The field should be maintained at a certain optimal level, sufficiently high to yield a high torque per unit ampere, but not too high to result in excessive saturation of the magnetic circuit of the motor. With fixed field, the torque is proportional to the armature current.

In the most commonly used, squirrel cage motors, only the stator current can be directly controlled, since the rotor winding is not accessible. Optimal torque production conditions are not inherent due to the absence of a fixed physical disposition between the stator and rotor field. And the torque equation is non-linear. In effect, independent and efficient control of the field and torque is not as simple and straightforward as the DC motors [8].

Space Vector Definition and Projection

Space vector notation allows the transformation of the natural instantaneous values of a three-phase system onto a complex plane located in the cross section of the motor. In this plane, the space phasor rotate with an angular

speed equal to the angular frequency of the three-phase supply system. A space phasor rotating with the same angular speed, for example, can describe the rotating magnetic field. Moreover, in the special case of the steady state, where the supply voltage is sinusoidal and symmetric, and the space phasor become equal to three-phase voltage phasors, allowing the analysis in terms of complex algebra. It is shown in Figure 3.1 the equivalent schematic for this new model [7] [9].

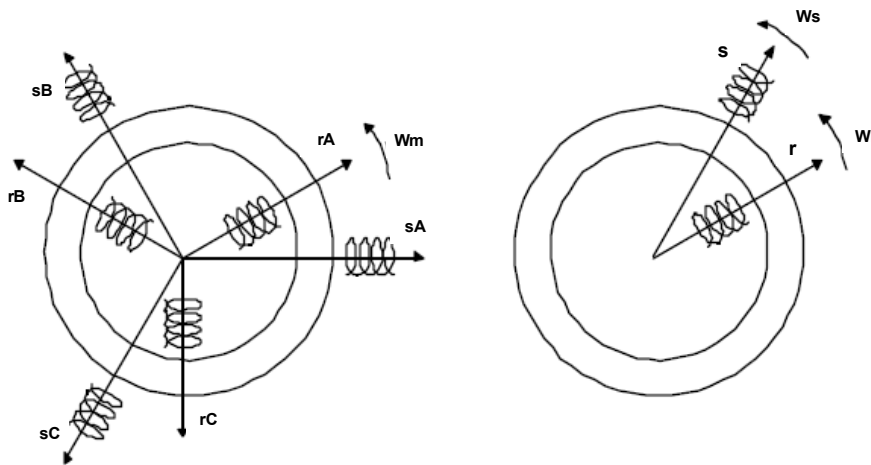


Figure 3.19: The schematic of rotating magnetic fields with rotor speed

With regard to the currents –the same could be done for any other quantity like voltages or fluxes–, the space vector can be defined as follows. Assuming the instantaneous currents in the stator phases are i_a , i_b , and i_c , then the complex phasor current is defined as in equation 3.1, and Figure 3.2 shows the space vector of the stator current and its components in three phase system axes (a, b, c). Notes

that $\alpha = e^{(j*2\pi/3)}$ and $\alpha^2 = e^{(j*4\pi/3)}$ and the factor C usually takes two values⁶: $2/3$ or $\sqrt{2/3}$. For more details see appendix A.2.

$$\underline{i}_s = C (i_a + \alpha i_b + \alpha^2 i_c) \quad (3.1)$$

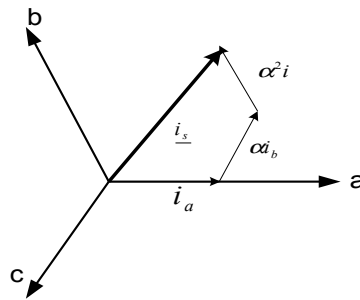


Figure 3.20: Stator current space vector and its components in (a,b,c).

In order to transform \underline{i}_s into a two time invariant coordinate system, two steps need to be done:

- **Clarke transformation: The (a,b,c) \rightarrow (α , β) projection**

The space vector can be reported in another reference frame with only two orthogonal axis called (α , β) as shown in Figure 3.3-a. The projection that modifies the three phase system into the α, β two dimension orthogonal system is

⁶ The factor $2/3$ makes the amplitude of any space phasor, which represents a three phase balanced system, equal to the amplitudes of one phase of the three-phase system. The factor $\sqrt{2/3}$ may also be used to define the power invariance of a three-phase system with its equivalent two-phase system

presented by equation 3.2 and equation 3.3 shows the inverse of Clarke transformation.

$$\begin{bmatrix} i_{s\alpha} \\ i_{s\beta} \end{bmatrix} = \begin{bmatrix} 1 & 0 \\ \frac{1}{\sqrt{3}} & \frac{2}{\sqrt{3}} \end{bmatrix} \begin{bmatrix} i_{sa} \\ i_{sb} \end{bmatrix} \quad (3.2)$$

$$\begin{bmatrix} i_{sa} \\ i_{sb} \\ i_{sc} \end{bmatrix} = \begin{bmatrix} 1 & 0 \\ -\frac{1}{2} & -\frac{\sqrt{3}}{2} \\ -\frac{1}{2} & \frac{\sqrt{3}}{2} \end{bmatrix} \begin{bmatrix} i_{s\alpha} \\ i_{s\beta} \end{bmatrix} \quad (3.3)$$

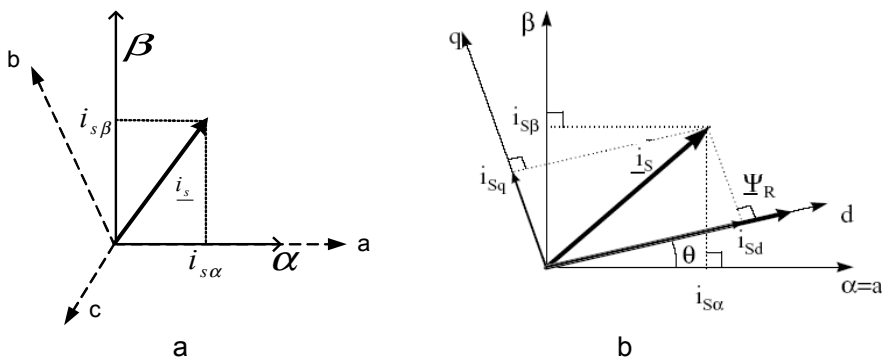


Figure 3.21: (a) Stator current space vector and its components in (α, β) and (b) Transformation from (α, β) to (d, q)

- **Park transformation: The $(\alpha, \beta) \rightarrow (d,q)$ projection**

This is the most important transformation in the FOC. In fact, this projection modifies a two phase orthogonal system (α, β) in the (d,q) rotating reference frame. If d axis is aligned with the rotor flux, Figure 3.3-b shows, for the current vector, the relationship from the two reference frame. And the flux and torque components of the current vector are determined by equations 3.4. These components depend on the current vector (α, β) components and on the rotor flux position; if the right rotor flux position is known then, by this projection, the d,q component becomes a constant. Equation 3.5 shows the inverse of Park transformation.

$$\begin{bmatrix} i_{sd} \\ i_{sq} \end{bmatrix} = \begin{bmatrix} \cos(\theta) & \sin(\theta) \\ -\sin(\theta) & \cos(\theta) \end{bmatrix} \begin{bmatrix} i_{s\alpha} \\ i_{s\beta} \end{bmatrix} \quad (3.4)$$

$$\begin{bmatrix} i_{s\alpha} \\ i_{s\beta} \end{bmatrix} = \begin{bmatrix} \cos(\theta) & -\sin(\theta) \\ \sin(\theta) & \cos(\theta) \end{bmatrix} \begin{bmatrix} i_{sd} \\ i_{sq} \end{bmatrix} \quad (3.5)$$

Application of FOC on Induction motor

Main principle: Decoupling

A general theory of AC motor control formulated by Blaschke 1972 [11] was applicable to any type of inverter and AC machine. It dealt with the interaction of flux and MMF vectors and demonstrated that moving reference frames tied to the rotor to a probably chosen flux wave presented a general

foundation for the control design because they permitted decouple of the flux and armature axes which had proved so valuable with DC machine.

Clearly, the dynamic interaction are greatly simplified if the machine is fed from current sources, as released by fast acting by current control loop, because this in fact removes the stator voltage. Equation 3.6 represents two scalar differential equations from the machine levels. This calls for a power converter of adequate control bandwidth, such as a PWM converter or a cyclo-converter [7].

$$R_S i_S(t) + \frac{d\psi_S}{dt} = R_S i_S(t) + L_S \frac{di_S}{dt} + M \frac{d}{dt} (i_R(t) e^{j\epsilon}) = u_S \quad (3.6)$$

Where

$$L_S i_S + M i_R(t) e^{j\epsilon} = \psi_S \quad (3.7)$$

The rotor voltage equation 3.8, assuming equal number of turns and the usual definitions of leakage factors, may be written as:

$$R_R i_R(t) + \frac{d\psi_R}{dt} = R_R i_R(t) + L_R \frac{di_R}{dt} + M \frac{d}{dt} (i_S(t) e^{-j\epsilon}) = u_R \quad (3.8)$$

Where:

$$L_R = \frac{1 + \sigma_R}{L_o}$$

As the rotor current vector can not be measured a cage motor it's eliminated by a stator based magnetizing current vector representing rotor flux.

$$\begin{aligned}\underline{i}_{mR} &= \underline{\psi}_R \frac{e^{j\varepsilon}}{L_o} = i_{mR} e^{j\rho} \\ &= \underline{i}_S + (1 + \sigma_R) \underline{i}_R e^{j\varepsilon}\end{aligned}\quad (3.9)$$

This results in

$$T_R \frac{d\underline{i}_{mR}}{dt} + (1 - j\omega T_R) \underline{i}_{mR} = \underline{i}_S \quad (3.10)$$

Where:

$$T_R = \frac{L_R}{R_R}$$

Splitting this equation in real and imaginary parts describing the magnitude and instantaneous angular velocity of the rotor flux wave gives equations 3.11 and 3.12.

$$T_R \frac{di_{mR}}{dt} + i_{mR} = \operatorname{Re}\left(\underline{i}_S e^{-j\rho}\right) = i_{sd} \quad (3.11)$$

$$\frac{d\rho}{dt} = \omega_{mR} = \frac{\omega + \operatorname{Im}\left(\underline{i}_S e^{-j\rho}\right)}{T_R i_{mR}} = \omega + \frac{i_{sq}}{T_R i_{mR}} \quad (3.12)$$

$\underline{i}_S e^{-j\rho}$ is the stator current vector as viewed by an observer moving with the rotor flux or, briefly, the field oriented stator current vector; i_{sd} and i_{sq} are its direct and quadrature current components, they are DC-quantities in steady state -equation 2.13-.

$$T(t) = \frac{2}{3} M \operatorname{Im}\left[\underline{i}_S \left(\underline{i}_R e^{j\varepsilon}\right)^*\right] \quad (3.13)$$

Correspondingly, the equation 3.13 for the instantaneous torque becomes equation (3.14), With $M=L_o$,

$$\begin{aligned}
 T(t) &= \frac{2}{3} \frac{L_o}{1 + \sigma_R} \text{Im} \left[\underline{i_S} \underline{i_{mR}}^* \right] \\
 &= \frac{2}{3} \frac{L_o}{1 + \sigma_R} \underline{i_{Sq}} \underline{i_{mR}} \\
 &= K \underline{i_{Sq}} \underline{i_{mR}} \tag{3.14}
 \end{aligned}$$

Which indicates that decoupled control of flux and torque of the AC machine is possible through the two components of the field oriented stator current vector. The magnitude of the flux is controlled by the direct component i_{sd} through a large field lag T_R and the torque by the quadrature component i_{sq} of the field oriented stator current vector. This is analogous to a DC machine, with T_R corresponding to the lag of the field winding.

The linearization and decoupling of the control plant by coordinate transformation and an inverse model are the main features of the field oriented control method. And since field orientation uses rotor flux as a reference, the magnitude and angular position of rotor flux wave are the most important variables and must be determined. Figure 3.4 represents the angular relations of current vector.

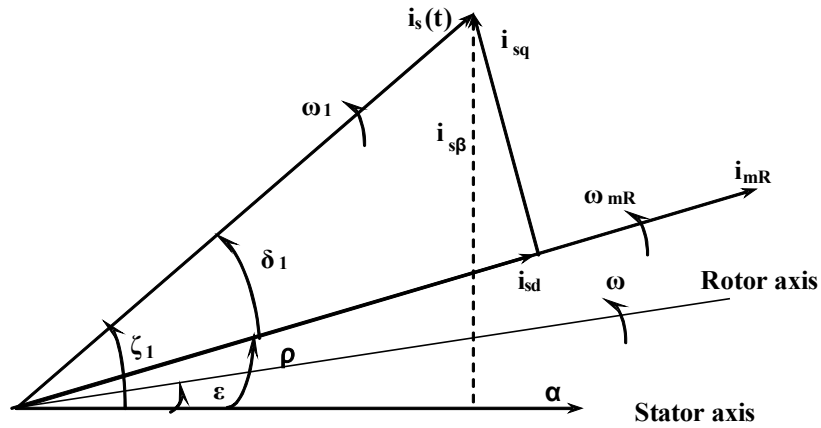


Figure 3.22: Angular relations of current vectors.

Mathematical model of Induction motor

The squirrel cage type of induction motor as differential equations for the stator current and rotor flux vector components presented in coordinate system XY rotating with arbitrary angular speed is shown in equations 3.15-3.19 [12].

$$\frac{di_{sx}}{d\tau} = -\frac{R_s L_r^2 + R_r L_m^2}{L_r w} i_{sx} + \frac{R_r L_m}{L_r w} \psi_{rx} + \omega_s i_{sy} + \omega_r \frac{L_m}{w} \psi_{ry} + \frac{L_r}{w} u_{sx} \quad (3.15)$$

$$\frac{di_{sy}}{d\tau} = -\frac{R_s L_r^2 + R_r L_m^2}{L_r w} i_{sy} + \frac{R_r L_m}{L_r w} \psi_{ry} - \omega_s i_{sx} - \omega_r \frac{L_m}{w} \psi_{rx} + \frac{L_r}{w} u_{sy} \quad (3.16)$$

$$\frac{d\psi_{rx}}{d\tau} = -\frac{R_r}{L_r} \psi_{rx} + (\omega_s - \omega_r) \psi_{ry} + R_r \frac{L_m}{L_r} i_{sx} \quad (3.17)$$

$$\frac{d\psi_{ry}}{d\tau} = -\frac{R_r}{L_r}\psi_{ry} - (\omega_s - \omega_r)\psi_{rx} + R_r \frac{L_m}{L_r}i_{sy} \quad (3.18)$$

$$\frac{d\omega_r}{d\tau} = \frac{L_m}{L_r J}(\psi_{rx}i_{sy} - \psi_{ry}i_{sx}) - \frac{1}{J}T_o \quad (3.19)$$

Where ψ_{rx} , ψ_{ry} , i_{sx} , i_{sy} are the rotor flux and stator current vectors in coordinate system XY rotating with arbitrary speed, ω_r is the angular speed of the rotor shaft, R_r , R_s , L_r , L_s are rotor and stator resistance and inductances respectively, L_m is a mutual inductance, J is the inertia, T_o is the load torque.

This model is higher order cross-sectional dynamic system with parameters that change with operating point. Therefore, this system could not be directly used in control synthesis and the idea of FOC should be applied in control process.

The basic scheme for the FOC

Figure 3.5 summarizes the basic scheme of torque control with FOC [10]: Two motor phase currents are measured. These measurements feed the Clarke transformation module. The outputs of this projection are designated $i_{s\alpha}$ and $i_{s\beta}$. These two components of the current are the inputs of the Park transformation that gives the current in the d,q rotating reference frame. The i_{sd} and i_{sq} components are compared to the references i_{sdref} (the flux reference) and i_{sqref} (the torque

reference). The outputs of the current regulators are v_{Sdref} and v_{Sqref} , they are applied to the inverse Park transformation. The outputs of this projection are v_{Saref} and v_{Sbref} which are the components of the stator vector voltage in the α,β stationary orthogonal reference frame. These are the inputs of the Pulse Width Modulator (PWM). The outputs of this block are the signals that drive the inverter. Note that both Park and inverse Park transformations need the rotor flux position θ . Obtaining this rotor flux position depends on the AC machine type (synchronous or asynchronous machine) and also depends on the control technique used (*see section 3.3.4*).

Knowledge of the rotor flux angle is essential for accurately applying the Clarke and Park transforms. If this angle is incorrect the flux and torque producing components of the stator current are not decoupled and true field oriented control is not achieved. Induction motors are asynchronous machines so the flux speed is not equal to the mechanical speed of the rotor due to the effect of slip.

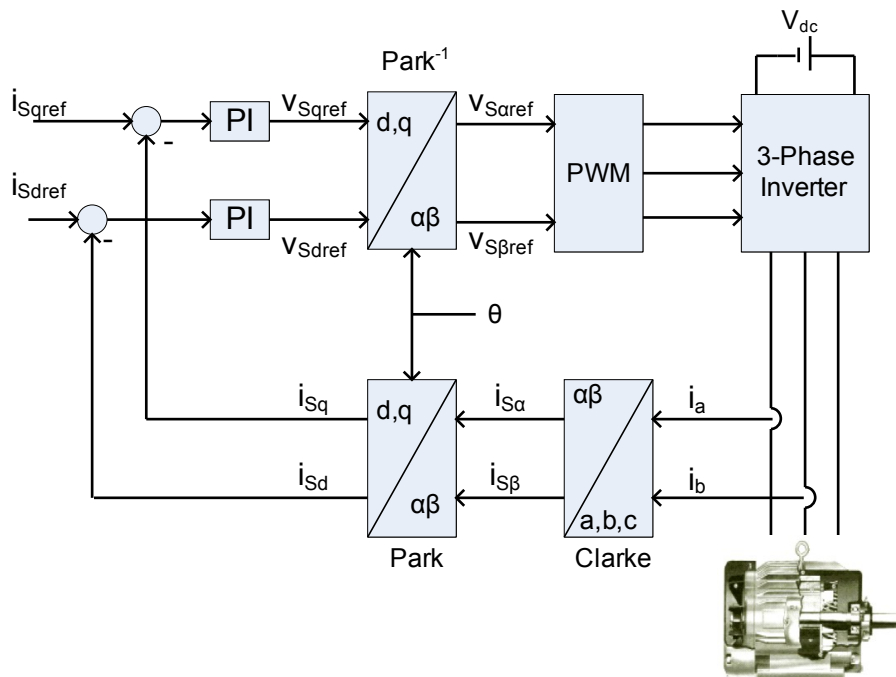


Figure 3.23: Basic scheme of FOC for AC-motor

Direct and Indirect Field Orientation Control

In Direct Field-Oriented Control (DFOC) strategy, both the instantaneous magnitude and position of the rotor flux are supposed to be available and known with high precision; i.e.: directly measured or estimated using for example a nonlinear state observer (*see chapter 5*). On the other hand, the position of the rotor flux space vector is obtained analytically in Indirect Field-Oriented Control (IFOC) strategy. IFOC is much more easier to be implemented than the DFOC, but the slip-speed calculation involves the rotor time-constant which is known as frequency and temperature dependent. The variations of this parameter should

then be tracked online in order to feedback its actual value to the speed controller and to the slip-speed calculation module [29].

In DFOC the flux –classically- may be measured by using a flux sensing element, an advantage of this method is that additional required motor parameters are not significantly affected by changes in temperature and flux level. However, the disadvantage is that a flux sensor is expensive and needs special installation and maintenance. To avoid using sensors, rotor flux can be estimated from terminal quantities (stator voltages and currents). This technique requires the knowledge of the stator resistance along with the stator, rotor leakage inductances and magnetizing inductance [30]. The flux angle could be found easily as shown in figure 3.6.

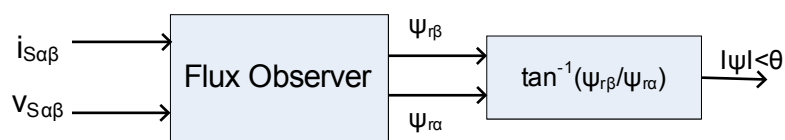
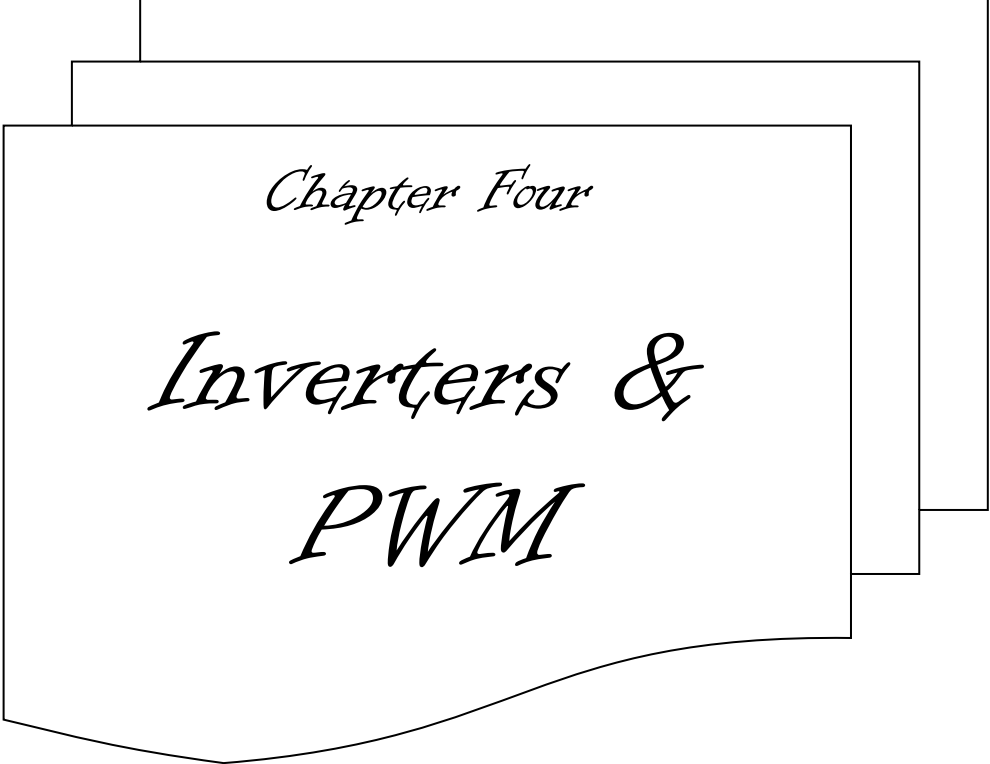


Figure 3.24: Calculation of rotor flux and rotor flux angle in Direct field Orientation.

In IFO, the slip-angle is computed and added to the rotor speed to find the synchronous speed. Therefore, one must calculate the slip-angle and estimate the rotor angle, more details are in chapter 6.



Chapter Four

*Inverters &
PWM*

INVERTERS AND PWM

Inverters

Three-phase inverter supplying voltage and current of adjustable frequency and magnitude to the stator is an important element of adjustable-speed drive system employing induction motor.

Inverters are dc-ac power converters and based on semiconductors power switches. Depending on the type of the dc power supplying, the inverter can be classified as voltage source inverter (VSI) or current source inverter (CSI), see figure 4.1. In practice, the dc is usually a rectifier typically of three-phase bridge configuration with the dc link connected between the rectifier and the inverter. The dc link is a simple capacitive or inductive or inductive-capacitive low pass filter [6].

Since neither the voltage through the capacitor nor the current through the inductor can change instantaneously, a capacitor output dc link is used for a VSI and an inductive output link is employed in CSI. In battery powered drive system such as for electric vehicles, the rectifier is, obviously not needed. However, the dc link is still used as an interface either to impose the current source input to a

CSI, or to protect the battery from the high frequency component of the supply current of VSI.

VSIs can be either voltage or current controlled [7]. In a voltage-controlled inverter, it is the frequency and magnitude of the fundamental of the output voltage that adjusted. Feed forward voltage control employed, since the inverter voltage depends only on the supply voltage and the states of the inverter switches, and therefore accurately predictable. Current-controlled VSIs require sensors of the output currents, which provide the necessary control feedback. Voltage-controlled VSIs are mostly used in scalar speed-control system based on the v/f principle.

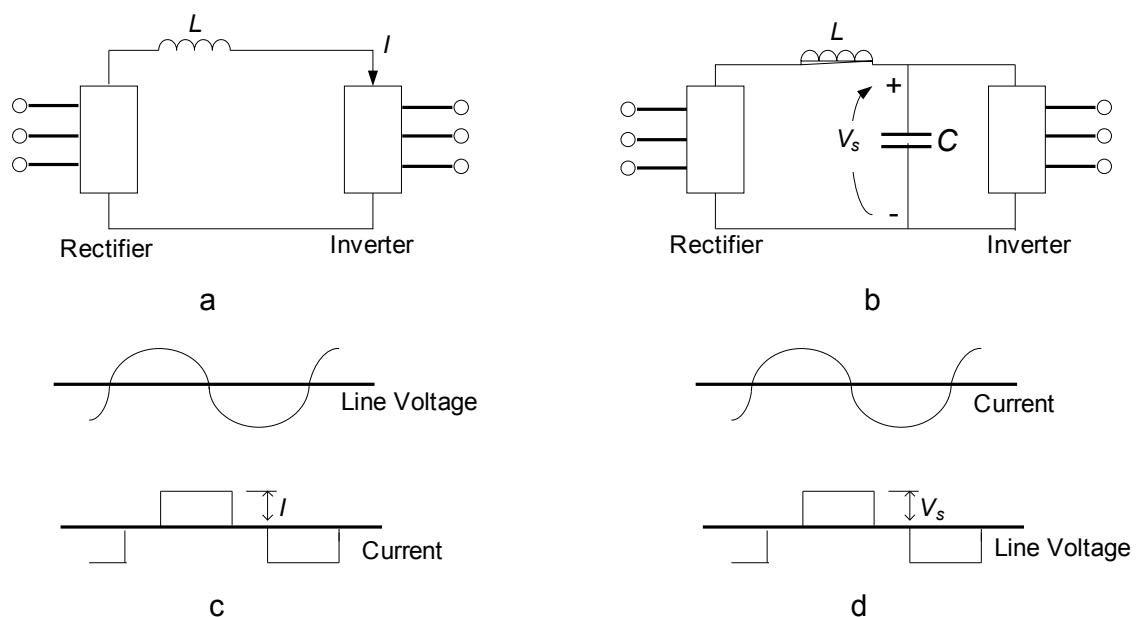


Figure 4.25: (a) CSI, (b) VSI, (c) waveform of current and voltage of CSI and (d) waveform of current and voltage of VSI

The type of semiconductor power switch used in an inverter depends on the volt-ampere rating of the inverter, as well as on other operating and economic

considerations, such as switching frequency or cost of the system. Taking into account the transient- and steady-state requirements.

Types of Switching Devices used in Inverters

The most known switches are mentioned below with some of the main features of them. Moreover, because there is considerable overlap between them, it is not possible to dogmatic and specify with device is best [14] [16] [17] [28], figure 4.2 shows the symbols of the mentioned below devices, and table 4.1 supplies a brief comparison between them:

- ◆ ***Bipolar Junction Transistor (BJT)***: historically BJT was the first to be used in power switching, they mainly used in applications ranging up to a few kilo-Watt (kW) and several hundred volts. The advantage of BJT is the power dissipation is small in comparison with the load power. On the other hand, the complexity and the cost of the bias-drive circuitry is the main disadvantage of BJT. That is because the power required in the biasing signal (base-emitter circuit) is tiny in comparison with the load power but it is not insignificant and in the largest power transistors can amount to several tens of watts.
- ◆ ***Metal Oxide Semiconductor Field Effect Transistor (MOSFET)***: Since 1980s the power MOSFET has gradually superseded BJT in inverters for drives. Its most principal advantage is that it is a Voltage-controlled device which requires negligible power to hold it in the “on” state. The gate drive circuitry is thus less complex and costly than the base drive

circuitry of an equivalent bipolar device. The disadvantage of MOSFET is that in the 'on' state the effective resistance of the drain-source is higher than an equivalent bipolar device so the power dissipation is higher and the device is rather less efficient as a power switch. MOSFETs are used in low and medium power inverters up to a few kW with voltages generally not exceeding 700 V.

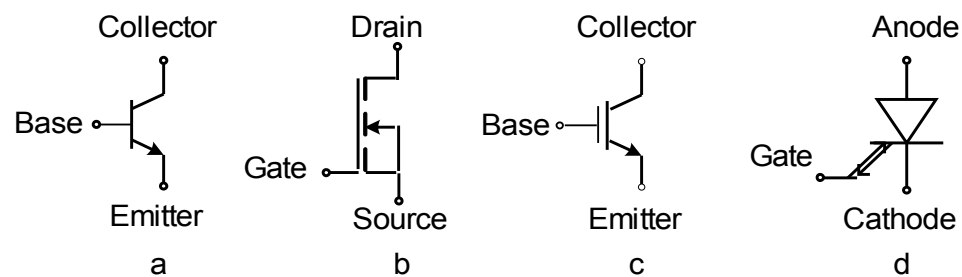


Figure 4.26: Symbols of different types of switches used in inverters, (a) BJT, (b) MOSFET (c) IGBT and (d) GTO.

- ◆ **Insulated Gate Bipolar Transistor (IGBT):** The IGBT is a hybrid device which combines the best feature of the MOSFET (i.e. ease of gate turn-on and turn-off from low-power logic circuits) and BJT (relatively low power dissipation in the main collector-emitter circuit). These obvious advantages give the IGBT the edge over the MOSFET and BJT, and account for the widespread take-up of the new technology amongst inverter drive manufacturers in the early 1990s. They particularly well suited to the medium power, medium voltage range (Up to several hundred kW). And it is the mostly used and developed type.

- ◆ **Gate Turn-Off Thyristor (GTO):** The GTO has a considerable higher voltage and current ratings (up to 5kV and 5kA) than the other three devices and is therefore used in high power inverters.

	<i>BJT</i>	<i>MOSFET</i>	<i>GTO</i>	<i>IGBT</i>
<i>Availability</i>	Late 70s	Early 80s	Mid 80s	Late 80s
<i>Voltage rating</i>	1kV	500V	5kV	3.3kV
<i>Current rating</i>	400A	200A	5kA	1.2kA
<i>Switching rate</i>	5kHz	1MHz	2kHz	100kHz
<i>Drive Circuit</i>	Difficult	Very simple	Very simple	Very simple
<i>State of technology</i>	Mature	Mature/Improve	Mature	Rapid improve

Table 4.1: Switches Comparisons

Quick comparison between VSI and CSI

In the current source inverter, a rectifier is connected to an inverter through a large series inductance L that the direct current is constrained to be constant. The output current waveform will be roughly a square wave. The line-to-line voltage will be approximately triangular. It is easy to limit over current conditions in this design, but the output voltage is swing widely in response to changes in load. CSI is mostly suitable for torque control technique, and it is suitable for high power range systems. Increasing the switching frequency of CSI gives a dynamic performance like the VSI [28].

In the voltage source inverter, a rectifier is connected to an inverter through a series inductor L and a parallel capacitor C that the voltage is constrained to be almost constant. The output line-to-line voltage waveform will be roughly a square wave and the output current flow will be approximately triangular. Here voltage variation is small but currents can vary widely with variation of the load. Figure 4.1 summarizes this section [6]. VSI is suitable for small and medium power ranges.

The frequency of both the currents and voltages of the inverters can be changed easily by changing the firing pulses on the gates of the switches.

Voltage Source Inverter

A diagram of the power circuit of three-phase VSI is shown in Figure 4.3 the circuit has a bridge topology with three branches (phases), Each consisting of two power switches and two freewheeling diodes. In the case illustrated, the inverter is supplied from an uncontrolled diode-based rectifier via a dc link that contains an LC filter as in the figure. Whilst this circuit represents a standard arrangement, it allows only positive power flow, i.e. from the supply system, typically a three-phase power line, to the load.

The capacitance C is chosen to be large enough to obtain adequately low voltage source impedance for the AC component in the DC circuit. The inductance L is presented to limit the capacitor charging current [7].

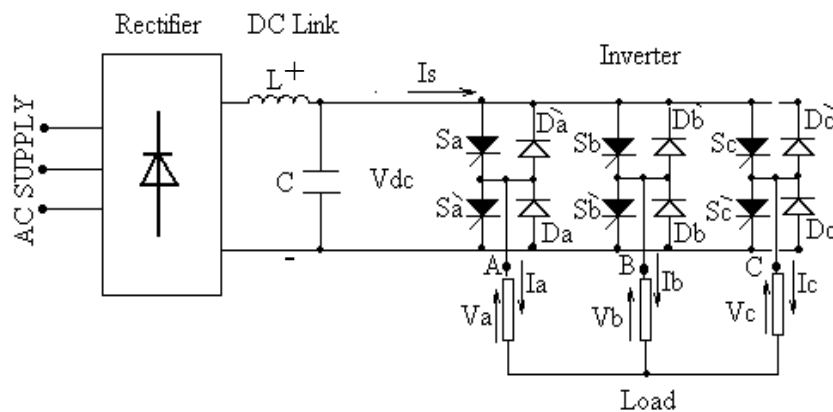


Figure 4.27: Circuit diagram of three phase VSI

Negative power flow, which occurs when the load feeds power back to the supply, is not possible the resulting negative dc component of the current in the dc link cannot pass the rectifier diodes. Therefore, in drive systems where the VSI-fed motor may operate as a generator, motor complex supply system must be used. These involve either a breaking resistance connected across the dc link (*represents a Dynamic breaking*) or replacement of the uncontrolled rectifier by a dual converter (*represents a regenerative breaking*). In the circuit shown in Figure 4.3, the power switches in a given branch must never both in the ON-state, since this constitute a short circuit.

Current Control of VSI Pulse Width Modulator

Introduction

Current controlled Pulse Width Modulation (PWM) inverter offer substantial advantages in eliminating stator dynamics in high performance AC

drives and are widely applied in such systems. A basic VSI-PWM system with current control is shown in figure 4.4. Presently, current controllers can be classified as hysteresis –which is the one implemented in this thesis-, ramp comparison or predictive controllers. Hysteresis controllers utilize some type of hysteresis in the comparison of the line currents to the current references [18][19].

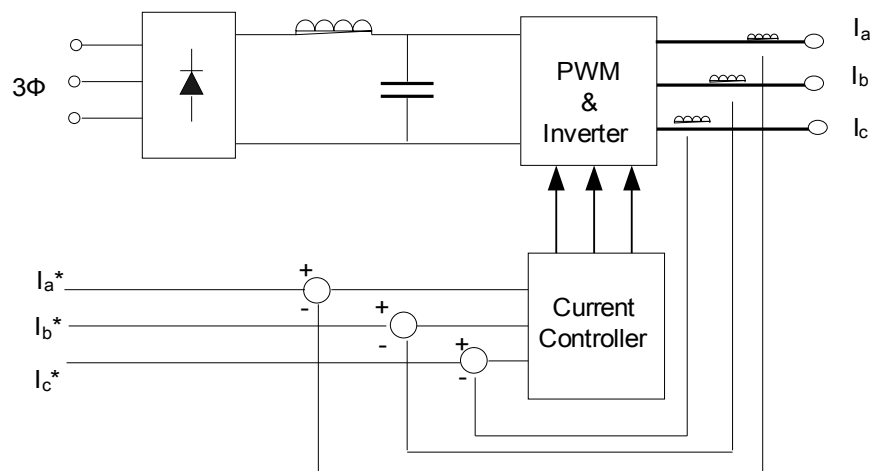


Figure 4.28: Basic diagram of PWM current controller

General properties

The concept of the voltage (current) vector is utilized because it is a very convenient representation of a set of three-phase voltages (or currents). As given in equation 3.1 which becomes as equation 4.1, where the actual voltages can be recovered from \underline{v} and the zero sequence component v_o using equation 4.2.

$$\underline{v} = \frac{2}{3}(i_a + \alpha i_b + \alpha^2 i_c) \quad (4.1)$$

$$\begin{aligned}
 v_a &= |v| \cos(\theta) + v_o \\
 v_b &= |v| \cos\left(\theta - \frac{2\pi}{3}\right) + v_o \\
 v_c &= |v| \cos\left(\theta + \frac{2\pi}{3}\right) + v_o
 \end{aligned} \tag{4.2}$$

Where θ is the angle between the voltage vector and the real axis.

Switching states

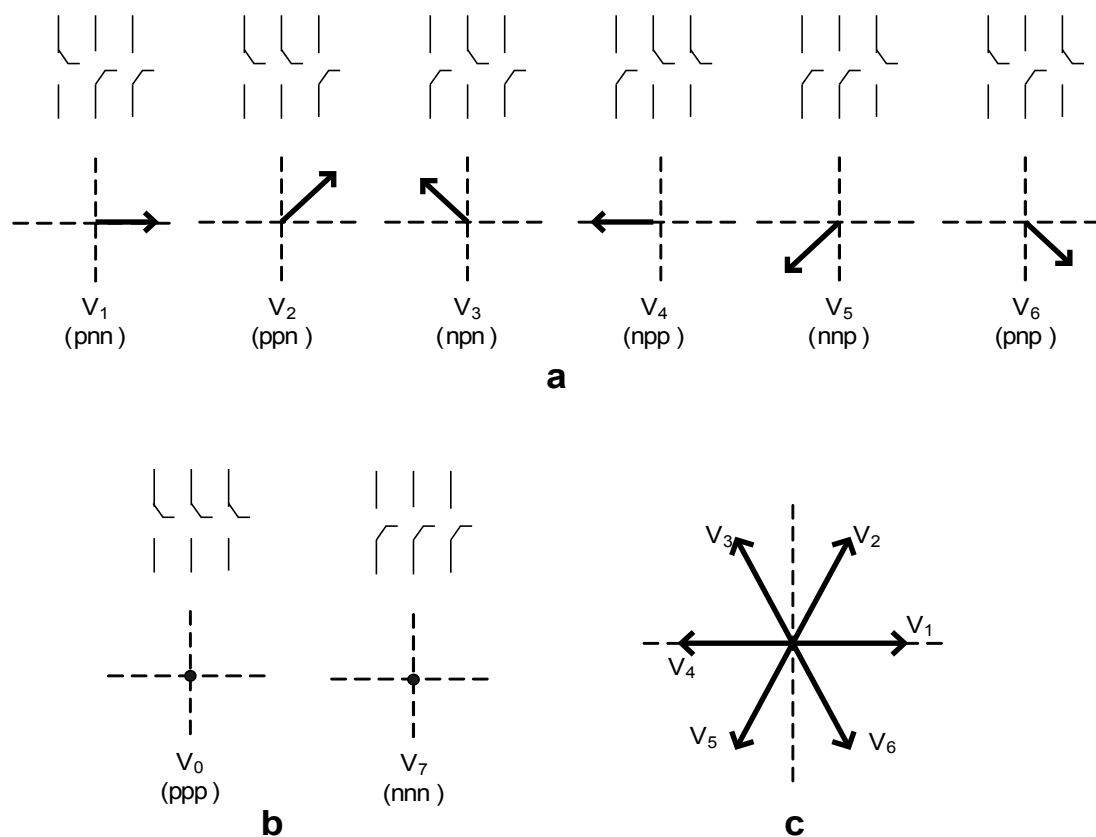


Figure 4.29: Eight switching state topology (a) The six nonzero voltage vectors, (b) the two zero voltage vectors and (c) nonzero voltages vectors associated with VSI inverter

A voltage source inverter can assume only eight distinct operational topologies. They are shown in Fig.4.5. Six out of these eight topologies produce a non-zero output voltage and are known as non-zero switching states and the

remaining two topologies produce zero output and are known as zero switching state.

Switching frequency

To determine the factors that influence the inverter switching frequency, let one phase of the load be described by equation 4.3.

$$v = Ri + Ldi / dt + e \quad (4.3)$$

Where:

- v Line to neutral load voltage,
- i Line current,
- e Counter EMF induced in the rotor,
- L Leakage inductance,
- R Stator resistor,

The time Δt in which the line current will increase by Δi can be found from equation 4.3, assuming that v and e do not change appreciably over the interval Δt and the stator resistance is negligible:

$$\Delta t = L \frac{\Delta i}{v - e} \quad (4.4)$$

This result shows that the inverter frequency is influenced by several factors: inductance and counter EMF of the load, DC bus voltage, and the current ripple [18]. The voltages v and e vary periodically. Therefore, the inverter switching frequency $1/\Delta t$ and the current ripple vary with the motor speed. The

current control loop should be designed in such a way that over the full range of motor operation the maximum switching frequency of the inverter power devices is not reached [7].

Hysteresis Controller: Three Independent Controllers

One version of hysteresis control –which is the widely used method because of its simplicity- uses three independent controllers, one for each phase. The control for one inverter leg is shown in figure 4.6. When the line current become grater (less) than the current reference by the hysteresis band the inverter leg is switched in the negative (positive) direction, which provide an instantaneous current limit within the hysteresis band. Therefore, the hysteresis band specifies the maximum current ripple assuming neither controller nor inverter delays (Figure 4.7).

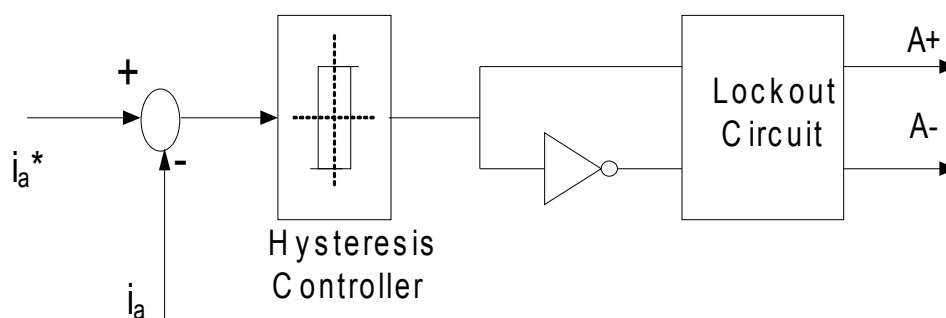


Figure 4.30: Hysteresis Controller for one phase

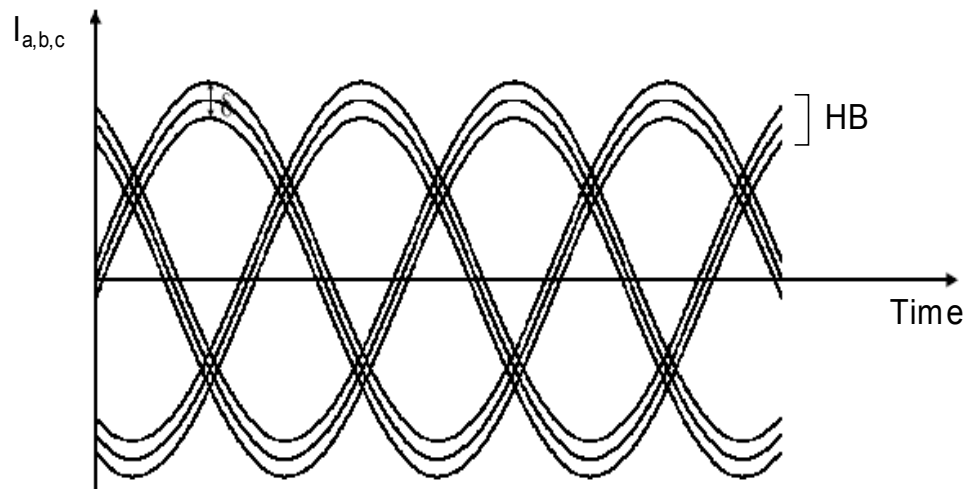
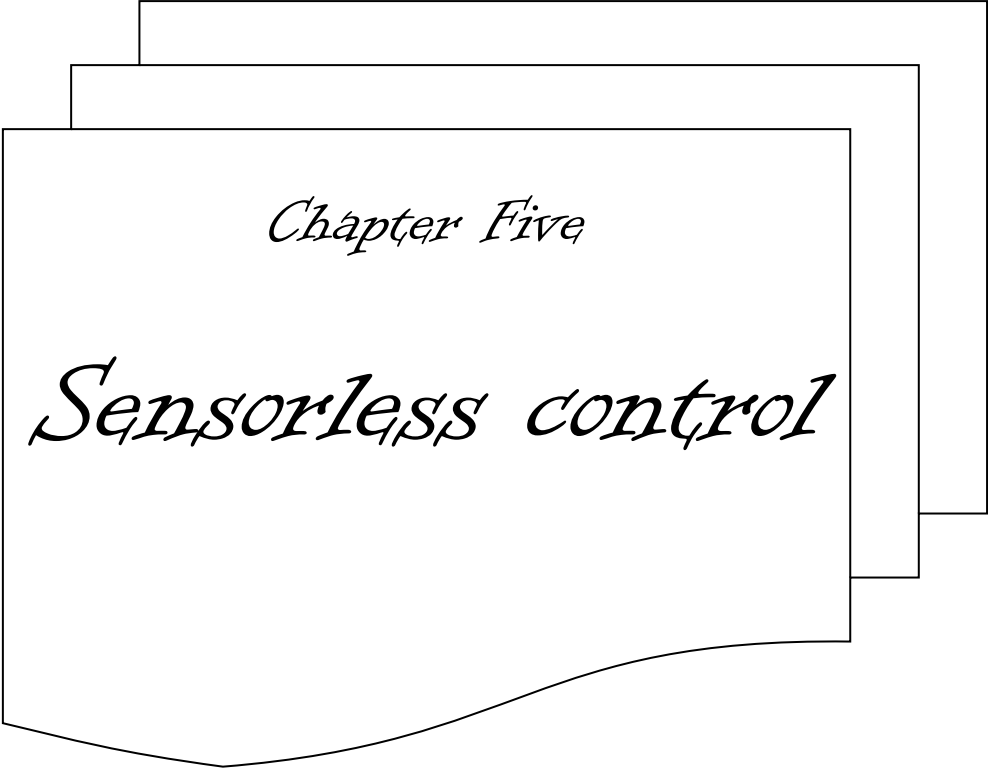


Figure 4.31: Hysteresis bands (HB) around the reference currents i_a ; i_b ; i_c



Chapter Five

Sensorless control

SENSORLESS CONTROL OF IM

Introduction

The interest for sensorless drives has been constantly rising during the last years. Sensorless control is an extension to the FOC algorithm that allows induction motors to operate without the need for mechanical speed sensors- the rotor speed is not measured but estimated- . These sensors are notoriously prone to breakage so removing them provides many benefits: it reduces the cost and size of the motor, lowers the sensitivity to noise, improves the drive's long term accuracy and reliability, on the other hand, systems require higher computational complexity [20]-[24].

As a general rule, the more complex they are, the better is their performance, especially in terms of low speed behavior, but also of the dynamic and static attitude. Sensorless drives have started to become a standard product, and there is currently a strong tendency of increasing their performance [25].

In high performance sensorless motor drives the two main control techniques used are Open Loop Estimators and Closed Loop Observers. In early literature, the terms observer and estimator are often used interchangeably

however most recent papers [20] define estimators as systems that use a model to predict the speed using the phase currents and voltages as state variables. The observed value of speed is then used by the FOC to adjust the PWM waveform in exactly the same way as an actual measured value.

Observers of an IM

As mentioned in the previous section, sensorless systems are used in many applications to avoid drawback of speed or flux sensor. Systems based on each of the known methods of speed estimation usually work correctly in the region of medium and high rotor angular velocity but they are unstable near zero angular velocity of the rotor. Errors of the estimated rotor angular velocity appear in transients. As the estimated rotor angular velocity is used in the observer or model of the induction motor the additional errors appear in transients of the estimated rotor flux [32].

A new speed observer, which has the ability to estimate very small rotor speed, was reported in [33] and [34] where the rotor angular velocity is calculated from simple relationship and used in the observer feedback signals. The rotor flux estimated in the new observer may be used in the control system.

Not all states are available for feedback in many cases and one needs to estimate unavailable state variables. Estimation of immeasurable state variables is commonly called *observation*. A device (or a computer program) that estimates or observes the states is called a state-observer or simply an observer. If the observer

observes all state variables of the system, regardless of whether some state variables are available for direct measurement, it is called a *full-order state-observer*. An observer that estimates fewer than the dimension of the state-vector is called *reduced-order state-observer* or simply a *reduced-order observer*. If the order of the reduced-order state-observer is the minimum possible, the observer is called *minimum-order state-observer* [31].

In open-loop estimators, especially at low speeds, parameter deviations have a significant influence on the performance of the drive both in steady state and transient -state. However, it is possible to improve the robustness against parameter mismatch and also signal noise by using closed loop observers.

Luenberger Observer

If differential equations 5.1 and 5.2 are a representation of a plant:

$$\frac{dx}{dt} = Ax + Bu + z \quad (5.1)$$

$$y = Cx \quad (5.2)$$

where x , u , y and z are vectors of state, control, output and disturbance variables, A , B and C are matrices of coefficients, the following Luenberger observer may be designed to estimate the disturbances (equations 5.3-5.5):

$$\frac{d\hat{x}}{dt} = A\hat{x} + Bu + \hat{z} + K_x (y - \hat{y}) \quad (5.3)$$

$$\frac{d\hat{z}}{dt} = \hat{K}_z (y - \hat{y}) \quad (5.4)$$

$$\hat{y} = C\hat{x} \quad (5.5)$$

where $\hat{\cdot}$ denotes variables estimated in the observer, K_x and K_z are matrices of gain coefficients.

Generally the coefficients K_z influence on speed of transients and the coefficients K_x are responsible for damping of variables errors in the observer. The system –Equations 5.3–5.5- acts properly if the disturbances are constant in steady states. For periodical disturbances, the errors $\mathbf{x} - \hat{\mathbf{x}}$ are not equal to zero what means that variables \mathbf{x} are estimated with errors. Special feedback has to be applied to damp the system. On the other hand, the system –Equations 5.3–5.5- may be improved if dynamics of variables \mathbf{z} is known. The equation 5.4 takes in such a case the following form:

$$\frac{d\hat{z}}{dt} = E\hat{x} + F\hat{z} + \hat{K}_z (\mathbf{x} - \hat{\mathbf{x}}) \quad (5.6)$$

where E and F are matrices defining dynamics of disturbances.

Flux Observer

The considerations in the previous section are useful for design and interpretation of observers of induction motor variables. The Luenberger observers are based on the equations 3.15-3.19 for components of stator current

and rotor flux vectors of the induction motor in the frame of references connected to the stator. This observer is represented in the set of equations (equation 5.7-5.10) [33]:

$$\frac{d\hat{i}_{sx}}{d\tau} = a_1 \hat{i}_{sx} + a_2 \hat{\psi}_{rx} + a_3 \omega_r \hat{\psi}_{ry} + a_4 u_{sx} - k_i (i_{sx} - \hat{i}_{sx}) \quad (5.7)$$

$$\frac{d\hat{i}_{sy}}{d\tau} = a_1 \hat{i}_{sy} + a_2 \hat{\psi}_{ry} - a_3 \omega_r \hat{\psi}_{rx} + a_4 u_{sy} + k_i (i_{sy} - \hat{i}_{sy}) \quad (5.8)$$

$$\frac{d\hat{\psi}_{rx}}{d\tau} = a_5 \hat{i}_{sx} - \hat{\psi}_{rx} \omega_r \hat{\psi}_{ry} (k_{f1} + i_{sx}) \hat{i}_{sx} - (k_{f2} - \omega_r) \hat{i}_{sy} \omega \hat{i}_{sy} - \quad (5.9)$$

$$\frac{d\hat{\psi}_{ry}}{d\tau} = a_5 \hat{i}_{sy} - \hat{\psi}_{ry} \omega_r \hat{\psi}_{rx} (k_{f1} + i_{sy}) \hat{i}_{sy} - (k_{f2} - \omega_r) \hat{i}_{sx} \omega \hat{i}_{sx} - \quad (5.10)$$

Where:

$$\begin{aligned} a_1 &= -\frac{R_s L_r^2 + R_r L_m^2}{w L_r} & a_4 &= \frac{L_r}{w} \\ a_2 &= \frac{R_r L_m}{w L_r} & a_5 &= \frac{R_r L_m}{L_r} \\ a_3 &= \frac{L_m}{w} & a_6 &= -\frac{R_r}{L_r} \\ w &= L_s L_r - L_m^2 \end{aligned} \quad (5.11)$$

In addition, $\hat{\cdot}$ denotes variables estimated in the observer and k_i , k_{f1} and k_{f2} are the gain coefficients of observer.

The scheme of the observer is presented in figure 5.1. The errors between measured and set value of the stator current vector components are used in feedback loops to improve dynamic properties of the observer. Usually high amplification coefficients are used in the feedback to achieve fast error reduction. There are at least six places where the amplified current errors appear in the

observer. The rotor angular velocity has to be *measured* or *estimated* in other structure and acts as the parameter in the flux observer [33]-[35].

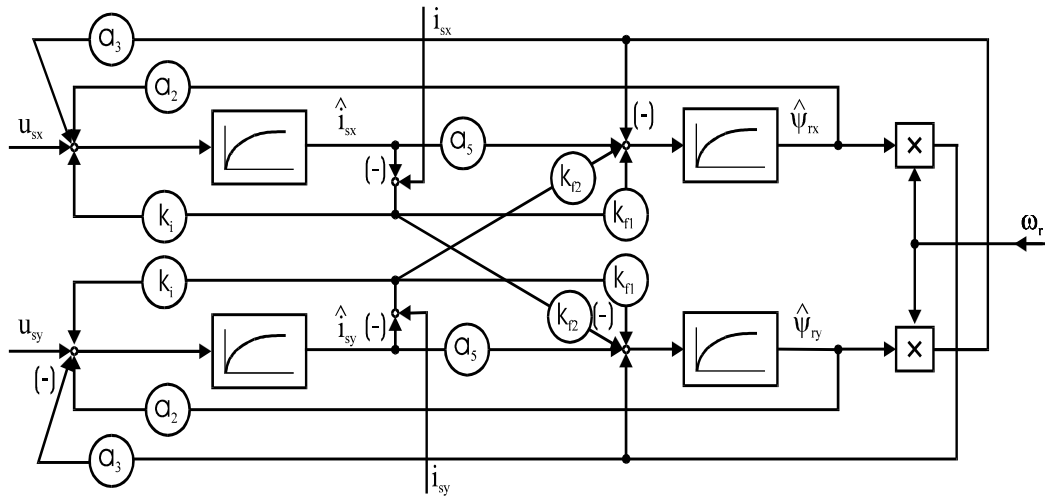


Figure 5.32: Structure of the conventional rotor flux observer.

Speed Observer

A Luenberger speed observer has been proposed for induction motor in [34] with structure of differential equations represented by equation 5.12-5.18.

$$\frac{d\hat{i}_{s\alpha}}{dt} = a_1 \hat{i}_{s\alpha} + a_2 \hat{\psi}_{r\alpha} + a_3 \zeta_\beta + a_4 u_{s\alpha} + k_3 \left(k_1 (i_{s\alpha} - \hat{i}_{s\alpha}) - \hat{\omega}_r \zeta_\alpha \right) \quad (5.12)$$

$$\frac{d\hat{i}_{s\beta}}{dt} = a_1 \hat{i}_{s\beta} + a_2 \hat{\psi}_{r\beta} - a_3 \zeta_\alpha + a_4 u_{s\beta} + k_3 \left(k_1 (i_{s\beta} - \hat{i}_{s\beta}) - \hat{\omega}_r \zeta_\beta \right) \quad (5.13)$$

$$\frac{d\hat{\psi}_{r\alpha}}{dt} = a_5 \hat{i}_{s\alpha} + a_6 \hat{\psi}_{r\alpha} - \zeta_\beta + k_2 (\hat{\omega}_r \hat{\psi}_{r\beta} - \zeta_\alpha) \quad (5.14)$$

$$\frac{d\hat{\psi}_{r\beta}}{dt} = a_5 \hat{i}_{s\beta} + a_6 \hat{\psi}_{r\beta} + \zeta_\alpha + k_2 (\hat{\omega}_r \hat{\psi}_{r\alpha} - \zeta_\beta) \quad (5.15)$$

$$\frac{d\zeta_\alpha}{dt} = k_1 (i_{s\beta} - \hat{i}_{s\beta}) \quad (5.16)$$

$$\frac{d\zeta_\beta}{dt} = -k_1 (i_{s\alpha} - \hat{i}_{s\alpha}) \quad (5.17)$$

$$\hat{\omega}_r = S \left(\sqrt{\frac{\zeta_\alpha^2 - \zeta_\beta^2}{\hat{\psi}_{r\alpha}^2 - \hat{\psi}_{r\beta}^2}} k - V_4 (V_f) \right) \quad (5.18)$$

where

- ◆ k_1, k_2, k_3 and k_4 are gain coefficients,
- ◆ a_1 - a_6 are the same as in equation 5.11.
- ◆ V and V_f are given by equation 5.19 and 5.20

$$V = \zeta_\alpha \hat{\psi}_{r\beta} - \zeta_\beta \hat{\psi}_{r\alpha} \quad (5.19)$$

$$\frac{dV_f}{dt} = \frac{1}{T_1} (V - V_f) \quad (5.20)$$

- ◆ S is the sign defined in step k by the following dependence taking the sign in the step $k - 1$ into account -equation 5.21-

$$S(k) = \begin{cases} 1 & \text{if } (\text{sgn}(\hat{\psi}_{r\alpha} \zeta_\alpha) = 1 \ \& \ \text{sgn}(\hat{\psi}_{r\beta} \zeta_\beta) = 1) \\ S(k-1) & \text{if } (\text{sgn}(\hat{\psi}_{r\alpha} \zeta_\alpha) \neq \text{sgn}(\hat{\psi}_{r\beta} \zeta_\beta)) \\ -1 & \text{if } (\text{sgn}(\hat{\psi}_{r\alpha} \zeta_\alpha) = -1 \ \& \ \text{sgn}(\hat{\psi}_{r\beta} \zeta_\beta) = -1) \end{cases} \quad (5.21)$$

The principle of work of this observer is based on estimation of disturbances appearing in the differential equations for stator current and rotor flux vector components. These disturbances are defined as new variables defined as equations 5.22 and 5.23:

$$\zeta_\alpha = \omega_r \psi_{r\alpha} \quad (5.22)$$

$$\zeta_\beta = \omega_r \psi_{r\beta} \quad (5.23)$$

Analysis of equations 5.22 and 5.23 results in equation 5.18 which makes it possible to determine the rotor angular velocity. The scheme of the observer is presented in figure 5.2.

High accuracy of the above speed observer in steady states and only small errors of estimated rotor angular velocity in transients for exactly known motor parameters may be observed. The other situation exists for the rotor flux vector. It has been shown in [33] that the angle between estimated and real rotor flux vectors is near zero but the amplitudes of these vectors may be greatly different.

Different estimating procedures may be applied to determine the stator and rotor resistances and leakage inductances. In many applications it is possible to apply a nonlinear dependence between the magnetizing current and mutual inductance. Great differences between the amplitudes of estimated and real rotor flux in the presented speed observer complicates the dependence between the mutual inductance and amplitude of estimated magnetizing current. This dependence may be calculated in complicated way because the gain coefficients of observer influence the amplitude of estimated rotor flux. The other way is to apply additional Luenberger observer and estimate the mutual inductance using the algorithm presented in [33].

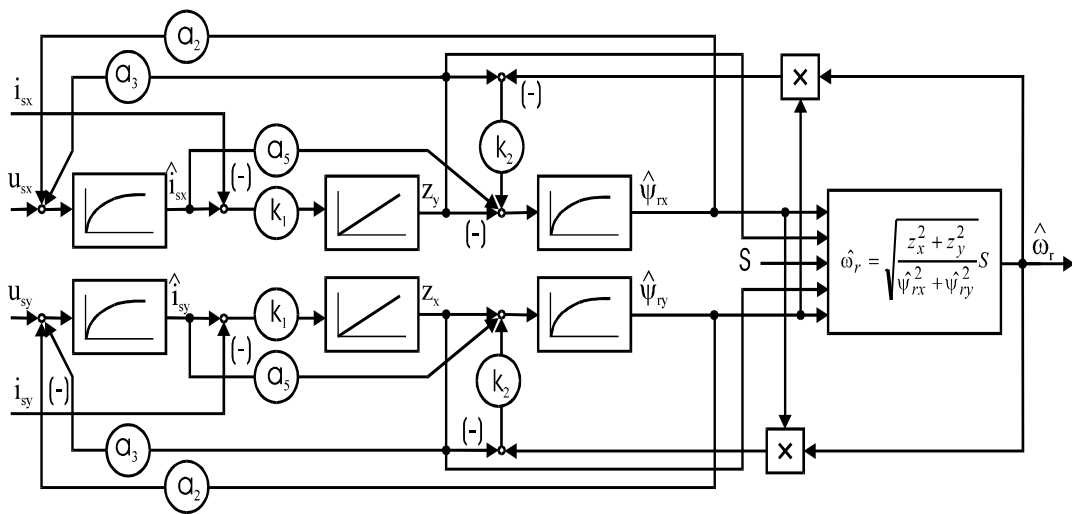


Figure 5.33: Structure of the proposed rotor flux and rotor speed observer.

Chapter Six

*Simulations and
Results*

SIMULATIONS AND RESULTS

Working with Simulink

Simulink is a software package that utilizes the computational tools of Matlab to analyze complex dynamic systems. The program is capable of solving both linear and non-linear processes so it is perfectly suited to simulating asynchronous induction motors. The first step in modeling a controller is to create a block diagram representation of its algorithm. This can be constructed from existing blocks in the Simulink library or from those created by the user. Although it is possible to incorporate Matlab m-files directly into Simulink, this significantly decreases the performance of the simulation. If it is necessary to use an m-file in the model, it should be structured as an S-function and cross-compiled into the standard block format. Fortunately, for the simulations in this thesis no S-Functions were required.

Once the block diagram has been developed, it can be simulated using any number of different solvers. These compute the internal state variables of the blocks by solving their respective Ordinary Differential Equations. Choosing the appropriate solver can significantly decrease the computation time and improve

the accuracy of the simulation. This decision is largely dependent on whether the controller model is implemented in discrete time using z variables, or continuous time using the Laplacian s variable. The main difference between a discrete and continuous model, is that the discrete time blocks respond to input changes with a fixed period and hold their outputs constant between successive samples. Although discrete time models can be solved using any of Simulink's solvers the fixed step (no continuous states) setting is usually the fastest. This assumes that the model is discrete and that every state variable is calculated at the same time.

In a continuous model, the state variables can be calculated at any time. This requires a solver that can operate at a rate that allows it to follow the dynamic behavior of the model. To do this a variable step solver is used which not only performs the calculations but also determines the step size for how frequently they should occur. Although determining step size increases the computational time it can improve the overall speed by avoiding unnecessary calculations. Finally, if a system has a mixture of continuous and discrete time blocks it must be solved using one of the Runge-Kutta variable solvers ODE23 or ODE45.

Fuzzy Logic Controller

In the system with not exactly known dynamic, and with difficult to describe analytical relationships, good results are obtained by using the fuzzy logic theory.

The system described in this paper has the mentioned characteristics, which are caused by non-precise variable identification and thus a complicated analytical system description. In the system presented, Mamdani type of fuzzy logic controller (FLC), presented in figure 6.1 is used for speed controller. The input signals for the controller are: control error, ' e ' and the change of error, ' Δe ' and the output is the change of control signal, ' Δu '. The controller consists of three elements: fuzzification block, block of rules (rules of inference) and defuzzification, which are related by proper relationships.

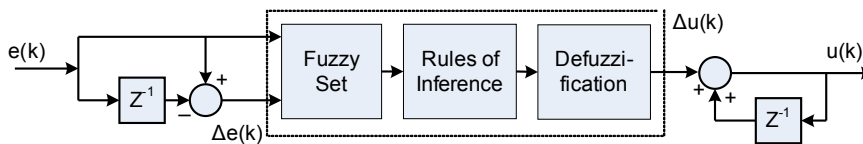


Figure 6.34: Fuzzy logic controller

On the basis of the values, ' e ' and ' Δe ', the fuzzy numbers are calculated in the fuzzification block using the membership function presented in figure 6.2. Simple membership functions for the following linguistic variables: ' NB ', ' NM ', ' NS ', ' Z ', ' PS ', ' PM ' and ' PB ' -negative big, negative medium, negative small, zero, positive small, positive medium and positive big respectively- are used.

The resulting block consists of logic table like, 'If...Then' which are described in table 6.1. Symbol ' B ' means big, symbol ' S ' means small, symbol ' M ' means medium and ' V ' means very. Based on the membership of fuzzy numbers to such sectors, which are defined in table 6.1, the output function is described, which is the fuzzy quantity of the control signal function. This quantity must be

subject to defuzzification, to identify a signal, which will be used to control the object.

		<i>e</i>						
		<i>NB</i>	<i>NM</i>	<i>NS</i>	<i>Z</i>	<i>PS</i>	<i>PM</i>	<i>PB</i>
Δe	<i>NB</i>	NVB	NVB	NVB	NB	NM	NS	Z
	<i>NM</i>	NVB	NVB	NB	NM	NS	Z	PS
	<i>NS</i>	NVB	NB	NM	NS	Z	PS	PM
	<i>Z</i>	NB	NM	NS	Z	PS	PM	PB
	<i>PS</i>	NM	NS	Z	PS	PM	PB	PVB
	<i>PM</i>	NS	Z	PS	PM	PB	PVB	PVB
	<i>PB</i>	Z	PS	PM	PB	PVB	PVB	PVB

 Δu

Table 6.2: Conclusion Rules

From many defuzzification methods, (*see chapter 1*) the Center of Area method (COA) is chosen. In the COA method, the quantity of the fuzzy set after defuzzification is described by:

$$y^* = \frac{\sum_{i=1}^n F(y_i) y_i}{\sum_{i=1}^n y_i} \quad (6.1)$$

Where:

n – Number of quantization levels

y_i – Value for i -th quantization function Δu for i -th quantization level

F_i – Value of membership function Δu for i -th quantization level.

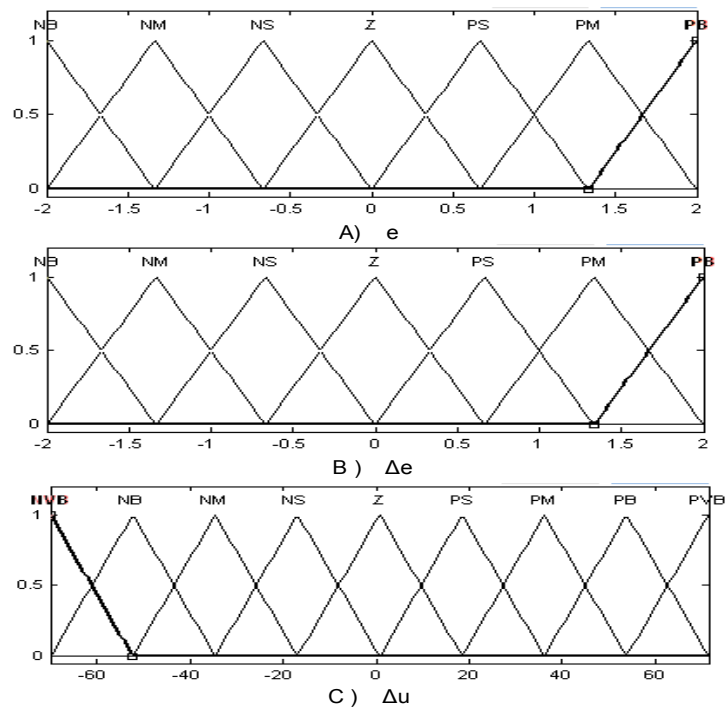


Figure 6.35: Membership functions plots for A) e , B) Δe and C) Δu

For the specified number of input signal samples, it is possible to elaborate a proper look-up table, which contains the error values. Figure 6.3 represents the control surface.

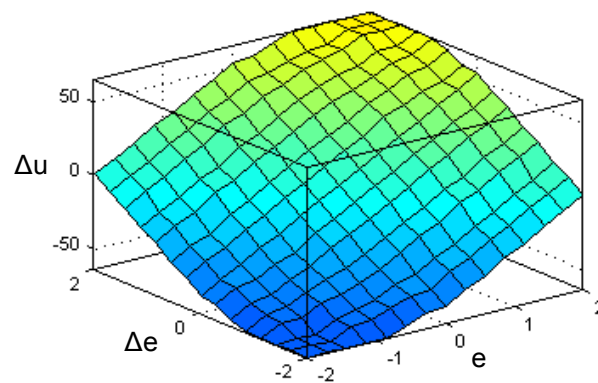


Figure 6.36: Control surface.

Induction Motor Model Implementation

For transient studies of adjustable speed drives, it is usually more convenient to simulate an induction machine and its converter on a stationary reference frame. Moreover, calculations with stationary reference frame is less complex due to zero frame speed (some terms cancelled).

The induction motor implemented here is a 400 KVA, and its parameters are shown in appendix A.4.1.

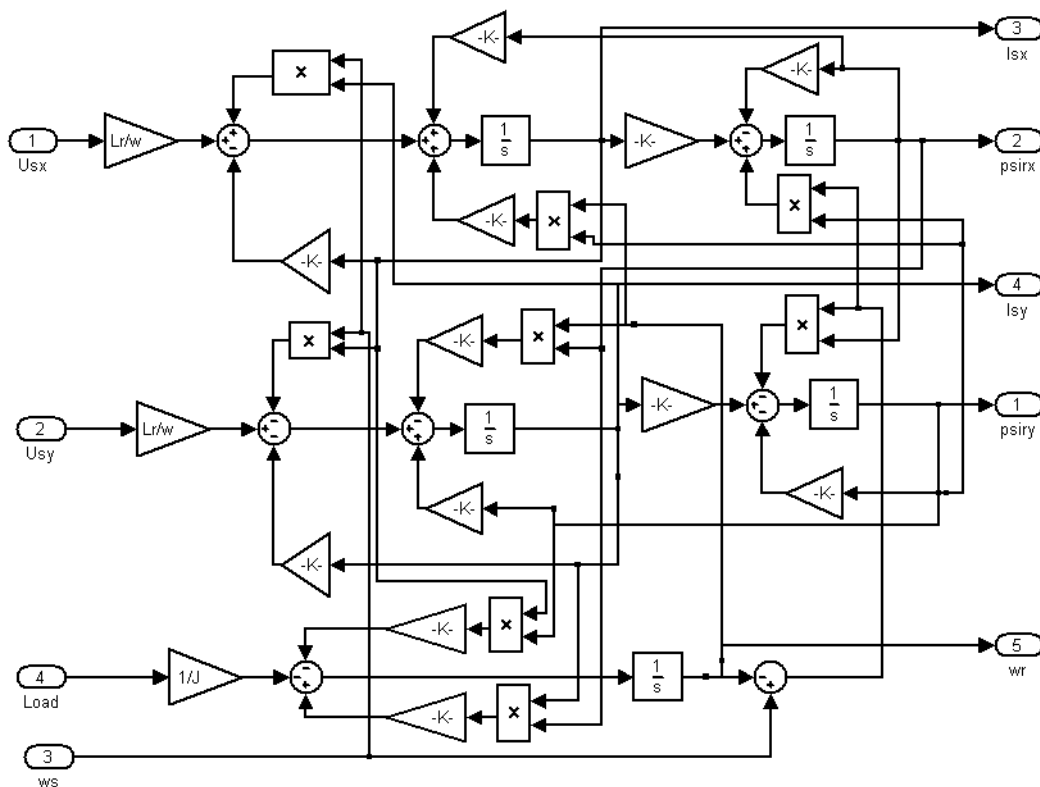


Figure 6.37: Squirrel Cage Induction Motor Model

Figure 6.4 shows a squirrel cage induction motor which is described in section 3.3.2 in the set of differential equations 3.15-3.19. Setting up the following conditions gives the simulation results shown in figure 6.5-a for no load and figure 6.5-b for full load ($M_o=1$ p.u.):

- Sinusoidal signal as $u_{s\alpha}$ and $u_{s\beta}$,
- Variable load torque M_o ,
- The synchronous speed (ω_s) is equal zero to obtain a simulation results in a stationary frame.

The simulation results show the following obvious notes:

- During the transient phase the starting current $i_{s\alpha}$ and $i_{s\beta}$ is high and the rotor flux ($\psi_{r\alpha}$ and $\psi_{r\beta}$) is building up until it reaches unity in steady state.
- The rotor speed plots show a small ripple at the beginning due to transient.
- The torque follows the reference load torque.
- The transient time at no load case is less than the transient time for the full load case.

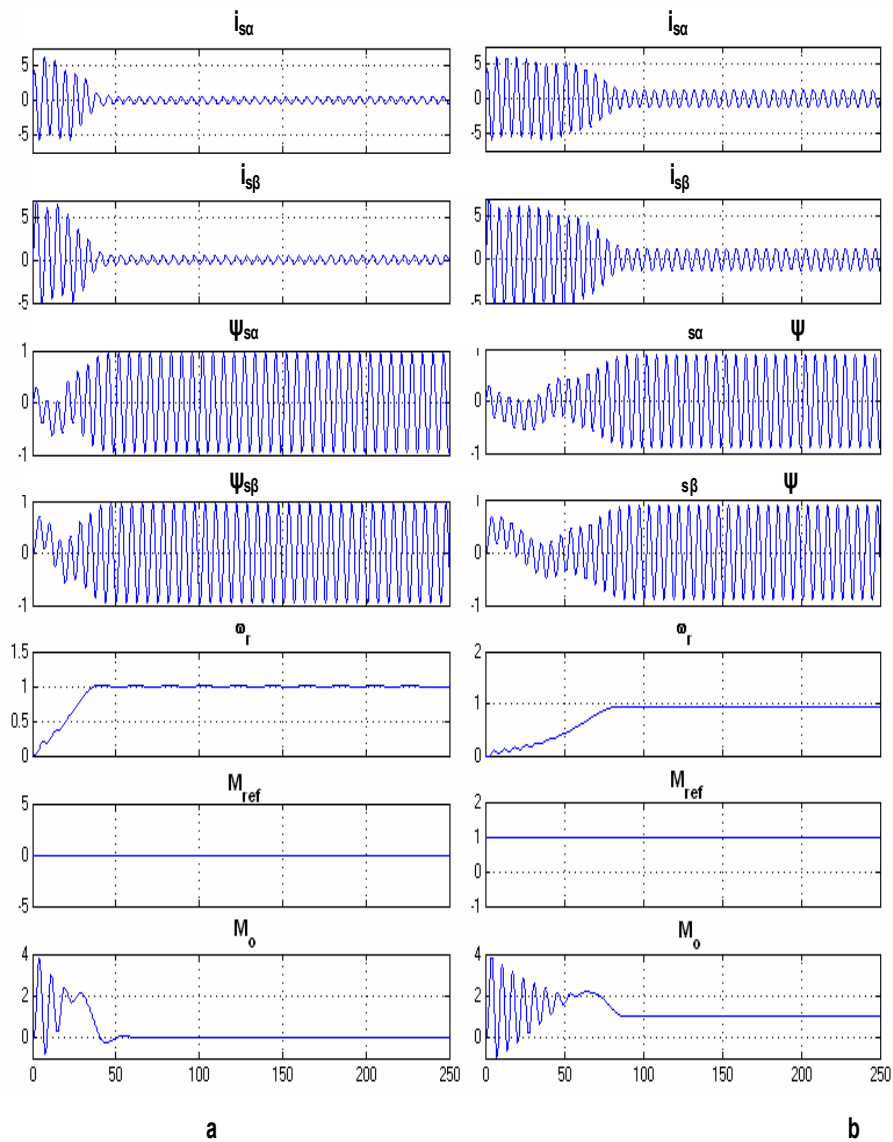


Figure 6.38: Simulation result in p.u. for IM model (a) No load and (b) Full load.

Implementing FOC with speed and flux measurements

The input of the induction motor block shown in figure 6.6 is the command $u_{s\alpha}$ and $u_{s\beta}$ and the mechanical torque load. Where the state variables as shown in the figure are the stator current ($i_{s\alpha}$, $i_{s\beta}$), the rotor flux ($\psi_{r\alpha}$, $\psi_{r\beta}$) and the rotor speed (ω_r). In the case of speed and flux measurements, three types of sensors should be used:

- The stator current sensor, which is easily handled because it can be placed on the input current phases.
- The flux sensor, which is placed in the air gap between stator and rotor.
- The speed sensor.

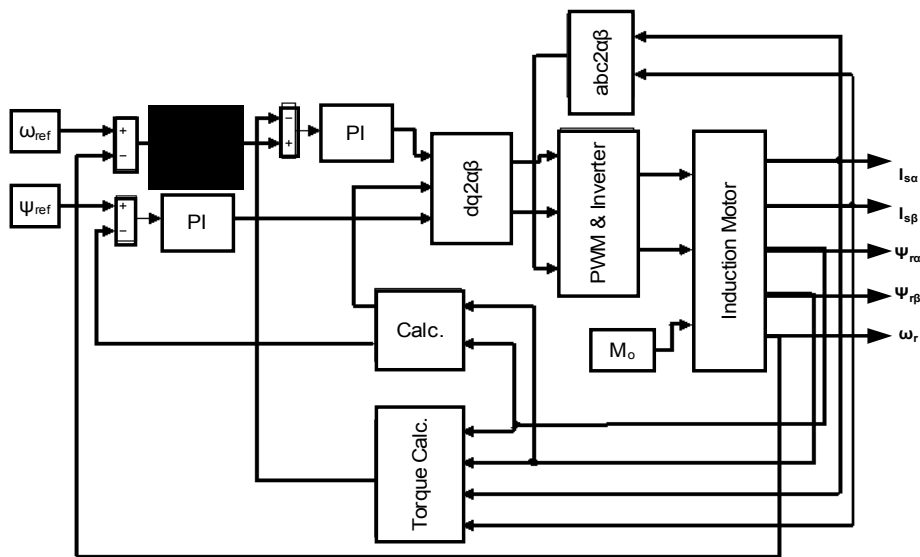


Figure 6.39: Simulink FOC model of induction motor.

According to figure 6.6, the rotor flux components are the inputs of the "Calc." block, and the output of this block is the *flux angle* and the *flux magnitude*. The flux angle is used in the transformation block " $dq2\alpha\beta$ ", which transforms *dq* frame to stationary frame ($\alpha\beta$), the flux magnitude is compared with the command flux, which generally equals one p.u, and the *measured speed* is compared with the *command speed*. The errors are compensated using PI controllers. The outputs of the PI controllers are the *command i_{sd}* and the *command torque* respectively.

Then command torque is compared with the calculated torque value which is output of "Torque Calc." block. The error is compensated using another PI that gives the command i_{sq} . The command values of i_{sd} and i_{sq} is transformed into $\alpha\beta$

coordinates using "*dq2αβ*" block. A detailed Simulink model for this system is shown in appendix A.4.3.

The current-controlled voltage source inverter PWM is driven by the command and measured currents. A transformation blocks converting $\alpha\beta$ to *abc* -"*abc2αβ*" block- and form *dq* to *abc* –build inside the "*PWM & Inverter*" block- are used.

The command currents are compared with actual currents using three independent hysteresis controllers. As mentioned in section 4.5.3. Figure 6.7 is a Simulink model of this controller.

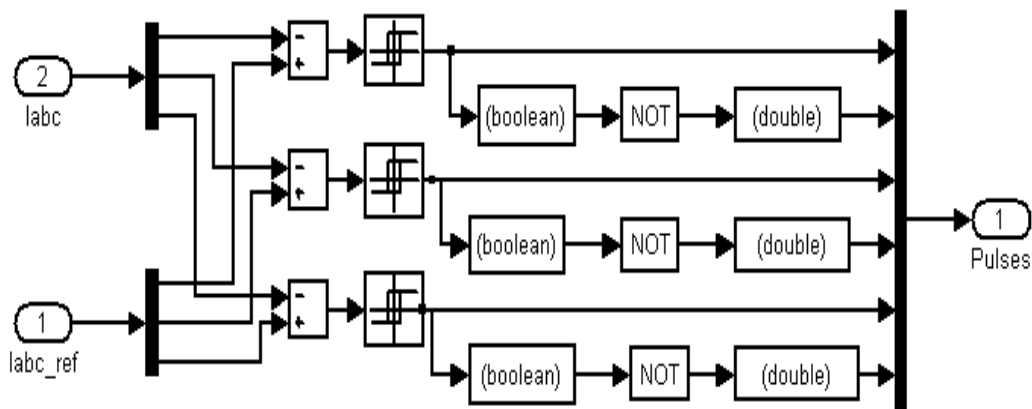


Figure 6.40: Pulse Generator using three independent hysteresis current controllers.

A fuzzy controller, which is designed in section 6.2, shown in figure 6.8, is tested with the same model shown above; the shaded PI controller is replaced by the FLC, and the simulation results for the different cases and different state variables shown in the following figures (6.9-6.14). Figures 6.9-6.12 are for a command speed equals one p.u. and a variable torque.

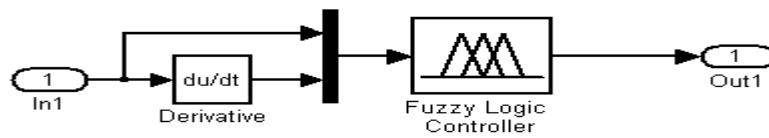


Figure 6.41: Simulink Fuzzy logic controller.

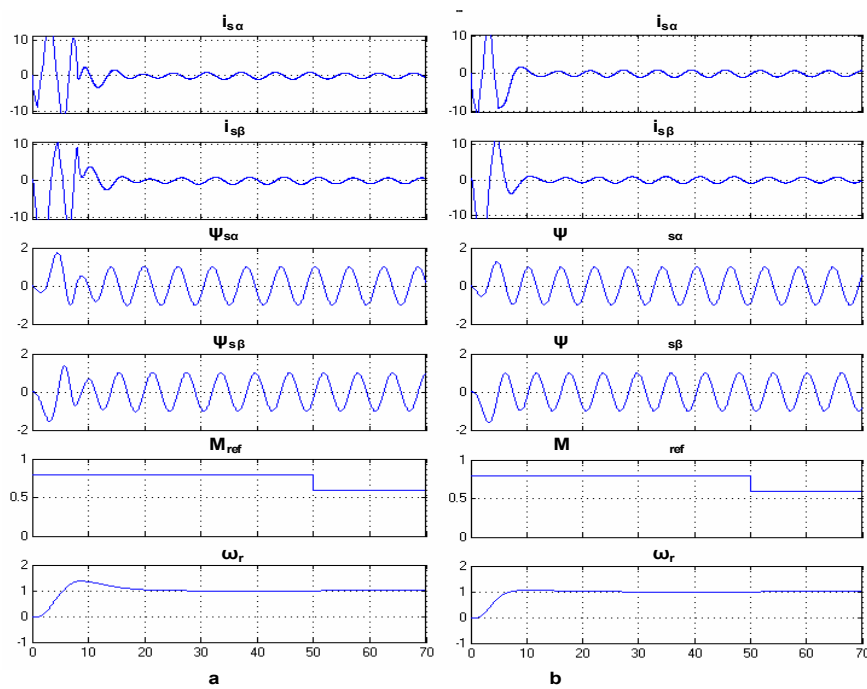


Figure 6.42: Simulation results for the control system (a) PI controller (b) FLC for speed=1p.u.

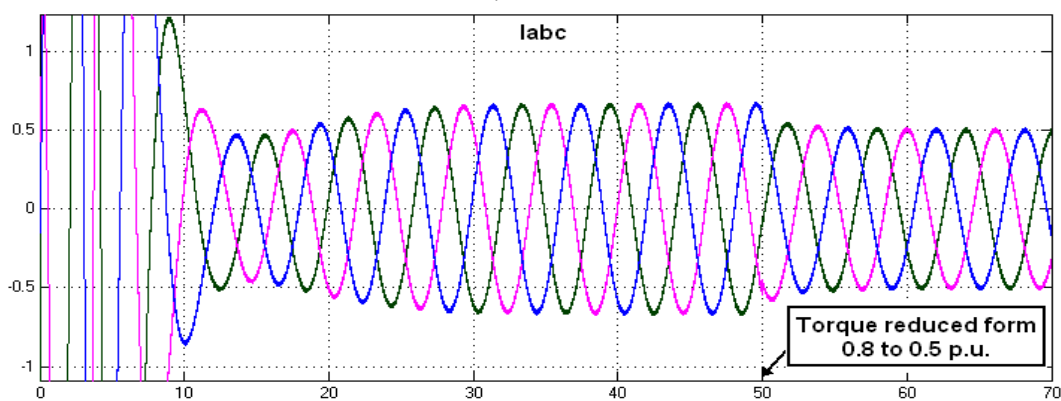


Figure 6.43: The measured i_{abc} in transient, steady state and applying disturbance (changing torque)

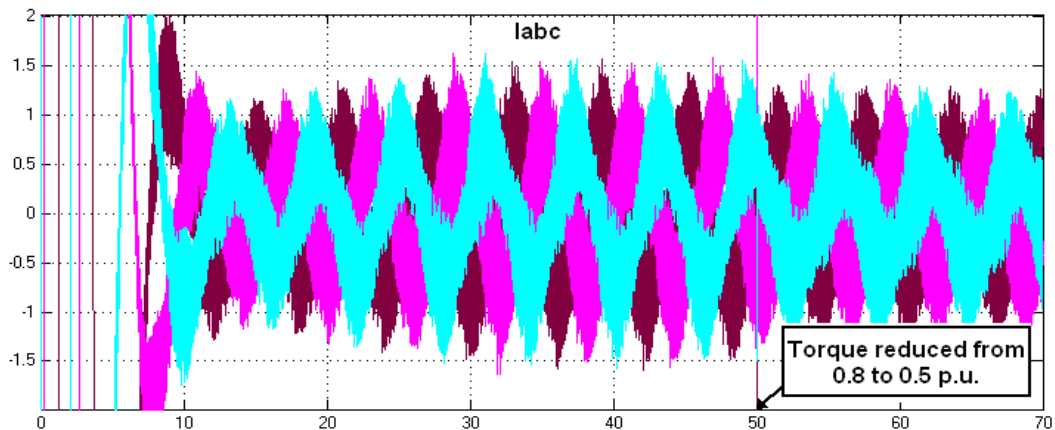


Figure 6.44: Command I_{abc} , very small change during changing the torque.

According to figure 6.12, the speed response of the PI controllers has 37% overshoot value, while the overshoot value of the FLC is 6.5%. While the steady state error for FLC is less than 0.3% while for PI controller the steady state error is 1%. Moreover, the FLC reaches steady state faster.

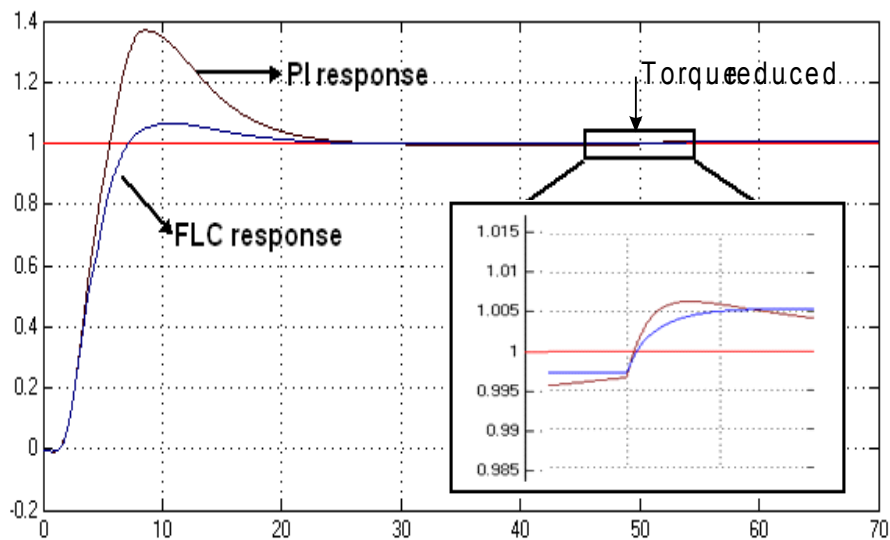


Figure 6.45: Speed response for FLC and PI controller

Figure 6.13 and 6.14 are for variable speed and variable torque.

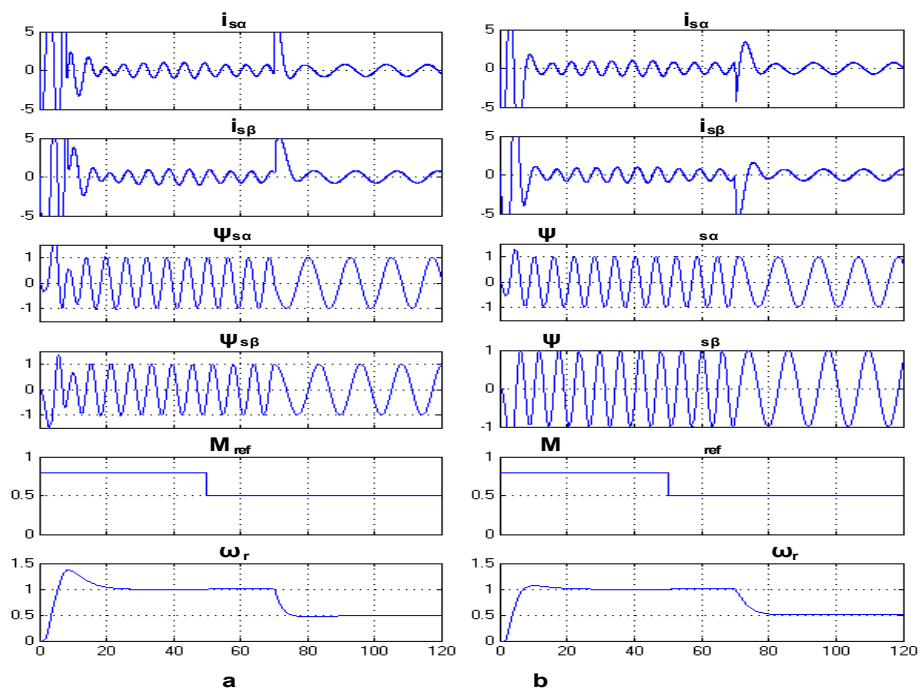


Figure 6.46: Simulation results for the FOC system (a) PI controller (b) FLC for variable speed.

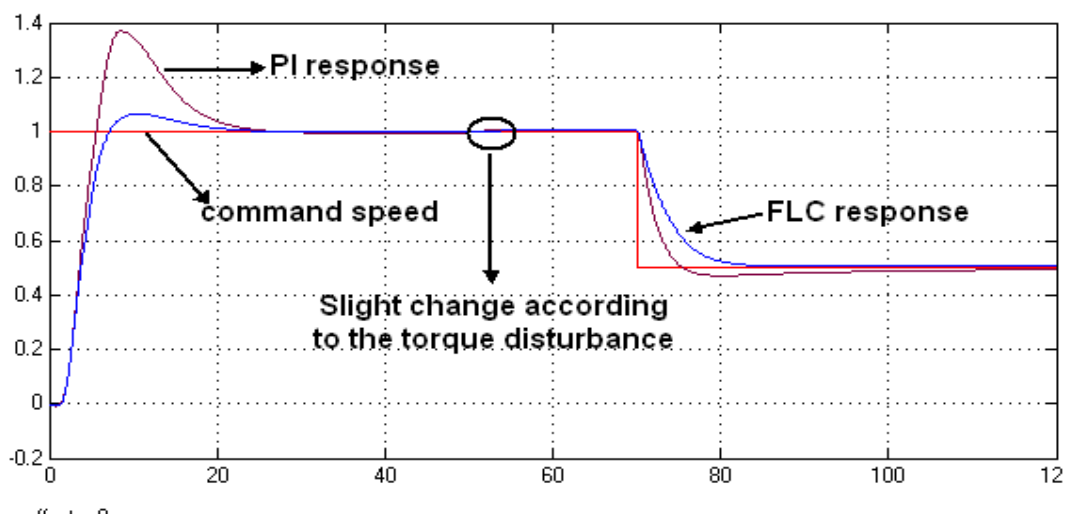


Figure 6.47: Speed response for FLC and PI controller for variable speed.

Implementing FOC with Luenberger Observer

Based on the implemented previously FOC of an induction motor, a Luenberger speed observer has been added to the model to obtain a senseless speed control at low speed operations, Luenberger system is represented using a set of differential equation (equations 5.12-5.18.) proposed in section 5.5. The k 's constants defined by trial and error technique.

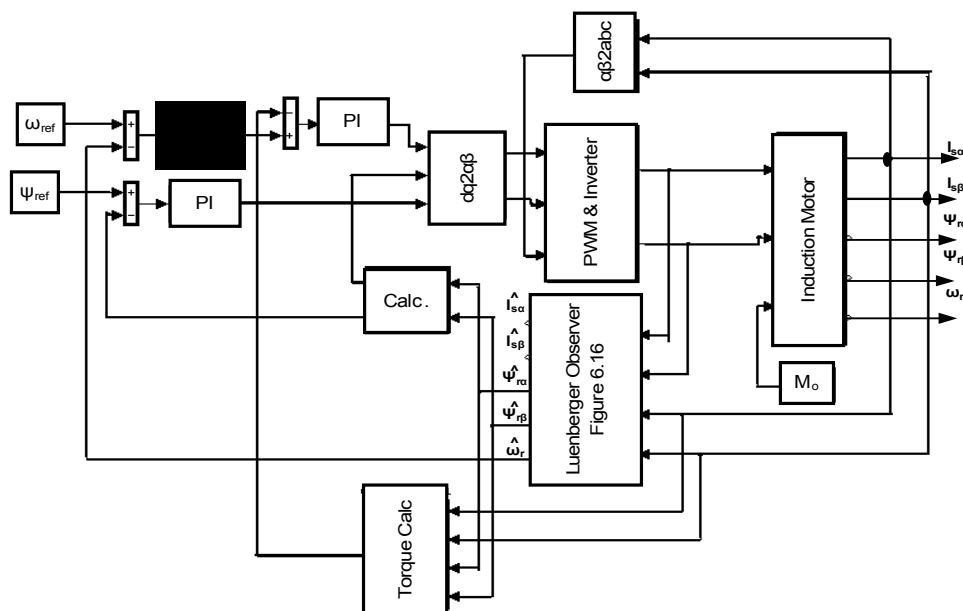


Figure 6.48: The control model with the observer system.

Figure 6.15 shows the Simulink control model with the Luenberger observer. In this model, there is no need for flux and speed sensors. The rotor flux and speed is estimated using Luenberger observer. Here, current and voltage sensors are needed because the inputs of the Luenberger observer are the measured stator current components ($i_{s\alpha}$, $i_{s\beta}$) and the measured stator voltage

components ($u_{s\alpha}$, $u_{s\beta}$). Figure 6.16 shows the Luenberger observer model. A detailed Simulink model for this system is shown in appendix A.4.4.

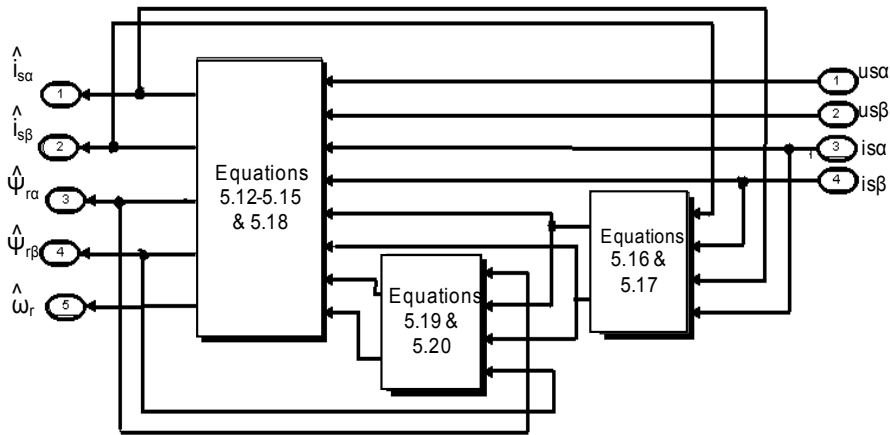


Figure 6.49: Luenberger speed observer

The outputs of this observer as shown in figure 6.16 are $\hat{i}_{s\alpha}$, $\hat{i}_{s\beta}$, $\hat{\psi}_{r\alpha}$, $\hat{\psi}_{r\beta}$ and $\hat{\omega}_r$. The estimated rotor flux components are used to calculate the flux angle and flux amplitude. Then the system behaves as described in section 6.4. In addition, the CC-VSI PWM and the FLC are as shown in section 6.4. The following figures are the results of the simulation results.

Figure 6.17 shows the simulation results for the state variables of the induction motor for the traditional PI controllers and Fuzzy Logic Controller. The stator current components are distorted and the width of the signal is proportional to the hysteresis band –section 4.5.3-. Figure 6.18 shows the rotor speed plot and the plot of the errors of the speed for the control system with the FLC and PI controllers. The steady state error (SSE) when using FLC is 3.0% and when using PI controller the SSE is 6.3% at command speed 0.3 p.u.

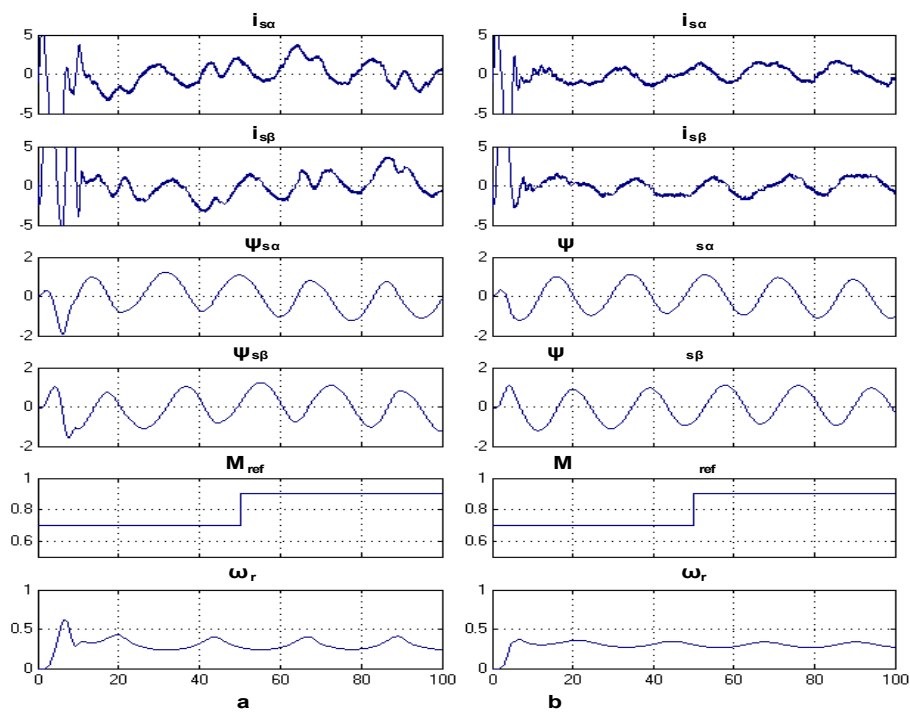


Figure 6.50: Simulation results for the sensorless control system (a) PI controller (b) FLC for constant speed and step change of load torque.

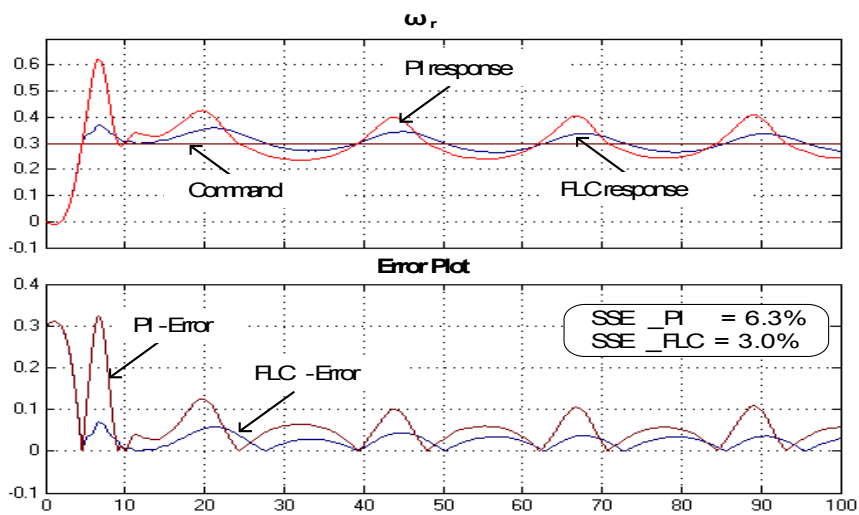


Figure 6.51: The plot of the rotor speed, and the Error plot at 0.3 p.u. command speed.

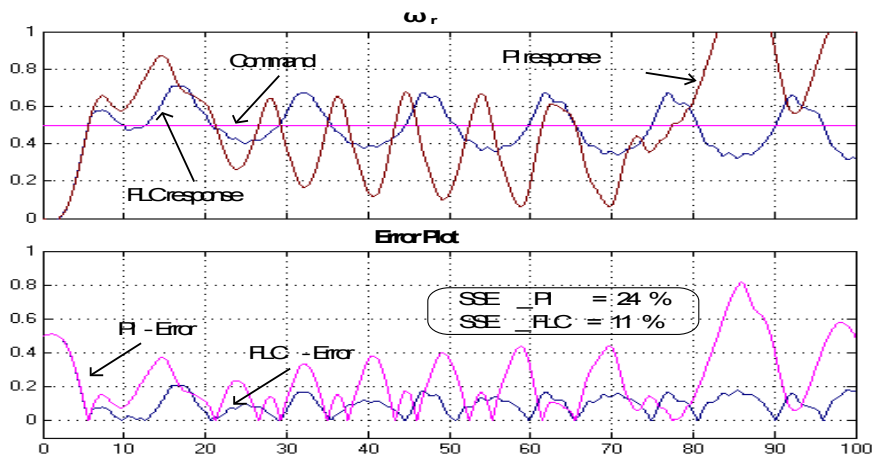


Figure 6.52: The plot of the rotor speed, and the absolute error plot at 0.5 p.u. command speed.

The steady state errors increase while the command speed increases. At a command speed 0.5 p.u. the SSE becomes 11% and 24% for FLC and PI controller respectively as shown in figure 6.19. While the SSE for a command speed equals to 0.1 p.u. as shown in figure 6.20 is 0.5% and 1.0% for FLC and PI controller respectively. The maximum overshoot values for the different cases shown above are 100% when using PI controllers and less than 30% for FLC.

Figure 6.21 shows the speed response at zero speed with a step change of torque. Notice that the SSE is very small with respect to the operation range and it is proportional with the step size, it is shown in this figure that the maximum SSE is less than 0.3%, and the overshoot value is 1%. Moreover, the actual torque follows the command value. Figure 6.22 shows the command and actual currents in the abc frame. Figure 6.23 and figure 6.24 show that the error increase with

increasing the command speed. And at last, figure 6.25 shows the results of the control system after a speed changes and step load torque change.

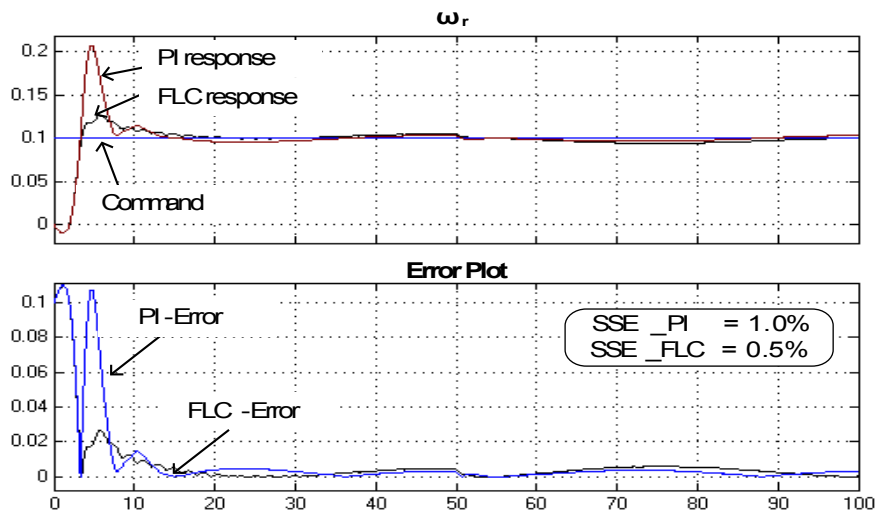


Figure 6.53: The plot of the rotor speed, and the absolute error plot at 0.1 p.u. command speed.

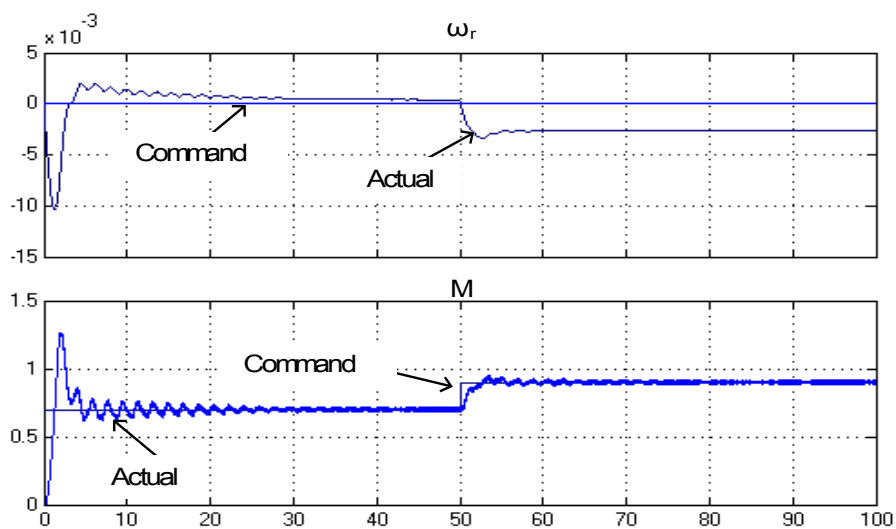


Figure 6.54: Speed response at zero speed with a step change of torque.

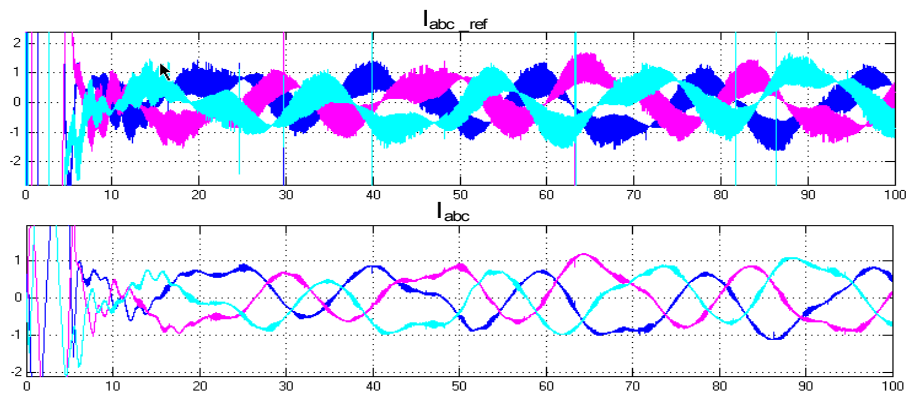


Figure 6.55: The iabc command and actual for the sensorless model.

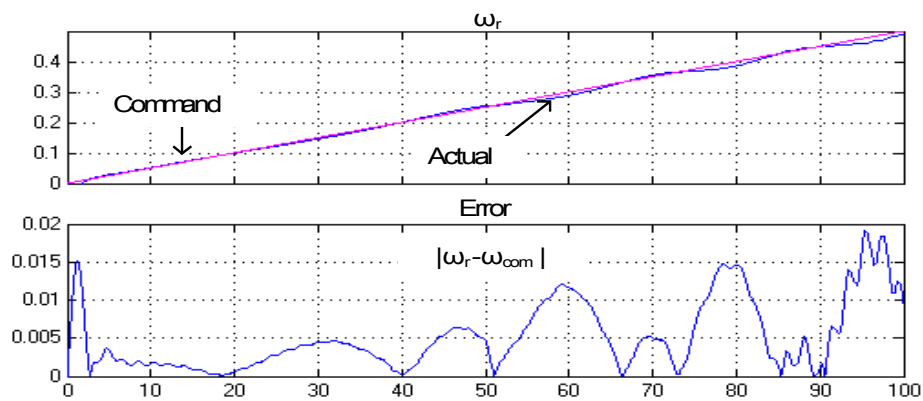


Figure 6.56: Result of control system after ramp speed change and the absolute error.

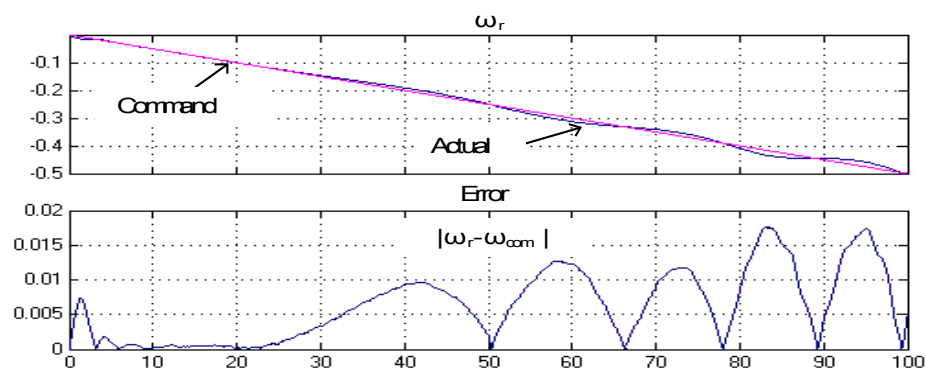


Figure 6.57: Result of control system after negative ramp speed change and the absolute error.

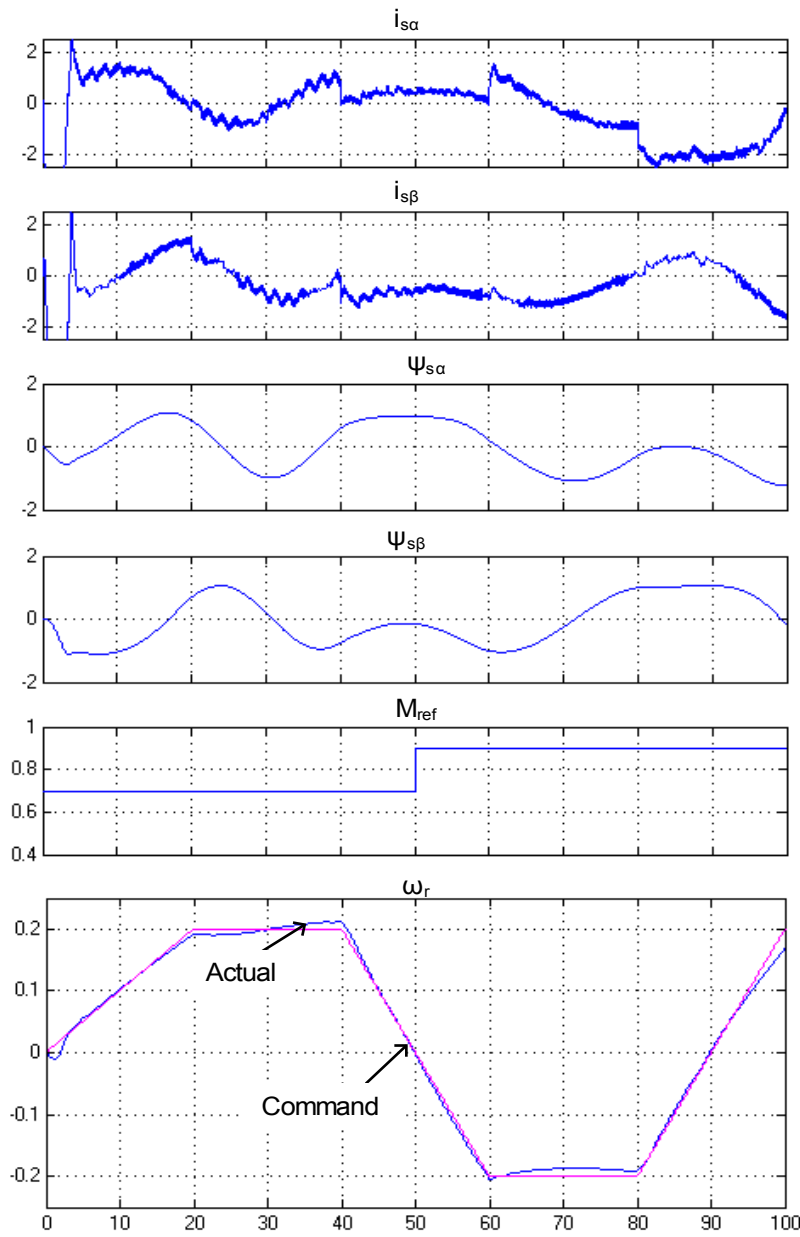
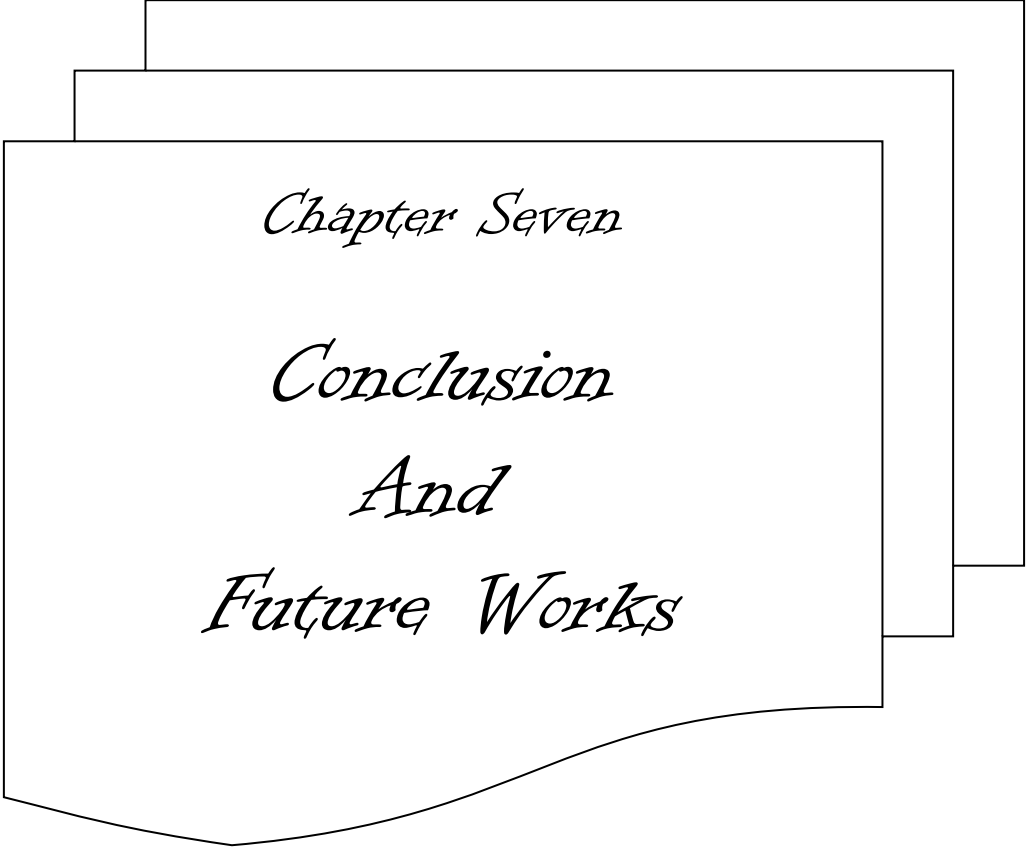


Figure 6.58: Results of control system after speed changes and step load changes. $i_{s\alpha}$, $i_{s\beta}$, $\psi_{r\alpha}$, and $\psi_{r\beta}$ are also shown.



Chapter Seven

Conclusion

And

Future Works

CHAPTER 7 CONCLUSION AND FUTURE WORKS

Conclusion

In this thesis, a sensorless vector control of induction motor, which is fed by voltage source inverter with hysteresis current controllers using speed observer system, is presented. The rotor speed was calculated using exact speed observer system, which mainly appropriate for lower speeds. In such way, benefits of induction motor, benefits of field orientation control and benefits of sensorless control are all combined together and a superior performance sensorless control model has been achieved. Moreover, using fuzzy logic controller increases the robustness of this system.

The Luenberger observer implemented in the thesis estimates the rotor speed in transients and steady states with small errors. The rotor speed was estimated at very low values, i.e. equal to zero.

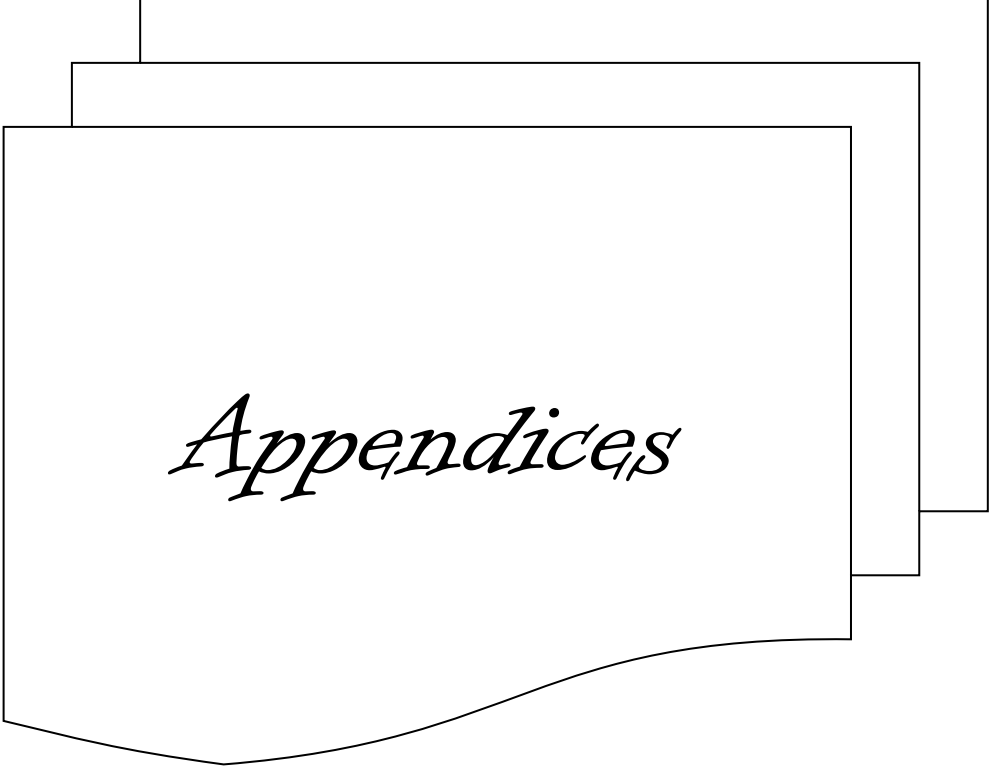
As simulation results show, very small amounts of errors have been noticed, and it was shown that the errors when using fuzzy logic is less than the error when using PI controller.

In the case of speed and flux measurements, errors are small for the high range of operation and increase when the command speed decrease. On the other hand, in the case of sensorless control using Luenberger states observer errors are inverse proportional to the speed.

Future Works

After the good results achieved by using sensorless control using Luenberger observer at low range of operations, other techniques of sensorless control may be implemented especially at high range of operation, such as, the use of power measurement (*see appendix A.3*) , the stator flux measurements and Kalman Filter and Extended Kalman Filter.

Another work may take place: testing other techniques of artificial intelligence such as Adaptive Fuzzy control, Artificial Neural Network or genetic algorithm or some compensation among these techniques.



Appendices

APPENDICES

Per Unit notation (p.u.)

Per Unit System

The per unit system is widely used in the power system industry to express values of voltages, currents, powers, and impedances of various power equipment. It is mainly used for transformers and AC machines.

For a given quantity (voltage, current, power, impedance, torque, etc.) the per unit value is the value related to a base quantity, equation A.1.

$$\text{Base value in p.u.} = \frac{\text{Quantity expressed in SI units}}{\text{Base value}} \quad (\text{A.1})$$

Generally, the following two base values are chosen:

- The base power = nominal power of the equipment
- The base voltage = nominal voltage of the equipment

All other base quantities are derived from these two base quantities. Once the base power and the base voltage are chosen, the base current and the base impedance are determined by the natural laws of electrical circuits, equations A.2 and A.3.

$$\text{Base Current} = \frac{\text{Base Power}}{\text{Base Voltage}} \quad (\text{A.2})$$

$$\text{Base Impedance} = \frac{\text{Base Voltage}}{\text{Base Current}} = \frac{(\text{Base voltage})^2}{\text{Base Power}} \quad (\text{A.3})$$

For AC machines, the torque and speed can be also expressed in p.u. The following base quantities are chosen:

- The base speed = synchronous speed
- The base torque = torque corresponding at base power and synchronous speed:

$$\text{Base Torque} = \frac{\text{Base Power (3 Phase) in VA}}{\text{Base speed in radians/second}} \quad (\text{A.4})$$

Per unit in Three phase

Power and voltage are specified in the same way as single phase systems. However, due to differences in what these terms usually represent in three phase systems, the relationships for the derived units are different. Specifically, power is given as total (not per-phase) power, and voltage is line to line voltage.

$$\begin{aligned} I_{base} &= \frac{P_{base}}{V_{base} \times \sqrt{3}} \\ Z_{base} &= \frac{V_{base}}{I_{base} \times \sqrt{3}} \\ Y_{base} &= \frac{1}{Z_{base}} = 1 \text{ p.u.} \end{aligned} \quad (\text{A.5})$$

Torque Constant

The value of torque constant can take two different values. These depend on the constant used in the space phasor. In the table A.2-1 both possibilities are shown, where '3→2' means the change from three axis to either two axis or space phasor notation. And '2→3' either two axis or space phasor notation to three axis.

	Non power invariant		Power invariant	
Torque constant	$3/2$		1	
Space phasor constant	3→2	2→3	3→2	2→3
	$2/3$	1	$\sqrt{2/3}$	$\sqrt{2/3}$

Table A.3: Torque constant values

A.2 Published Works

Simulink Models and Parameters

Induction Motor Parameters

The implemented induction motor is shown in the following m file.

%All parameters are in p.u.

Rr= 0.045;
Rs= 0.045;
Lm=1.85;
Lr=1.927;
Ls=1.927;
J=59;

% The following parameter are the coefficients of induction motor equations

Wr=Ls*Lr-Lm*Lm;
a1=-(Rs*Lr^2+Rr*Lm^2)/(Lr*Wr);
a1s=-(Rs*Lr^2)/(Lr*Wr);%for obs
a1r=-(Rr*Lm^2)/(Lr*Wr);
a2=(Rr*Lm)/(Lr*Wr);
a3=Lm/Wr;
a4=Lr/Wr;
a5=-Rr/Lr;
a6=Rr*Lm/Lr;

PWM & Inverter Simulink model

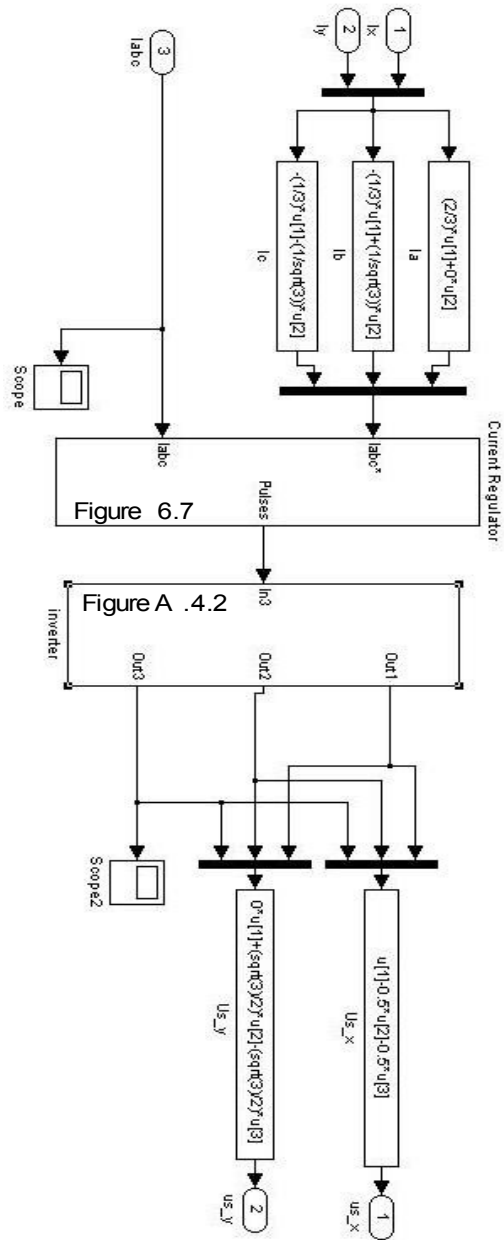


Figure A.4.1 PWM and Inverter with transformations calculations

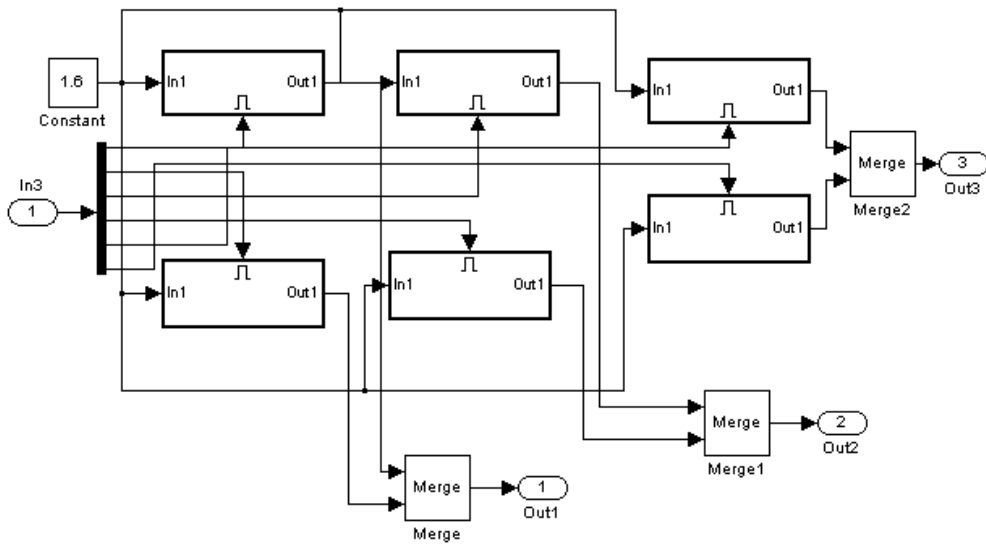


Figure A.4.2: The inverter model

A.4.3 Simulink model of the control system with speed and flux measurements

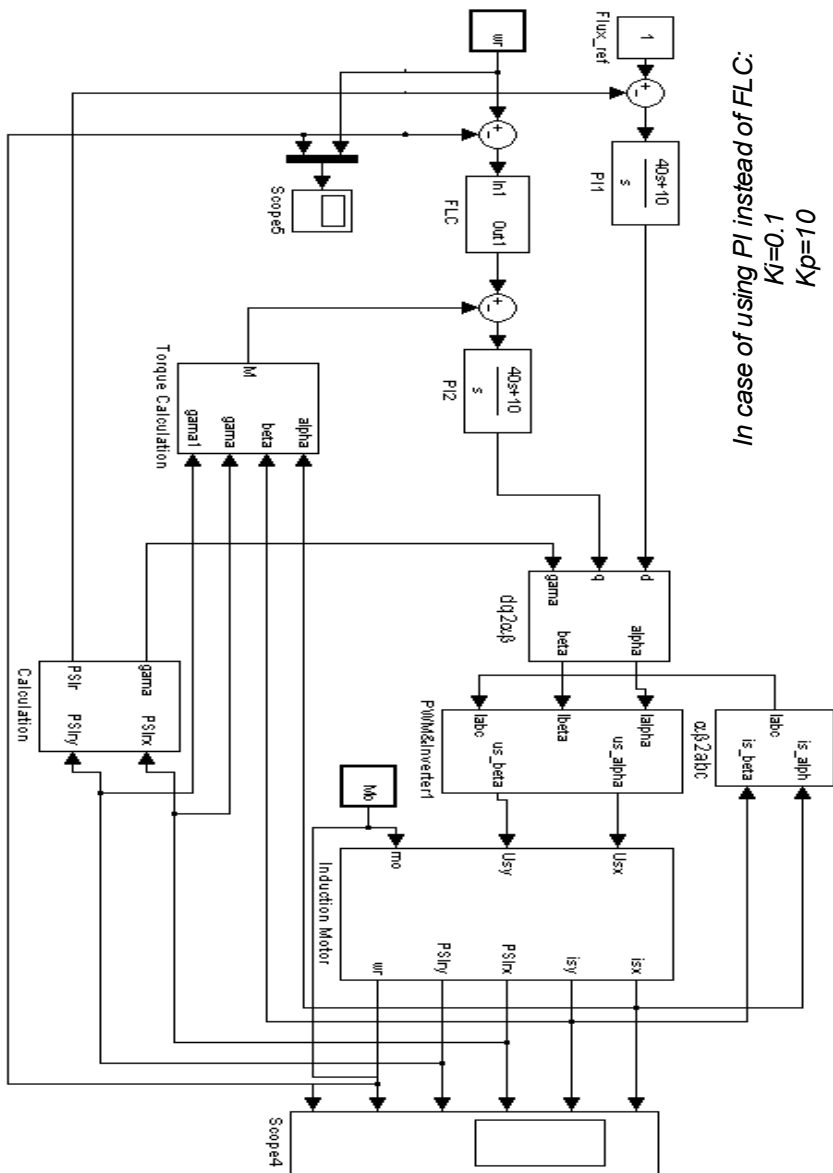


Figure A.4.3: Complete Simulink model the control system with sensors

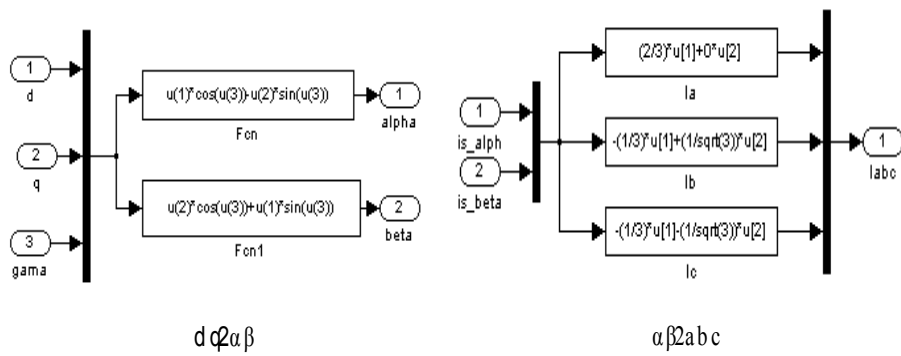


Figure A.4.4: Transformation blocks

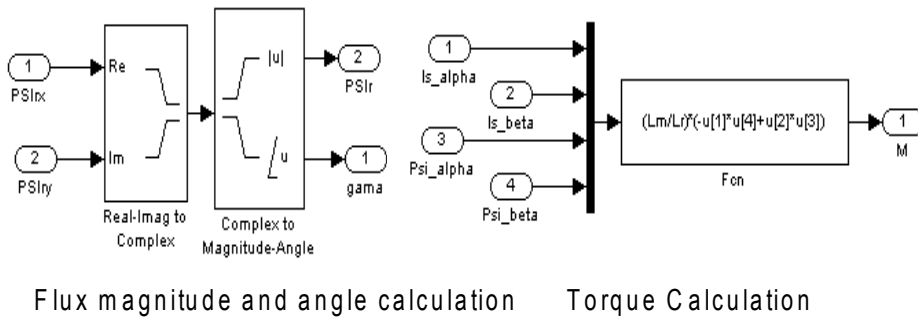


Figure A.4.5: Calculation Blocks

A.4.4 Simulink model for the sensorless control system

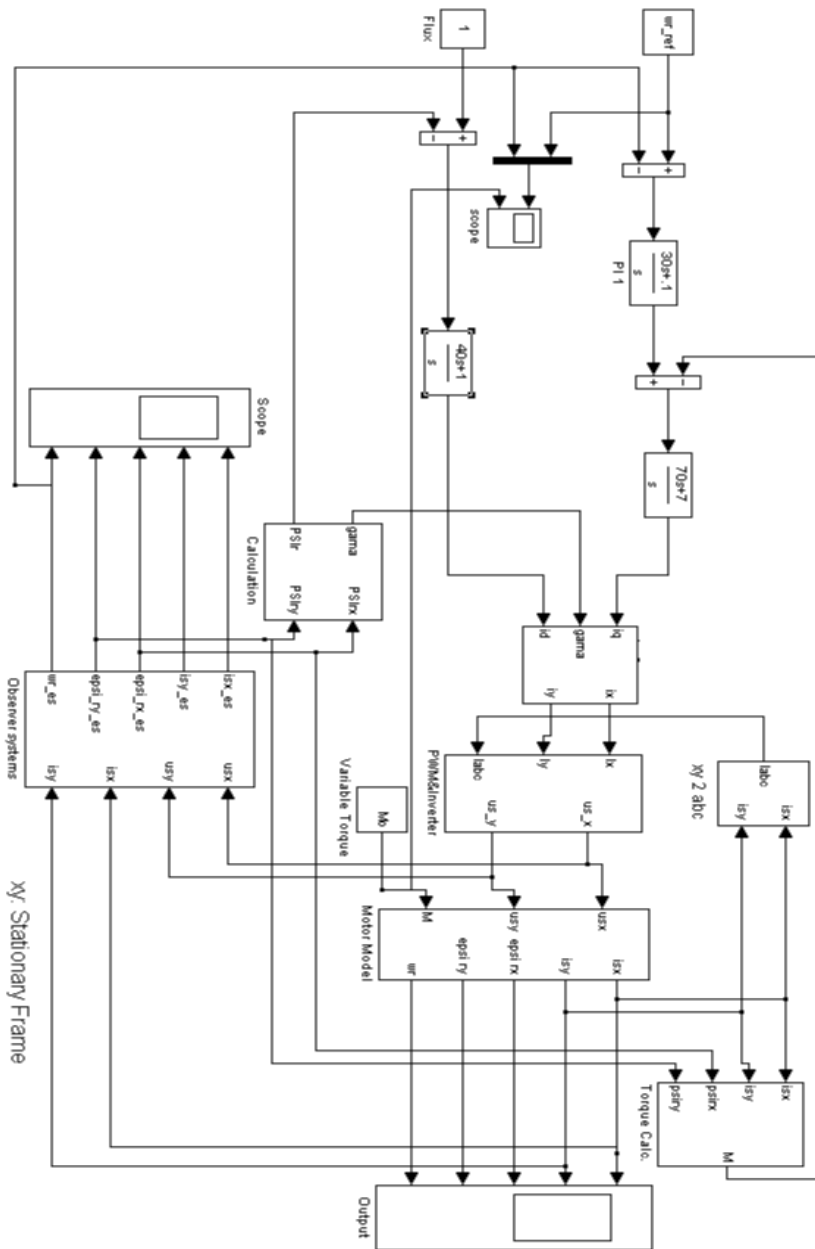


Figure A.4.6: The sensorless control system using PI.

REFERENCES

- [1] Bartk., *Neural Networks and Fuzzy systems*, Prentice Hall, 1992.
- [2] J. Nie and D. Linkens, *Fuzzy-Neural Control*, Prentice Hall, 1955.
- [3] Program for research into Intelligent Systems, *Fuzzy Logic*, National University of Singapore-School of Computing.
<http://www.comp.nus.edu.sg/~pris/FuzzyLogic/HistoricalPerspectiveDetail.html> (August, 2004)
- [4] [Abdul Aziz S.](#) and [Jeyakody P.](#), *Fuzzy logic report*, Imperial College-London.
http://www.doc.ic.ac.uk/~nd/surprise_96/journal/vol4/sbaa/report.html (August, 2004)
- [5] Zadeh, lotfi, *Foreword (Fuzzy Logic Toolbox)*, Mathworks website, January, 1995.
<http://www.mathworks.com/access/helpdesk/help/toolbox/fuzzy/fp637.html> (August, 2004).
- [6] Chapman S., *Electric Machinery Fundamentals*, 3rd edition, McGraw-Hill, 1999.
- [7] Kazmierkowski M. and Tunia H., *Automatic Control of Converter-Fed Drives*, PWN ltd, 1994.
- [8] Abu-Rub H., Krzemiński Z., *System Control of Induction Motor*, ICRAM'95 (International Conference on Recent Advances in Mechatronics), Istanbul.

-
- [9] Zhang L., Wathanasarn C., Hardan F., *An efficient Microprocessor-Based Pulse Width Modulator using Space Vector Modulation Strategy*, IEEE 1994.
- [10] Di Gabriele R., Parasiliti F., Tursini M., *Digital Field Oriented Control for induction motors: implementation and experimental results*, Universities Power Engineering Conference (UPEC'97).
- [11] Blaschke F. (1972): *The principle of field orientation as applied to the new transvector closed loop control system for rotating field machines.* - Siemens Rev., Vol.39, No.5, pp.217-220.
- [12] Al-Batran A., Abu-rub H., Guzinski J. and Krzeminski Z., *Fuzzy logic based sensorless control of induction motors*. EPNC (Electromagnetic Phenomena in Nonlinear Circuits), pp. 87-88, Poznan/Poland, 2004.
- [13] Boldea I. and Nasar S., *Vector Control of AC Drives*, CRC Press, 1992.
- [14] Boldea I. and Nasar S., *Electric Drives*, CRC Press, 1998.
- [15] Vas P., *Sensorless Vector and Direct Torque Control*, New York, O. University Press, (1998).
- [16] Hughes A., *Electric Motors and Drives*, 2nd edition, Newnes, 1990.
- [17] Mazda F., *Power Electronics handbook*, 3rd edition, Newnes, 1997.
- [18] Brod D., Novotny D., *Current Control of VSI-PWM Inverter*, IEEE Transactions on Industry Application, Vol. [A-2], NO 4, 1985, p.p. 562-570.
- [19] Plunkett A., *A current-controlled PWM transistor inverter drive*, in conference. ref. 1979, 14th Annual. IEEE Ind. Industrial Application Society, p.p. 785-792.

-
- [20] Franklin G., Power J., Workman M., *Digital Control of Dynamic Systems*, Addison-Wesley Publishing Company, Massachusetts 1990.
- [21] Ilaş C., Magureanu R.: *A General Adaptation Mechanism and its Applications to Induction Motor Direct Field Oriented Drive*, Conf.Rec.IEEE-ISIE'96, Warsaw, Poland, June 1996.
- [22] Abu-Rub H., Hashlamoun W., *A comprehensive analysis and comparative study of several sensorless control system of asynchronous motor*, ETEP journal (European Trans. On Electrical Power), Vol. 11, No. 3, May/June 2001.
- [23] Abu-Rub H., Guzinski J., Krzeminski Z., and Toliyat H., *Speed Observer System for Advanced Sensorless Control of Induction Motor*, IEEE Transactions on Energy Conversion, Vol. 18, No. 2, June 2003, pp. 219-224
- [24] Krzemiński Z.: *Sensorless control of induction motor based on new observer*. Int. Conf. on Intelligent Motion and Power Conversion, PCIM'2000, Nuremberg, 2000.
- [25] Rajashekara K., Kawamura A., Matsuse K.: *Sensorless Control of AC Motor Drives- speed and position sensorless operation*, IEEE Press, 1996, ISBN 0780310462.
- [26] Krzemiński Z. (1999): *A new speed observer for control system of induction motor*. IEEE Int. Conf. on Power Electronics and Drive Systems, PESC'99, Hong Kong, 1999.

-
- [27] Cleland J. and Turner M., *Fuzzy Logic Control of Electric Motors and Motor Drives: Feasibility Study*, Environmental Protection Agency (EPA), USA, 1996. <http://www.epa.gov/ORD/WebPubs/projsum/600sr95175.pdf> (October, 2004)
- [28] Kerkman R., Skibinski G., and Schlegel D., *AC Drives: Year 2000 (Y2K) and Beyond*, IEEE – APEC '99, March 14-18, 1999.
- [29] Ouhrouche M., Léchevin N. and Abourida S., *RTLab Based Real-Time Simulation of a Direct Field-Oriented Controller for an Induction Motor*, Proceedings of the 7th International Conference on Modeling and Simulation of Electric Machines, Converters and Systems, Montreal, Canada, Aug 18-21, 2002.
- [30] Gabriel R., Leonhard W. and Nordby C., *Field oriented control of standard AC motor using microprocessor*, IEEE Tran. IA, vol.16, no.2, pp.186.192, 1980.
- [31] Ogata K., *Modern Control Engineering*, 3rd edition, Prentice-Hall, Inc. 1997.
- [32] Orłowska-Kowalska T. and Wojsznis P. (1996). *Comparative study of rotor flux estimators sensitivity in the speed sensorless induction motor drive*. Proc. of IEEE Int. Conf. ISIE'96, Warsaw.
- [33] Krzemiński Z., *A new speed observer for control system of induction motor*. IEEE Int. Conference on Power Electronics and Drive Systems, PESC'99, Hong Kong.

- [34] Krzemiński Z., *Sensorless control of induction motor based on new observer*. Int. Conf. on Intelligent Motion and Power Conversion, PCIM'2000, Nuremberg.
- [35] Krzemiński Z., *Speed and Rotor Resistance Estimation in Observer System of Induction Motor*, 4th European Conf. on Power Electronics, Florence, September 3-6, 1991.
- [36] Abu-Rub H., *Systems Control of Induction Motor Synthesis on the Basis of Variables Identification using the Power Measurements, (Ph.D. thesis)*, Technical University of Gdańsk, Poland, (1995).
- [37] Bose B., *Technology trends in microcomputer control of electrical machines*, IEEE Transaction on Industrial Electronics, vol. 35, NO 1, February 1988.
- [38] Holtz J., *Sensorless control of induction motors*, Proceedings of the IEEE, Vol. 90, No. 8, Aug. 2002.
- [39] Joetten R. and Maeder G., *Control methods for good dynamic performance induction motor drives based on current and voltage as measured quantities*, IEEE Trans. Industrial Applications, vol. IA-19, no. 3, pp. 356-363, 1983.
- [40] Hillenbrand F., *A method for determining the speed and rotor flux of the asynchronous machine by measuring the terminal quantities only*, in Proc IFAC, Lausanne, Switzerland, 1983, pp. 55-62.
- [41] Schauder C., *Adaptive speed identification for vector control of induction motors without rotational transducers*, in Proc IAS, Florence, 1989, vol.3, pp. 493-499.
- [42] Boussak M., Capolino A. and Phuoc T., *Speed measurement in vector-controlled induction machine by adaptive method*, in Proc EPE, 1991, pp. 653-658.

-
- [43] Baader U., Depenbrock M. and Gierse G., *Direct self control (DSC) of inverter-fed induction machine - a basis for speed control without speed measurement*, IEEE Trans. on Industrial Applications, vol. 28, pp. 581-588, May/June 1992.
- [44] Tajima H. and Hori Y., *Speed sensorless field orientation control of the induction machine*, IEEE Trans. on Industrial Applications, vol. 29, pp. 175-180, 1993.
- [45] Du T. and Brdys A., *Shaft speed, load torque and rotor flux estimation of induction motor drive using an extended Luenberger observer*, in Proc. Sixth Int. Conf. on Electrical Machines and Drives, Oxford, UK, 1993, pp.179-184.
- [46] Tsuji M., and others, *A speed sensorless vector-Controlled method for induction motor using q-axis flux*, in Proc. IPEMC, Hangzhou, China, 1997, pp.353-358.
- [47] Cipolla-Ficarra, Griva G., Profumo F., *Comparison of different on-line algorithms for rotor time constant estimation in induction motor drives*, PEMC97, 3/192-3/196
- [48] Holtz J. and Quan J., *Drift and Parameter compensated Flux Estimator for Persistent Zero Stator Frequency Operation of Sensorless Controlled Induction Motors*, IEEE Trans. On Industry Applications, Vol. 39, No. 4, July/Aug. 2003, pp. 1052-1060.

A.3 Published Work

Electromagnetic Phenomena in Nonlinear Circuits, 28 - 30 June 2004, Poznań, POLAND

FUZZY LOGIC BASED SENSORLESS CONTROL OF INDUCTION MOTORS

Abdul-Fattah Al-Batran*, Haithem Abu-Rub*, Jaroslaw Guzinski**, Zbigniew Krzeminski**

* Electrical Engineering Department, Birzeit University, Palestine, E-mail: haithem@birzeit.edu

** Faculty of Elect. & Control Eng., Gdansk University of Technology, 80-952 Gdansk – Poland, E-mail: jarguz@pg.gda.pl

Abstract: In this paper, it is presented sensorless speed control of induction motors using fuzzy logic controller. The rotor angular speed is estimated using observer system or power measurement. The control system with speed observer is appropriate for extremely low speed and with power measurement is appropriate for higher speed operation. The proposed methods are applied to the field oriented control, however, may be used in any type of induction motor control system. In presented paper, simulation results are shown.

I. Introduction

Since the introducing of the idea of vector control of induction motors [11], this type of machine almost replaced the separately excited dc motors in adjustable electrical drives. To deal with induction motor as separately excited dc motor it is important to find two input orthogonal values. These values could be the direct and quadrature components of stator current. The decoupling between the input and the output in this coupled and complicated machine obtained as a result of using the idea of vector representation and transformation from one frame to other. If our coordinate system rotates with of rotor flux then the electromagnetic torque could be controlled by only one component while the second one is kept constant.

The application of vector representation and the advancement in power electronics, microprocessors and digital electronics cause a revolution in the use of a complicated squirrel cage induction motors.

Speed sensor has many defects and presents many problems like spoiling of the raggedness and simplicity of ac motors. Also this factor is expensive [1, 2, 3, 6, 7, 8, 10].

It has been proposed in the paper sensorless version of the system control. In this paper the rotor speed is calculated using exact speed observer system [1, 2] and from the differential equations in steady state and using power measurement. The calculated speed is used in the feedback to make it possible to linearize a dynamic of the control system.

The performance of sensorless controlled induction motors is poor at very low speed and zero stator frequency. There are limits of stable operation at very low speed that should be solved.

When the field oriented control system is used for sensorless drive system, the field angle, and also the mechanical speed, are estimated using the stator current vector and the stator voltage vector as input variables. Their accurate acquisition is a major concern for stable operation at very low speed. The reason is the limited accuracy of stator voltage acquisition and the presence of offset and drift components in the acquired signals [5].

The direct measurement of the stator voltages at the machine terminals is most accurate, but hardware requirements are quite substantial. The switched stator voltage waveforms require a large signal acquisition bandwidth, and the electric isolation must be maintained between the power circuit and the electronic control system. However, the processing of the analog signals introduces errors and offset. Using the reference voltage of the PWM modulator avoids all these problems. This signal is readily available in the control unit, and it is free from harmonic components. It does not exactly represent the stator voltages, though, as distortions are introduced by the dead time effect which cannot be completely eliminated even by the most sophisticated compensation strategies [5].

The using of exact speed observer system solves the limiting occurred at low speed region. The used observer system is appropriate for zero and extremely low speed.

The application of fuzzy logic attracts the attention of many scientists from all over the world [4]. The reason for this trend is the many advantages over traditional algorithmic methods in fuzzy environment. The speed in sensorless drive system is not exactly obtained and represents a fuzzy condition. Therefore fuzzy logic controller (FLC) is a good solution for sensorless control.

The used model of induction motor is fed by the voltage source inverter. Simulation results in real time have been carried out.

II. Induction motor description

The squirrel cage type of induction motor as differential equations for the stator current and rotor flux vector components presented in coordinate system XY rotating with arbitrary angular speed is:

$$\frac{di_{sx}}{d\tau} = \frac{R_s L_r^2 + R_r L_m^2}{L_r w} i_{sx} - \frac{R_r L_m w}{L_r w} i_{sy} + \omega_s i_{sy} - \frac{L_m}{L_r} \frac{d\psi_{rx}}{d\tau} \quad (1)$$

$$\frac{di_{sy}}{d\tau} = \frac{R_s L_r^2 + R_r L_m^2}{L_r w} i_{sy} - \frac{R_r L_m w}{L_r w} i_{sx} + \omega_s i_{sx} - \frac{L_m}{L_r} \frac{d\psi_{ry}}{d\tau} \quad (2)$$

$$\frac{d\psi_{rx}}{d\tau} = \frac{R_r}{L_r} \psi_{rx} + \omega_s \psi_{ry} - \frac{L_m}{L_r} i_{sx} \quad (3)$$

$$\frac{d\psi_{ry}}{d\tau} = \frac{R_r}{L_r} \psi_{ry} - \omega_s \psi_{rx} - \frac{L_m}{L_r} i_{sy} \quad (4)$$

$$\frac{d\omega_r}{d\tau} = \frac{L_m}{L_r J} (\psi_{rx} i_{sy} - \psi_{ry} i_{sx}) - \frac{1}{m\theta} \quad (5)$$

$$w = \delta L_r L_s ; \delta = 1 - \frac{L_m^2}{L_r L_s}$$

Where $\psi_{rx}, \psi_{ry}, i_{sx}, i_{sy}, u_{sx}, u_{sy}$ are the rotor flux, stator current and voltage vectors in coordinate system XY rotating with arbitrary speed, ω_r, ω_s are angular speed of the rotor shaft and reference frame, R_r, R_s, L_r, L_s are rotor and stator resistance and inductances respectively, L_m is a mutual inductance, J is the inertia, m_0 is the load torque.

III. Vector control system

The idea of vector control of AC machines depends on vector representation and transformation from one coordinate system (stationary) to the rotating one (Fig. 1) The produced torque T_e in the machine has the next form:

$$T_e = \frac{L_m}{L_r J} (\psi_{rd} i_{sq} - \psi_{rq} i_{sd}) \quad (6)$$

where dq are the variables in rotating frame. If our coordinate system rotates with of rotor flux ψ_r then the electromagnetic torque could be controlled by only one component while the second one is kept constant. This happens because the imaginary component of rotor flux ($\psi_{rq}=0$) which gives the next form:

$$T_e = \frac{L_m}{L_r J} (\psi_{rd} i_{sq}) \quad (7)$$

If we keep constant i_{sd} then the rotor flux will keep constant. By this way the produced torque will linearly depends on the imaginary component of stator current (i_{sq}). The vector control system is shown at Fig. 2.

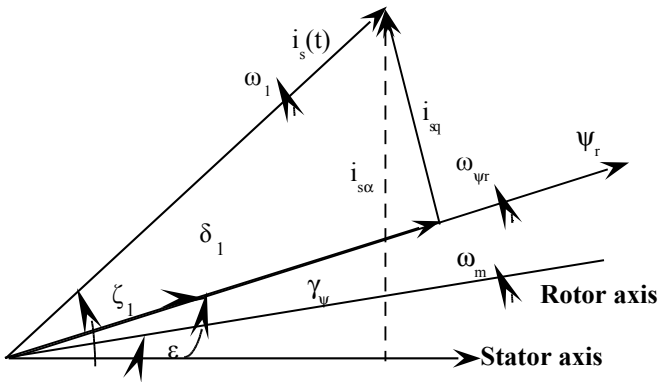


Fig 1. Angular relations of current vectors.

IV. Speed estimation

A. Rotor Speed Observer System

A new speed observer system has been proposed for the first time in [2]. The differential equations of the speed observer modified in this paper are as follows:

$$\frac{d\hat{i}_{sx}}{dt} = a_1 \hat{i}_{sx} + a_2 \hat{\psi}_{rx} + a_3 \omega_r \hat{\psi}_{ry} + a_4 u_{sx} + k_i (i_{sx} - \hat{i}_{sx}) \quad (8)$$

$$\frac{d\hat{i}_{sy}}{dt} = a_1 \hat{i}_{sy} + a_2 \hat{\psi}_{ry} - a_3 \omega_r \hat{\psi}_{rx} + a_4 u_{sy} + k_i (i_{sy} - \hat{i}_{sy}) \quad (9)$$

$$\frac{d\hat{\psi}_{rx}}{d\tau} = a_5 \hat{i}_{sx} + a_6 \hat{\psi}_{rx} - \zeta_y - k_2 (\hat{\omega}_r \hat{\psi}_{ry} - \zeta_y) \quad (10)$$

$$\frac{d\hat{\psi}_{ry}}{d\tau} = a_5 \hat{i}_{sy} + a_6 \hat{\psi}_{ry} + \zeta_x + k_2 (\hat{\omega}_r \hat{\psi}_{rx} - \zeta_x) \quad (11)$$

$$\frac{d\zeta_x}{d\tau} = k_1 (i_{sy} - \hat{i}_{sy}) \quad (12)$$

$$\frac{d\zeta_y}{d\tau} = -k_1 (i_{sx} - \hat{i}_{sx}) \quad (13)$$

$$\hat{\omega}_r = S \left(\sqrt{\frac{\zeta_x^2 + \zeta_y^2}{\hat{\psi}_{rx}^2 + \hat{\psi}_{ry}^2}} k - V_4(V_f) \right) \quad (14)$$

where $\hat{\cdot}$ denotes estimated variables, k_1, k_2, k_3 are the observer gains, S is the sign of speed. The values ζ_x, ζ_y are the components of disturbance vector and V is the control signal obtained through experiments and V_f is the filtered signal V .

The coefficients k_1 to k_4 in the speed observer system have small values. Therefore, the operation of the observer system is stable and maintains small transient errors. The values of the coefficients significantly affect the quality of the calculated speed during transients. In [17], it is shown that the coefficient k_2 may depends on the rotor speed,

$$k_2 = a + b \cdot |\hat{\omega}_r| \quad (15)$$

where a and b are constant coefficients and $\hat{\omega}_r$ is the estimated and filtered rotor speed.

The simulation and experimental tests showed that it is necessary to choose different values of the coefficients for different speeds, torques and transients to minimize speed estimation errors.

The speed observer may be used in different control systems for rotor flux and speed estimation. In [1, 2] the observer system was used for nonlinear control system. For vector control system this observer till now was not used. Therefore in this paper we apply the observer system in field oriented control system. The control signals are defined as follows:

$$V = \hat{\psi}_{rx} \zeta_y - \hat{\psi}_{ry} \zeta_x \quad (16)$$

$$\frac{dV_f}{d\tau} = \frac{1}{T_1} (V - V_f) \quad (17)$$

This method of speed computation is appropriate for extremely low speed operation. Below will be presented other simple method appropriate for high speed region.

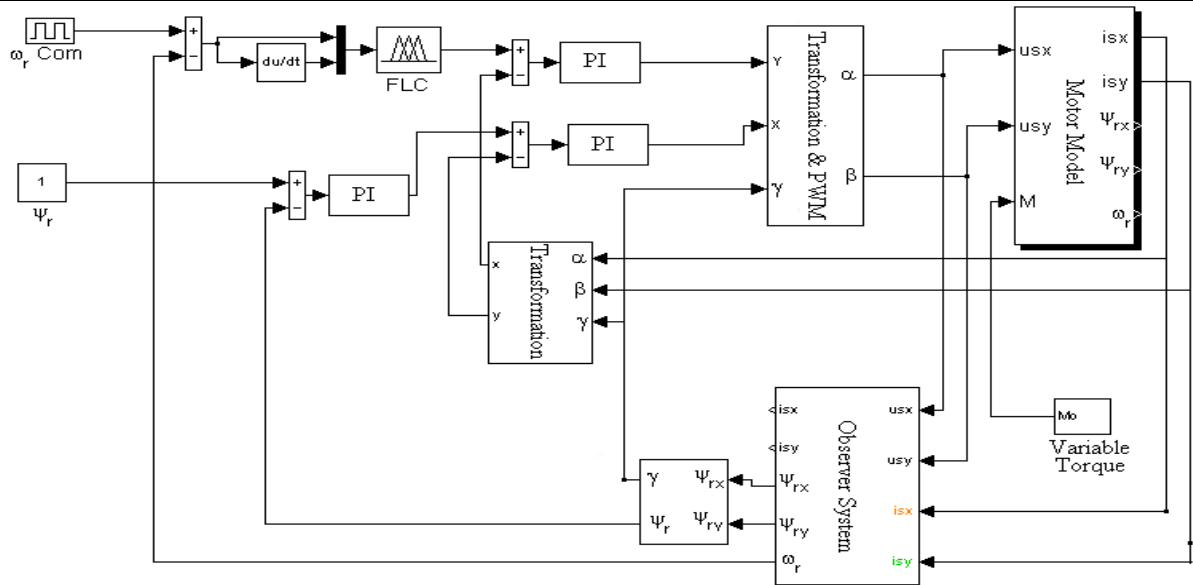


Fig 2. Vector control system of induction motor

B. Rotor angular speed calculation using power measurement

Rotor angular speed in a presented control system may be determined by using the differential equations of stator current and rotor flux vectors products (equations 1 to 4). Rotor angular speed presents in deferent depends of stator and rotor deferential equations. In steady states the left-hand sides of equations (1 to 4) are equal to zero. This property, together with using new variables and power definitions, provides a lot of equations for rotor speed [3]:

$$\omega_r = \frac{-a_2 x_{12} - s_i i_s^2 + a_4 Q}{i_s^2 + a_3 x_{22}} \quad (18)$$

where; $a_2 = \frac{R_r L_m}{L_r \omega}$; $a_3 = \frac{L_m}{\omega}$; s_i is the slip frequency and Q is the imaginary reactive power [9]. x_{12} and x_{22} are new variables defined below.

The equations of used power is:

$$Q = u_s \beta^i i_s \alpha - u_s \alpha^i i_s \beta \quad (19)$$

where α and β denote a stationary frame. The slip frequency is:

$$s_i = \frac{R_r x_{12}}{L_r x_{22}} \quad (20)$$

and the new variables are [1, 2]:

$$x_{12} = \psi_r \alpha^i i_s \beta - \psi_r \beta^i i_s \alpha \quad (21)$$

$$x_{22} = \psi_r \alpha^i i_s \alpha + \psi_r \beta^i i_s \beta \quad (22)$$

The stator flux vector is presented as next:

$$\psi_s = (u_s - R_s i_s) dt \quad (23)$$

Where u_s, i_s, R_s are stator voltage, current and resistance respectively.

The expressions of stator flux and rotor flux vectors are will known:

$$\psi_s = L_s i_s + L_m i_r \quad (24)$$

$$\psi_r = L_r i_r + L_m i_s \quad (25)$$

Taking into account the above equations get the expression of rotor flux vector components in stationary coordinate system:

$$\psi_{r\alpha} = \frac{L_r}{L_m} \psi_s \begin{pmatrix} \alpha \\ \beta \end{pmatrix} \begin{pmatrix} L_s i_s \\ L_m i_r \end{pmatrix} \quad (26)$$

$$\psi_{r\beta} = \frac{L_r}{L_m} \psi_s \begin{pmatrix} \beta \\ -\alpha \end{pmatrix} \begin{pmatrix} L_s i_s \\ L_m i_r \end{pmatrix} \quad (27)$$

This method is appropriate for speed not close to zero operation.

V. Fuzzy logic controller

In the system with not exactly known dynamic, and with difficult to describe analytical relationships, good results are obtained by using the fuzzy logic theory.

The system described in this paper has the mentioned characteristics, which are caused by non-precise variable identification and thus a complicated analytical system description. In the system presented, Mamdani type of fuzzy logic controller (FLC), presented in Fig. 3. is used for speed controller. The input signals for the controller are: control error, 'e' and the change of error, 'Δe' and the output is the change of control signal, 'Δu'. The controller consists of three elements: fuzzyfication block, block of rules (rules of inference) and defuzzyfication, which are related by proper relationships.

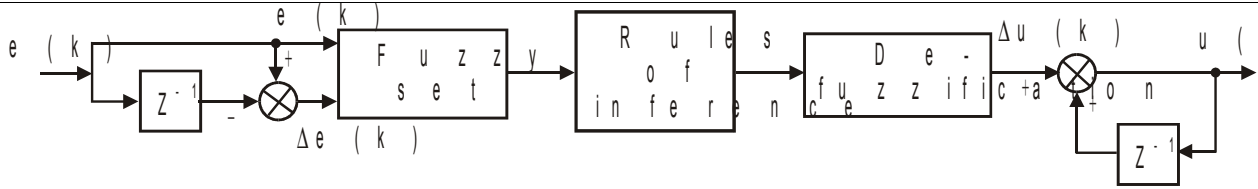


Fig 3. Fuzzy Logic Controller (FLC)

On the basis of the values, 'e' and 'Δe', the fuzzy numbers are calculated in the fuzzy membership function pres... functions for the three lin... - zero and 'P' - positive... consists of logic table like... Table 1. Symbol 'B'' me... small. On the basis of the... such sectors, which are de... is described, which is the... function. This quantity m... identify a signal, which w... From many defuzzificati... method (COA) is chosen... the fuzzy set after defuzz...

$$y^* = \frac{\sum_{i=1}^n F(y_i) y_i}{\sum_{i=1}^n y_i}$$

where:

- n – Number of quantization levels
- y_i – Value for i-th quantization function Δu for i-th quantization level
- F_i – value of membership function Δu for i-th quantization level.

For the specified number of input signal samples, it is possible to elaborate a proper look-up table, which contains the error values.

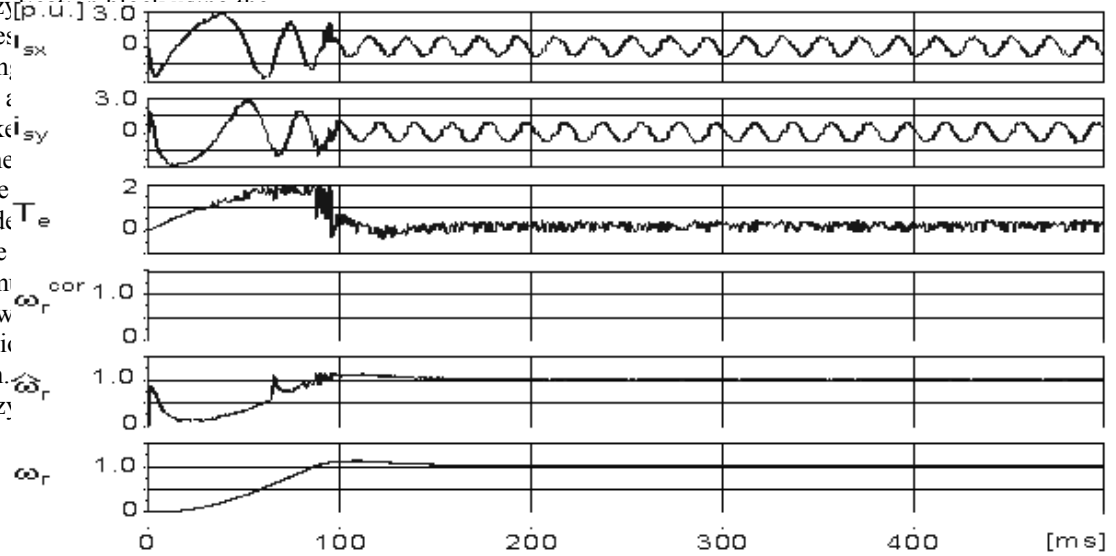


Fig. 4. Results for step changes of the rotor speed set values and of the load torque. Data of a 3 kW squirrel cage motor have been used in investigations. The results are presented for extremely low speed region.

The results show very good operation in the region very close to zero speed and at zero speed. The speed error when operating on zero region does not exceed 1.5%. This error increasing when speed increases.

Figure 4. shows the response of sensorless control system with PI controller and power measurement. The indexes XY denote the stationary components.

F

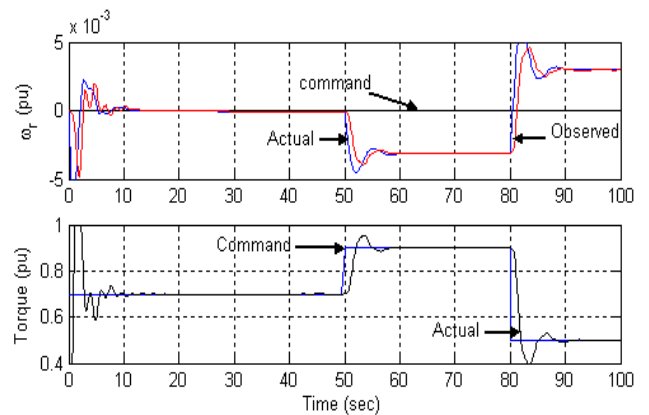


Fig. 5. Results of control system with speed observer system at zero command speed

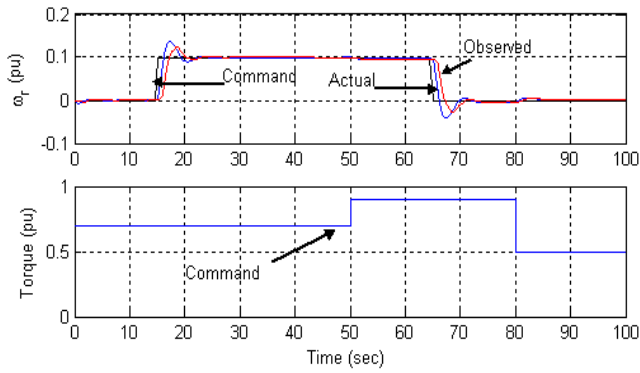


Fig. 6. Results of control system with observer system after speed step change

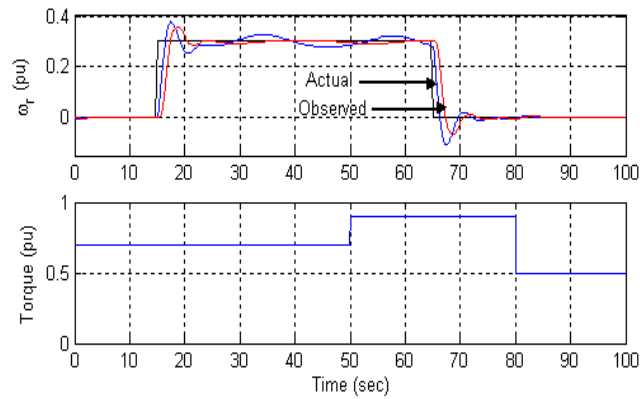


Fig. 7. Results of control system with speed observer system after speed and load changes

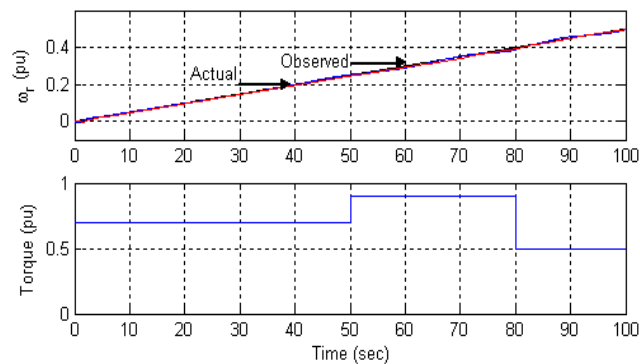


Fig. 8. Results of control system with speed observer system after ramp speed change and step load changes

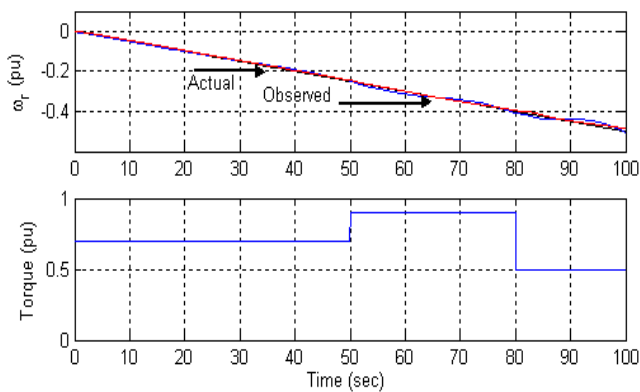


Fig. 9. Results of control system with speed observer system after ramp speed change and step load changes

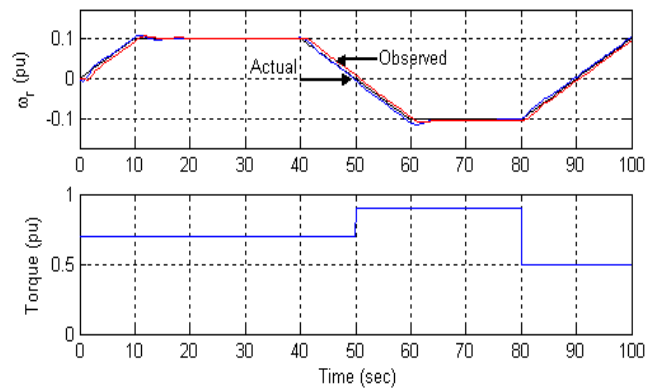


Fig. 10. Results of control system with speed observer system after speed and step load changes

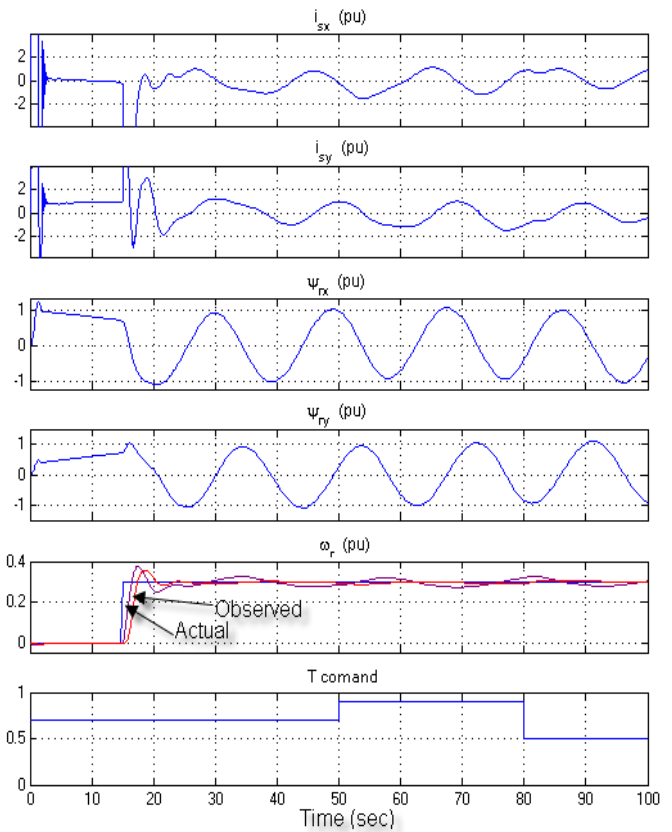


Fig. 11. Results of control system with observer system after speed and step load changes

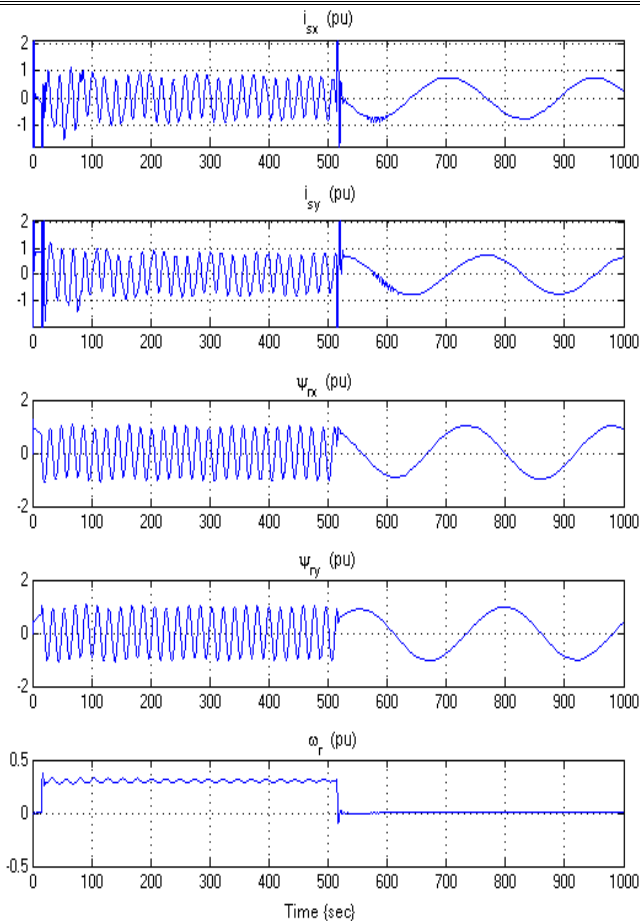


Fig. 12. Results of control system with observer system after speed step change

VII. Conclusion

In the presented paper a sensorless vector control of induction motor using speed observer system is presented. The rotor speed was calculated using exact speed observer system, which mainly appropriate for lower speeds. Other method of speed calculation is power measurement. This method could be used for higher speed computation because the limitation resulted from voltage measurement at lower speeds.

Simulation results are presented for the system with fuzzy logic speed controller. All presented results show that the proposed sensorless control system works very well at extremely low speeds.

References

[1] Krzemiński Z.: Sensorless control of induction motor based on new observer. Int. Conf. on Intelligent Motion and Power Conversion, PCIM'2000, Nuremberg, 2000.

[2] Krzemiński Z. (1999): *A new speed observer for control system of induction motor*. IEEE Int. Conf. on Power Electronics and Drive Systems, PESC'99, Hong Kong, 1999.

[3] Abu-Rub H., Hashlamoun W., A comprehensive analysis and comparative study of several sensorless control system of asynchronous motor, accepted to ETEP journal (European Trans. On Electrical Power), Vol. 11, No. 3, May/June 2001.

[4] B. K. Bose, "Expert system, fuzzy logic and neural network application in power electronics and motion control" *Proc. of the IEEE vol. 82 No. 8* August 1994

[5] Holtz J. and Quan J., Drift and Parameter compensated Flux Estimator for Persistent Zero Stator Frequency Operation of Sensorless Controlled Induction Motors, *IEEE Trans. On Industry Applications*, Vol. 39, No. 4, July/Aug. 2003, pp. 1052-1060.

[6] H. Abu-Rub, J. Guzinski, Z. Krzeminski, and H. Toliyat, "Speed Observer System for Advanced Sensorless Control of Induction Motor", *IEEE Transactions on Energy Conversion*, Vol. 18, No. 2, June 2003, pp. 219-224

[7] J. Guzinski, H. Abu-Rub, and H.A. Toliyat, "An Advanced Low-Cost Sensorless Induction Motor Drive," *IEEE Transactions on Industry Applications*, vol. 39, No. 6, November/December 2003, pp. 1757-1764.

[8] Orłowska-Kowalska T., Wojsznis P. Kowalski C.T. (2001): *Dynamic Performance of Sensorless Induction Motor Drive with Different Flux and Speed Observers* Proc. of 9-th European Conference on Power Electronics and Application EPE 2001 Graz, Austria 2001

[9] Akagi H., Kanazawa Y., Nabae A. (1983). "Generalised Theory of the Instantaneous Reactive Power in Three-Phase Circuits, IPEC, Tokyo.

[10] Guzinski J., Abu-Rub H., Sensorless Control System of the Induction Motor, PCIM'01 (38 International Intelligent Motion Conference, Germany, June 2001).

[11] Blaschke F. (1971). "Das Prinzip der Feldorientierung, die Grundlage für Transvector-regelung von Drehfeldmaschine". *Siemens Z.* Vol.45, str. 757-760.